PHASE EQUILIBRIA AND CRYSTALLIZATION OF THE LITHIUM OXIDE - ZINC OXIDE - SILICA SYSTEM

Thesis submitted to the Department of Glass Technology, Faculty of Metallurgy, of the University of Sheffield, in partial fulfilment of the requirements for the degree of Doctor of Philosophy.

January 1964.

Anthony Hon-Team Lam.

TEXT CUT OFF IN THE ORIGINAL

Summary

The phase equilibria in the glass forming region of the lithium oxide-zinc oxide-silica ternary system were investigated by the quenching technique with a vertical gradient furnace. The glass forming limit on the low silica side was found to be near the fifty mole per cent silica line, being higher in silica at the lithium oxide rich side. The refractive indices of the glasses were measured by the Beche line technique. Zinc oxide was found to increase the refractive indices of the glasses more than the lithium oxide.

Tridymite, lithium disilicate, lithium metasilicate, zinc orthosilicate and two ternary compounds were found as primary phase crystals. One of the ternary compounds was identified conclusively as $Li_2O.ZnO.SiO_2$. The other ternary compound was tentatively identified as $2Li_2O.4ZnO.3SiO_2$. The optical properties and the x-ray diffraction patterns of these two ternary compounds are very similar and they form solid solutions with each other. Also zinc orthosilicate dissolves in $2Li_2O.4ZnO.3SiO_2$ to form solid solutions. Continuous solid solution was found along the $Li_2O.ZnO.SiO_2$ - $2ZnO.SiO_2$ join with up to 60 mol % of zinc orthosilicate dissolved in $Li_2O.ZnO.SiO_2$ in the specimens quenched from above 1500°C.

Two eutectic points and two reaction points were found in the compositions investigated. The eutectic point of the composition triangle SiO_2 - $Li_2O.2SiO_2$ - $Li_2O.ZnO.SiO_2$ was found at Li_2O 25.5 mol % ZnO 10 mol %, SiO_2 64.5 mol % and 955° ±5°C. The eutectic point of the composition triangle SiO_2 - $Li_2O.ZnO.SiO_2$ - $2Li_2O.4ZnO.3SiO_2$ was located at Li_2O 16.5 mol %, ZnO 23 mol %, SiO_2 60.5 mol % at 1050° ±5°C. The reaction point of the composition triangle $Li_2O.2SiO_2$ - $Li_2O.SiO_2$ - $Li_2O.ZnO.SiO_2$ was found at Li_2O 27.5 mol %, ZnO 9.8 mol %, SiO_2 63.7 mol % at 976° ±5°C. The reaction point between the SiO_2, $2ZnO.SiO_2$ and $2Li_2O.4ZnO.3SiO_2$ was located at Li_2O 15.7 mol %, ZnO 24.6 mol %, SiO_2

59.7 mol % and 1068° ±5°C. The two-phase regions were found below the solidus temperature in the composition triangle of SiO_2 - $Li_2O.ZnO.SiO_2$ - $2Li_2O.4ZnO.3SiO_2$.

Extraneous lines were found to be included in the lithium disilicate and lithium metasilicate data in the X-Ray Powder Data File. The present powder data of lithium disilicate were indexed as orthorhombic crystal with cell parameters a_o = 5.80Å, b_o = 14.66Å and c_o = 4.806Å, and that of the lithium metasilicate were indexed as pseudo-hexagonal orthorhombic crystal with cell parameters a_o = 5.43Å, b_o = 9.41Å and c_o = 4.660Å.

The crystallization characteristics of five glasses of this ternary system were studied. Uniform crystallization was found to occur in all the specimens. Big lithium disilicate crystals were found in specimens of four glasses. A high concentration of tiny crystals was found in every specimen.

A hot stage microscope with a microfurnace was constructed to study the crystal growth in glasses of this system. Three glasses were investigated. The usual hump shaped growth rate versus temperature curves were obtained. The growth of the crystals were found to be linear with time. The maximum growth rate of lithium metasilicate, lithium disilicate, $Li_2O.ZnO.SiO_2$ and tridymite in these glasses were found to be about 3,500, 400, 70 and 20 micron per minute respectively.

.....

Acknowledgments.

The author wishes to thank Professor R. W. Douglass for his valuable advice and constant encouragement during the course of this work.

He also wishes to thank Dr. J. O. Isard, Mr. R. F. R. Sykes, Mr. C. Moxon and all members of the staff of the Department of Glass Technology, who willingly gave their help and advice when it was sought.

The author appreciates the assistance given by Mr. J. Lewins of the Department of Glass Technology in the preparation of electron micrographs.

He also takes this opportunity to thank Dr. J. G. Morley of Rolls-Royce Research Laboratories, Derby, England, for his advice on the detailed design of the hot stage microscope used in the present study; and Mr. R. E. Carr of Research and Development Centre, Anchor Hocking Glass Corp., Ohio, U.S.A., for his encouragement, and introducing the author to the interesting field of nucleation and crystallization.

Finally, the author wishes to thank the International Lead Zinc Research Organization, New York, U.S.A., for the financial help given during the present investigation.

LIST OF CONTENTS.

LIST OF FIGURES.

LIST OF TABLES

INTRODUCTION

1. The Invention of the Glass-ceramic process.

In 1957, Corning Glass Works of U.S.A. announced the invention of a new process of forming ceramic articles which they described under the trade name Pyroceram. This kind of new material is now collectively termed as glass-ceramic. This process has since been proved to be important not only on the commercial side but also in the technology and science of ceramics.

This process is essentially a controlled crystallization. The raw material is melted and formed into glass articles according to conventional methods used in the glass industry. These articles are then converted into largely crystalline ceramics by heat treatment, which can be roughly divided into a nucleation heat treatment and a crystal growth heat treatment at a higher temperature. Nucleating agents, such as titanium oxide, or metal constituents are added to the glass batch to control the subsequent crystallization. These nucleating agents dissolve in the melt and in the nucleation heat treatment, they affect the structure of the glass to provide numerous nucleation sites. During the crystal growth heat treatment, a lot of tiny crystals are developed and these convert the original glass articles into ceramic articles having the same size and containing more than 50% crystalline materials.

2. The advantage of the glass ceramic process.

The ceramic material made by this process can be transparent with a slight tan or opaque with the attractive appearance of fine china. This material is generally stronger and harder than the parent glass, and has greater scratch and impact resistance.

Its thermal, electrical and chemical resistant properties depend on the properties of both the glass matrix and the constituent crystalline phases. By choosing suitable composition and heat treatment, to yield the crystalline phase having the desired physical properties, material of unusual properties can be obtained. Using compositions in Li_2O - Al_2O_3 - SiO_2 - TiO_2 system, Corning Glass Works is able to produce materials having good chemical durabilities and thermal expansion coefficient ranging from negative to positive. Some nose cones of missiles and artificial satellites made by this process with compositions of the MgO - Al_2O_3 - SiO_2 - TiO_2 system have unusual electrical properties with extremely low temperature coefficient and good thermal shock resistance. Although this material is poly-phase, it is essentially homogeneous due to the extreme small size of the crystalline phase. Its physical properties are essentially isotropic.

Another advantage of this process is that the conventional glass forming processes can be used to form the articles. The glass forming processes have been developed to a very high standard of engineering, because they are rapid, automatic and can be carried out to close tolerance with the elimination of all porosity. Therefore these provide means of forming with low cost.

With this process, compositions which cannot be used successfully before can now be used. For examples, the commercial Pyroceram tablewares contain essentially β-Spodumene solid solution crystals. If articles with this composition are made from crystalline materials and fired as in the conventional porcelein process, the resultant articles will be very weak and have a very poor finish, because β-Spodumene bodies are difficult "to glaze". With this new process, the composition range of ceramic materials is extended and a new kind of material with unusual microstructure can be formed commercially.

3. Effects on the ceramic science and technology.

Probably, it is suitable to point out in here the implication of the invention of this process. Actually this process bridges an important gap in the material technology. Not long ago, metallurgy, ceramic technology and glass technology were more or less completely separate branches of material technology. Although they all utilize natural or processed materials to produce utensils or engineering materials, their manufacturing process and their approach were vastly different and the properties of their products were not the same. With the appearance of cermet, the division of ceramic technology and metallurgy vanished. In the glass-ceramic process, the conventional manufacturing methods of the glass industry are used to form the articles, which are heat treated to control the microstructure and hence the physical properties of the product as in the metallurgy industry and the final product is similar to that of the ceramic industry. Therefore the three main branches of the material technology are now unified. Also it is needless to say that the research work which leads to the invention of this process embraces the approach and the concepts of the previously divided branches of the material science.

Phase transformation has been an important field in science. Usually overheating, if it happens, is not very large, but undercooling can be very great. The transformation of more random structure to a more ordered structure, e.g. the condensation of supersaturated vapour, and the re-crystallization of undercooled liquid is more difficult than the change from the ordered structure to the disordered structure. This is attributed to the necessity of the formation of the nuclei as an essential step in the transformation of random structure to ordered structure. Some progress has been made in very simple systems, but in more complex systems knowledge is still very limited.

The ability of a system to form glass on undercooling depends upon the kinetics of crystallization. Since the composition ranges of different systems that form glasses are very wide, and the temperature ranges and time intervals in which the phenomena can be studied are so wide, glass is a very good medium for the study of the mechanism of phase transformation. Actually glass formation is a very important and fundamental field in the study of the science of Glass. This field was neglected, possibly due to the seemingly unrelated nature between glass formation and the normal day-to-day production, and the lack of suitable instruments for the study.

Recrystallization or devitrification as it is called in the glass industry, has been an embarrassing occurrence in the normal production of glass. Therefore previous research work had been concentrated on the prevention of it, and its mechanism was seldom studied in any depth. With the invention of the glass-ceramic process devitrification has been changed from a liability to an asset, and the possibilities are unlimited. This has stimulated and revived the interest in the mechanism of crystallization. A lot of work has been done since the announcement of this process, and some advance has been made. However, the mechanism of crystallization is still far from fully understood yet.

4. The choice of the present program.

In the patents [1-6] taken out by the Corning Glass Works, more than ten glass forming systems are said to be suitable for the glass ceramic process. From the research of other workers, more systems were found. In the main patent[1] of the Corning Glass Works, alkali or alkali-earth aluminosilicate systems are used. The commercial Pyroceram products are mainly made of magnesium aluminosilicate and lithium aluminosilicate system. Both magnesium and lithium have high field strengths.

There is a certain amount of similarity between aluminium oxide and zinc oxide. They are both amphroteric and their electronegativities are both 1.5. It is known that the co-ordination number of the aluminium ion in small amounts in silicate glasses is four and that of zinc ion in glass and in zinc ortho-silicate is also four.

From experience, the glass industry has learned that both zinc oxide and aluminium oxide are beneficial in the developing of opacity during the production of fluoride opal glass in which re-crystallization of tiny crystals in the glass occurs. Also in the manufacture of ruby glass, in which recrystallization processes are also involved, zinc oxide is found to be beneficial. It was felt that zinc oxide would help the re-crystallization process in the glass ceramic process, therefore, the lithium oxide - zinc oxide - silicate system was chosen for the present study.

The knowledge of the phase equilibria in the system is very helpful in the understanding of a study of this nature. Unfortunately, no information about the phase equilibria of this ternary system was found in the literature, so the phase diagram of the glass forming region was first studied. The present thesis is divided into two parts. The first part concerns the study of the phase equilibria and the second part deals with the crystallization of glasses in this ternary system.

PART A PHASE EQUILIBRIA OF LITHIUM OXIDE - ZINC OXIDE - SILICA SYSTEM.

I. LITERATURE SURVEY.

No reliable information was found on the phase equilibria of the ternary lithium oxide - zinc oxide - silica system. However two of the binary systems had been investigated.

1. The lithium oxide - silica system.

The lithium oxide - silica system had been investigated by a number of workers. Due to the high tendency to devitrification of Glasses in this system, it is possible to obtain the approximate location of the melting point curves by thermal analysis. This method was used by Riche and Endell, Ballo and Dittler, Schwarz and Sturm, Wallace, F. M. Jaeger and H. S. Van Klooster.(7) However, their results did not agree with each other, possibly due to the inherent errors in this method.

Reliable results were provided by the work of F. C. Kracek.(8) He used the quenching technique to investigate the liquidus temperature in the composition range between silica and lithium metasilicate. With compositions having higher than fifty mole percent of lithium oxide, thermal analysis with the heating up curve technique was used. With a low heating rate of 3°-4°/min. an agreement to within 0.5°C was obtained between the data of the heating up curve and that of the quenching technique on the melting point of lithium metasilicate. A petrological microscope was used to examine the specimen to identify the crystals.

Lithium orthosilicate, lithium metasilicate and lithium disilicate were found as primary phases in this system. Lithium orthosilicate decomposes at 1255°C before its melting point is reached, the composition of the liquid phase being 34.2 mole percent silica. The eutectic point between lithium orthosilicate and lithium metasilicate is at 1024°C, 38.1 mole percent silica.

FIG. 1.

THE SYSTEM LITHIUM OXIDE – SILICA.

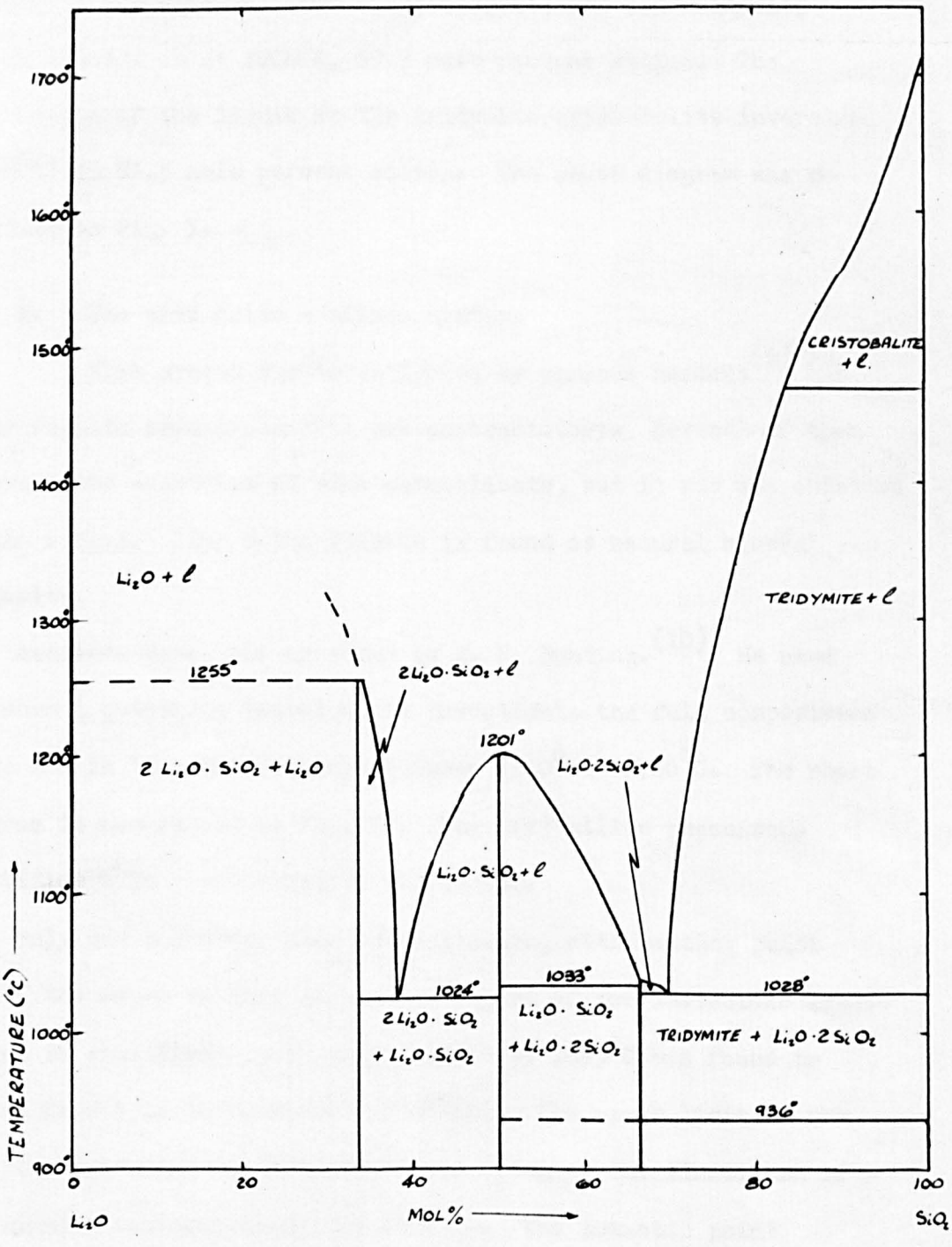

Lithium metasilicate melts at 1201 ± 1°C and its liquidus curve meets the incongruent melting point curve of lithium disilicate at 1033° and 66.7 mole percent silica, within 0.05% of the lithium disilicate composition. The lithium disilicate and tridymite eutectic point is at 1028°C, 69.7 mole percent silica. The composition of the liquid at the tridymite-crystabolite inversion (1470°C) is 83.5 mole percent silica. The phase diagram was reproduced as Fig. I.

2. The zinc oxide - silica system.

This system was investigated by various workers(9) but their results were incomplete and contradictory. Several of them reported the existence of zinc metasilicate, but it was not obtained by the others. Zinc orthosilicate is found as natural mineral willemite.

Accurate data was provided by E. N. Bunting.(10) He used the normal quenching technique to investigate the full composition range and in temperature range between 1300° to 1700°C. The phase diagram is reproduced as Fig. II. The crystalline phases were identified with a petrological microscope.

Only one compound, zinc orthosilicate, with melting point 1512°C was found in this system. A region of two immiscible liquid phases in equilibrium with crystabolite at 1695°C was found to extend from 2 to 34 mole percent silica. The upper limit of the two liquid regions was not determined owing to the limitation of the working temperature of the furnace. The eutectic point between tridymite and zinc orthosilicate was found at 1432°C and 49.1 mole percent zinc oxide. The other eutectic point between zinc oxide and zinc orthosilicate was found at 1507°C and 77.5 mole percent zinc oxide.

FIG. 2.

THE SYSTEM ZINC OXIDE — SILICA.

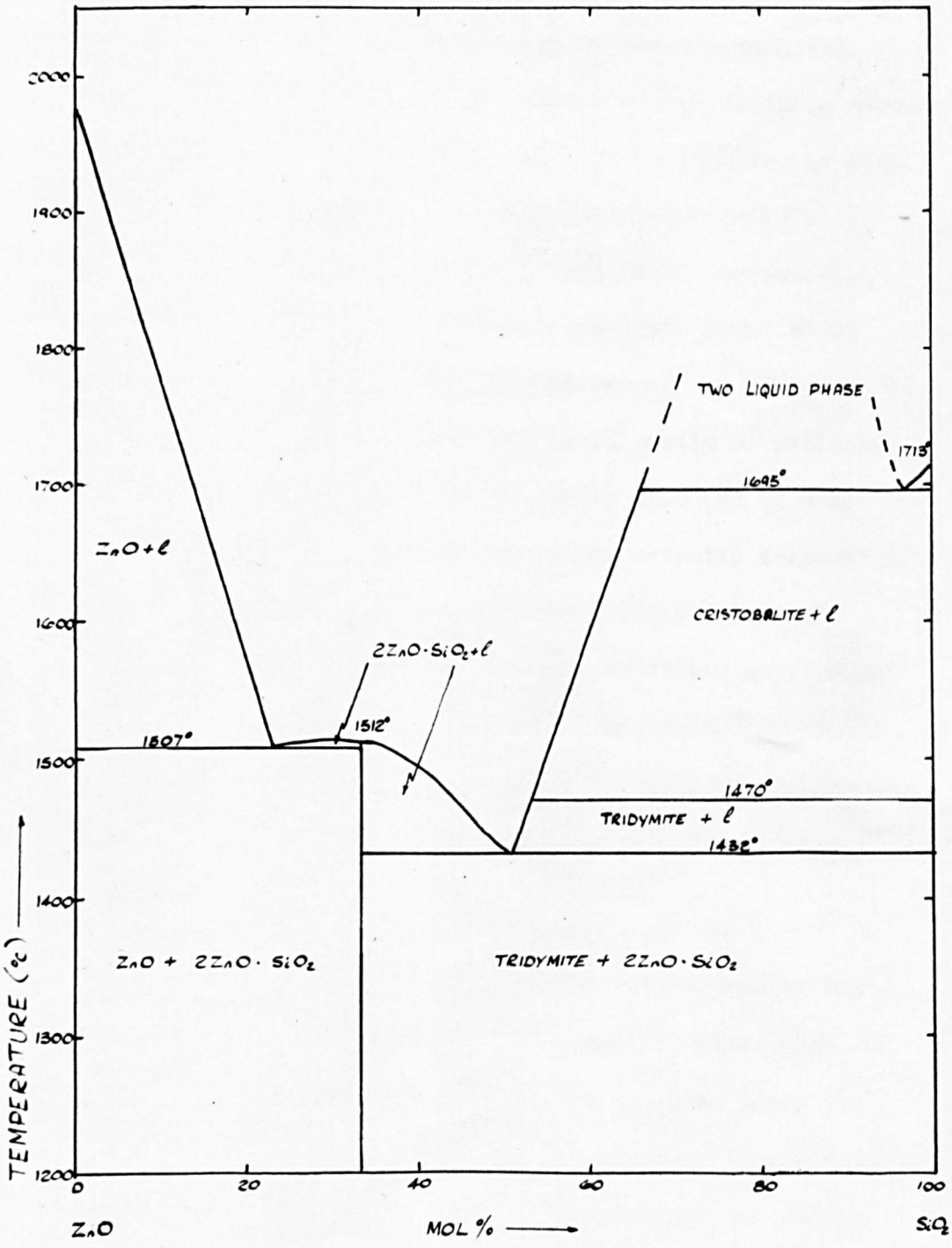

A special platinum iridium alloy button was used in an induction furnace to determine the melting point of zinc oxide which was found to be 1975°C. An optical pyrometer with an accuracy of ± 25°C was used to measure the temperature. Volatilization of zinc oxide at high temperature was minimized by putting platinum iridium alloy sponge on top of the specimen.

The existence of zinc metasilicate was specially examined. Specimens containing 49.1 and 51.0 mole percent zinc silicate were heat treated at various temperatures from 1100° - 1350°C. At high magnification of 1000X tridymite and zinc orthosilicate were identified. At low magnification of 100X and 200X, the material appeared to be homogeneous. One eutectic point was found to be at 49.1 mole percent of zinc oxide. A high percentage of eutectic mixture would be found in the sample and could easily be mistaken to be zinc metasilicate. Specimens containing 51.6 and 65 mole percent zinc oxide were heat treated above the eutectic temperature and quenched samples were examined by X-ray diffraction. Only zinc orthosilicate X-ray pattern was found. Specimens containing 48.3 and 51.6 mole percent zinc oxide were heat treated at 1350°C and examined by X-ray, tridymite and zinc orthosilicate were found. Therefore the absence of zinc metasilicate was proved conclusively.

3. Lithium oxide - zinc oxide - silicate system.

H. S. Van Klooster[11] investigated a few compositions along 50 mole percent silica lines in this system. Zinc metasilicate was said to be present, and a simple eutectic phase diagram along the zinc metasilicate and lithium metasilicate join was reported. Since the absence of zinc metasilicate was proved conclusively by E. W. Bunting,[10] the data reported by Van Klooster was considered very inaccurate, and was not considered.

I. M. Stewart and G. J. P. Buchi[12] recently published the result of their work on the phase relationships in the system of lithium oxide - zinc oxide - silica. They prepared specimens by pressing the raw material into compacts with an organic bonding agent which was subsequently burnt out at low temperature. The compacts were heat treated in the temperature range 925° to 1300°C for one or two hours, then the specimens were examined by X-ray diffraction. The temperature and duration of the heat treatment for individual compositions were established by trial and error in the preliminary work. The final heat treatment time and temperature chosen were that which gave a non glassy specimen, the diffraction pattern of which was sharp. From the results of eighteen compositions investigated, they concluded that two ternary compounds $Li_2O \cdot ZnO \cdot SiO_2$ and $4\ Li_2O \cdot 10\ ZnO \cdot 7\ SiO_2$ existed. The X-ray diffraction powder data of these ternary compounds was very similar. The pattern of $Li_2O \cdot ZnO \cdot SiO_2$ was indexed on the basis of a primitive tetragonal cell of parameter $a_o = 11.47$ Å , $c_o = 10.78$ Å , and that of $4\ Li_2O \cdot 10\ ZnO \cdot 7\ SiO_2$ on the basis of an orthorhombic cell of parameter $a = 7.93$ Å , $b = 9.13$ Å, $c_o = 12.80$ Å. A composition triangle diagram was published. The liquidus temperature of the compositions was not investigated and no optical properties of the ternary compounds were given.

II. EXPERIMENTAL WORK.

1. RAW MATERIAL.

Purest grade of lithium carbonate, zinc oxide and sand were used as the source of lithium oxide, zinc oxide and silica for the preparation of the specimens. Adequate quantities of raw material were obtained at the start of the present work to ensure the uniformity of the raw material.

Lithium carbonate of reagent grade was not available, so chemically pure grade was used. The analysis given by the supplier J. Preston Ltd., is as follows:

Moisture	less than 1.5%
Analysis on dry sample:	
Li_2CO_3	not less than 98.5%
AS_2O_3	less than 5 p.p.m.
Pb	less than 10 p.p.m.
Cl, Ca, Mg, SO_4	Passes agreed tests in B.P.C.49

The moisture content was redetermined and found to be 0.13%. The lithium content was determined by flame photometer technique and found to be 99.2% expressed as lithium carbonate. This factor was used for correction.

Through the generosity of Amalgamated Oxide Ltd., chemically pure zinc oxide was received with a limit chemical analysis as follows:

Moisture	0.05 - 0.15%
Analysis on dry sample:	
Zinc oxide ZnO	99.90 - 99.75%
Silica and insoluble matter	Nil - Trace
Lead oxide PbO	0.025% max.
Cadmium Oxide CdO	0.002 - 0.008%
Copper Oxide CuO	0.002%
Ferric Oxide Fe_2O_3	Nil - 0.0015%
Alumina Al_2O_3	Nil
Manganous Oxide MnO	0.0002%
Lime CaO	Nil
Chlorine Cl_2	Nil
Sulphur Trioxide SO_3	0.01 - 0.015%
Arsenic	2 pts./million

The moisture content was redetermined and found to be 0.10%. No other chemical analysis was done. The moisture content was used for correction.

Belgium sand was used as the source of silica. It was first digested with concentrated hydrochloric acid over a steam bath for longer than sixteen hours and then washed with distilled water until free of chloride and dried. The purity as determined by the hydrofluoric decomposition method was found to be 99.9%. The moisture content was found to be 0.01%.

All the compositions were calculated to be correct to 0.001%. The raw materials necessary to give forty or fifty grammes of specimen were weighed on an analytical balance. Obviously, the composition of the finished specimen would not be accurate to this order due to loss in handling of the raw material and during melting. However, it was felt that it would be advisable to eliminate any possible additional error, because not much extra work was necessary to achieve this order of accuracy in calculation and weighing.

2. MELTING TECHNIQUE.

(1) Furnace.

Most of the compositions were melted in a normal Silit Rod vertical furnace with maximum working temperature of 1500°C. During the first part of the work, the temperature of this furnace was controlled by a transformer and a rheostat; later, a Cambridge mechanical controller was added. Several compositions with high founding temperatures were melted in a platinum-rhodium wound vertical furnace. This furnace was controlled by a Variac, a rheostat, and a Cambridge optical controller, and had been operated up to 1650°C.

(2) Preliminary Work.

Before preparing specimens for the actual measurement of liquidus temperature, the melting behaviour of this system was surveyed, as it is known that a substantial amount of zinc oxide is quite difficult to incorporate into ordinary commercial glasses and that lithium glasses have a very strong tendency to devitrify.

Owing to the large number of compositions necessary to establish the phase diagram, it was not practical to analyse all the specimens. Therefore a melting technique with minimum

volatile loss had to be developed. The technique of putting the raw material into the furnace at the founding temperature was tried, and found to be unsuitable because of the very high and variable loss by volatilisation. To avoid this uncontrolled loss of raw material due to vigorous chemical reaction between the raw material at high temperature, the technique used by previous workers in the Department investigating the liquidus temperature of glasses, was used. The procedure consists of sintering the raw material at a low temperature (e.g. about 800°C) up to six hours and subsequently melting the partially reacted material at higher temperature with the aid of a mechanical stirrer. This worked fairly well with low zinc oxide glass, but considerable unexpected difficulties of segregation were encountered in melting high zinc oxide compositions in the preliminary work stage. Even the mechanical stirrer did not improve the homogenity to a sufficiently high standard. The main difficulty was that some material stuck on the side wall of the platinum crucible. When the sintered material was put into the melting furnace, a fair amount of material was partly melted and stuck on the side wall of the crucible. Later the bulk of the material melted down and left some material stuck onto the side wall unmelted. Therefore some modifications were introduced. Also it was found that the glasses attacked the platinum crucible slightly. However the attack was so slight that platinum crucibles were used throughout this study.

(3) Melting Procedure.

The modified procedure of melting was to sinter the mixed raw material in platinum crucible at 750° to 900°C. according to the composition for up to six hours. The raw material became a loosely bound mass, which was crushed inside the crucible, and then packed into cone shape to minimise the

contact area with the side wall. This would reduce the volume of the sintered mass into about one half. The sintered material was put into the melting furnace at about 1000° to 1100°C. and the temperature of the furnace was then raised to the required founding temperature. When sufficient melt was formed, a mechanical stirrer was lowered to stir the melt continuously until a homogenous specimen was obtained. The specimen was cast into rod form and annealed at about 500°C. in a muffle furnace. The tendency to crystallization was very high. A number of specimens partly devitrified after casting. The stirrer was a refractory rod covered by a platinum shield and driven by a motor.

Occasionally, a small amount of partially melted material was found on the side wall of the crucible, when very high percentage of zinc oxide glasses were melted. The crucible was taken out of the furnace and tilted to get some of the melt onto the partially melted material. Shortly afterwards the crucible was put back into the furnace, stirring was started while the melt was still fairly viscous. This normally would eliminate any partially melted material on the side wall. Most of the compositions were melted at 1300° to 1400°C for up to six hours with continuous stirring. The melting temperature was kept low and time was kept short to minimise the loss by volatilisation. The melt was normally fairly fluid, so the specimen was homogeneous as was confirmed by reproducibilities of the liquidus temperature determinations. Either forty or fifty gramme of specimen was melted for each composition. The amount of glass needed for the determination of liquidus temperature was small but it was easier to obtain more homogeneous specimens with a bigger melt than with a few grammes. Some of the specimen rods were used, to study the crystallization characteristics. The specimens of about twenty compositions were weighed with the platinum crucible and platinum stirrer shield. By comparing with the weight expected, it was found that less than 0.2% of

weight loss occurred in most cases, with maximum loss of 0.5% in one case. Therefore the calculated composition of most specimens would be correct to ± 0.2% with a few extreme cases of ± 0.5%. The loss of zinc oxide seemed to be higher than that of the lithium oxide, as specimens containing high zinc oxide tended to have higher loss. It was felt that this technique of preparation of specimens was satisfactory for the present study.

3. Heat treatment.

(1) Apparatus.

For the liquidus temperature determination by quenching technique, a constant temperature furnace is normally used, but this method is very time consuming. It is found from previous work done in the Department that a vertical gradient furnace is much more efficient. However the original vertical gradient furnace was a nichrome-wound furnace with a maximum working temperature about 1100°C. Judging from the phase diagrams of the binary systems, the liquidus temperatures of some of the compositions in the system were expected to be higher than 1100°C, therefore a special Pt-Rh wound vertical gradient furnace was made, the construction of which was shown diagramatically in Fig. IIIa and IIIb. To obtain the desired temperature gradient, the furnace was rewound three times. Finally, the temperature range of the lower six specimen cones was about 50°C at 1000°C. The furnace was balanced by counterweight and could be lowered quickly to chill the specimen.

The specimen holder was made of a thermocouple grade Pt-Rh wire. Nine loops of the same type of wire were welded at one inch apart onto the vertical wires. An insulated thermocouple grade platinum wire was welded on the middle of each loop to form a thermocouple at each loop. These thermocouples passed through the refractory stopper of the furnace and were soldered to compensating leads in an insulated box situated above the refractory stopper. Following an

FIG 3a QUENCHING FURNACE UNIT.

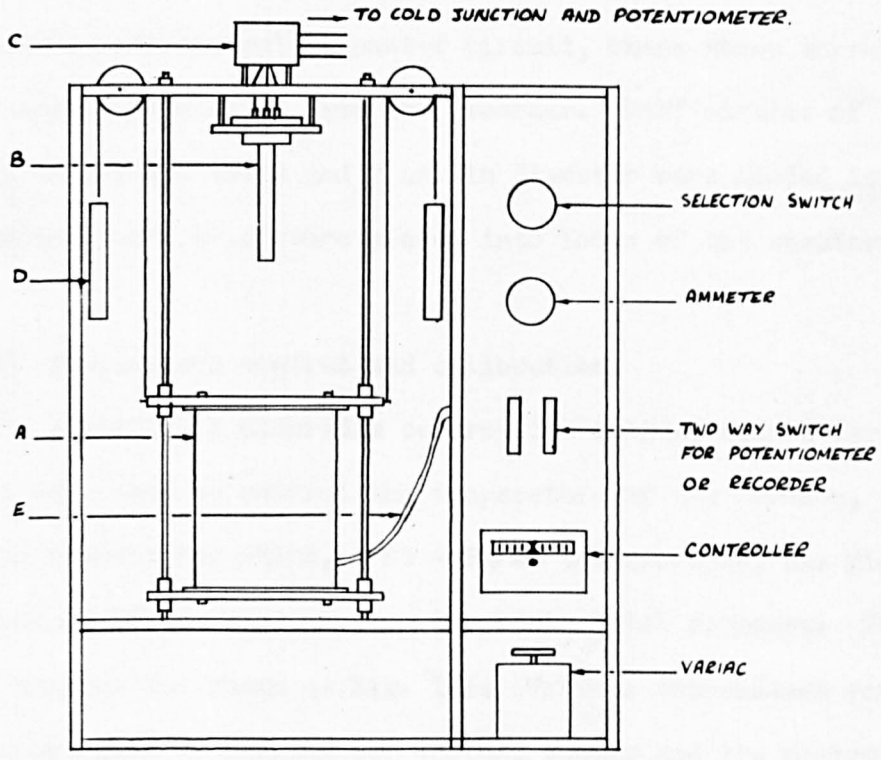

FIG 3b. SPECIMEN HOLDER.

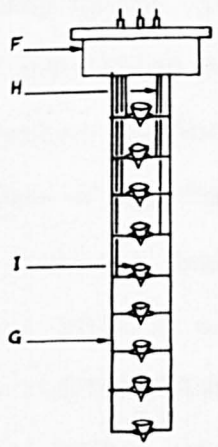

A GRADIENT FURNACE.
B SPECIMEN HOLDER.
C JUNCTION BOX.
D COUNTER WEIGHT
E POWER & CONTROL-COUPLE. LEADS TO FURNACE.
F REFRACTORY STOPPER.
G Pt/13% Rh WIRE FRAME
H Pt WIRE (ONE SIDE OF THE THERMOCOUPLE
I SPECIMEN CONE

ice-junction, the thermocouples were connected by copper leads to a ten point selection switch which was used to connect each thermocouple to the usual potentiometer, and galvanometer circuit for temperature measurement. Also three thermocouples could be connected to a Cambridge multi-point temperature recorder so that permanent records were obtained for each experiment over the whole duration of heat treatment. When the temperature of the specimens was measured with the potentiometer circuit, these three thermocouples were disconnected from the recorder. Half circles of platinum of 0.1 mm. thick and 2 cm. in diameter were folded into the specimen cones which were placed into loops of the specimen holder.

(2) Temperature control and calibration.

A Variac, a Cambridge centre-line optical controller and a rheostat were used to control the temperature of the furnace, the detecting element for which, a Pt - Pt/Rh thermocouple, was placed very close to the furnace winding to obtain quick response. The circuit diagram was shown at Fig. III. Various temperature ranges could be obtained by varying the voltage supply and the control point in the Cambridge centre-line controller. With proper combination of the setting in the Variac and rheostat, the temperature of the furnace could be controlled to within $\pm$ 2°C. During the course of the work, the controller did not function very well several times, and the temperature of the furnace fluctuated up to $\pm$ 5°C. As soon as the control limit was found to increase beyond $\pm$ 3°C, the controller was readjusted until it achieved the best performance.

The thermocouples in the specimen holder assembly were initially calibrated by inserting a standard thermocouple into each specimen cone in turn. For the seven lower thermocouples, the maximum difference between the standard thermocouple and the corresponding thermocouple in the specimen holder assembly was less than 3°C, with

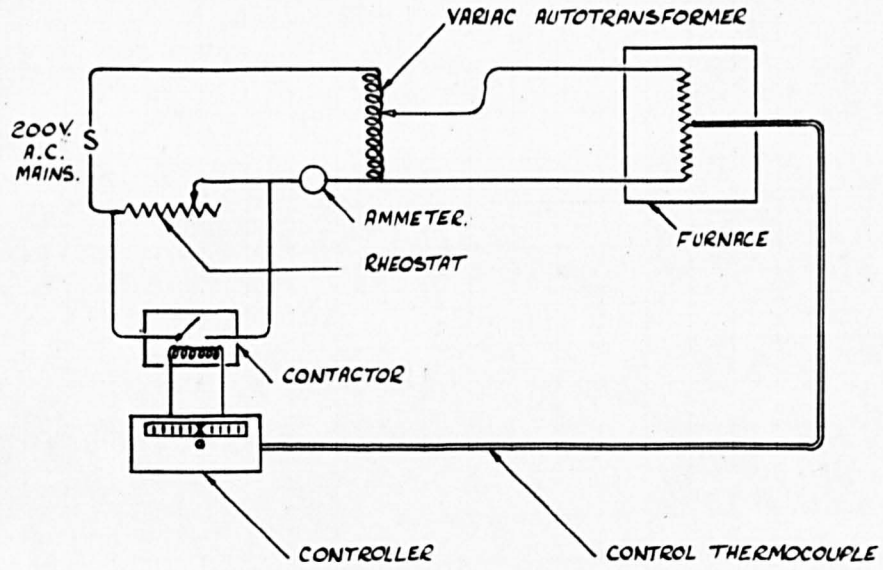

FIG 3c TEMPERATURE CONTROL CIRCUIT.

the error for the middle one of about 1°C. The top thermocouple was found to give a temperature about 15°C higher than thatof the standard thermocouple, and the second one about 10°C higher. The temperature gradient of this part of the furnace was very steep, and heat might be conducted from the hot zone of the furnace along the thick Pt-Rh wire frame to the top two thermocouples so that they registered higher temperatures. Therefore the top position was not used and the second one was used only on exploratory runs. Since it was not attempted to determine the liquidus temperature with an accuracy of better than ± 5°C, it was felt that the present design did not introduce any significant error in establishing the phase diagram.

After the specimen holder had been properly wired up into the heat treatment unit, it was not possible to calibrate the thermocouples periodically by the same technique. Therefore three glasses, the liquidus temperatures of which were determined in the first month of the present work to an accuracy of ± 2°C, were used to re-calibrate the thermocouples every two months. The liquidus temperatures of these three glasses were redetermined and found to be within ± 3°C of the original data. Although the appearance of the thermocouples was affected by heat, the calibration did not change.

(3) Determination of liquidus temperature.

The quenching technique was used to determine the liquidus temperatures of compositions inside the glass forming region and was described in this section. For compositions just outside the glass forming region, a hot stage microscope was used. The construction of this hot stage microscope and the experimental procedure was described in the sections about the study of rate of crystal growth.

In the quenching technique, the specimen rod was crushed into small pieces. Several pieces of the glass being investigated, were placed in each of the platinum specimen cones. The weight of each

was up to 0.2 gm. After the heat treatment furnace had attained a steady condition of the desired temperature range, the furnace was raised to the upper position to heat treat the specimens. The temperatures of the top, the middle and the bottom cones were recorded with a multi-point recorder. A potentiometer was used to measure accurately the temperature of each specimen for five or six times over the heat treatment period. The mean temperature was taken as the temperature of the specimen. The fluctuation of the specimen temperature was assessed by measuring the temperature continuously for three control cycles, the two extremes were taken as the range of fluctuation. After the predetermined time of heat treatment had elapsed, the furnace was lowered and the specimens were chilled in air. The time taken for the specimen to cool from 1200°C to below 500°C was less than 15 seconds. Normally, no secondary growth was found in the specimen, although the glasses in this system had a high tendency to devitrify.

After the cones were cooled, they were unfolded to release the specimens, which were examined by petrological microscope and X-ray diffraction. The specimen cones were reformed after they were cleaned in hydrofluoric acid and hydrochloric acid. Each cone could be re-used for about ten times. In this way, a range of temperature was covered by each experiment and each specimen was subjected to individual heat-treatment. When the selected temperature range was correct, the liquidus temperature of that specimen could be determined to ± 5°C. at once. If one experiment could not yield the liquidus temperature to the desired accuracy, then further experiments were done on different temperature ranges. Normally two or three experiments were necessary to determine the liquidus temperature. When it was necessary to determine the liquidus temperature more accurately, e.g. those compositions used for re-calibration of the thermocouples, additional experiments were done to narrow the limits.

The duration of heat treatment ranged from one hour to six hours. When there were no other experimental complications, longer heat treatment time was normally used to ensure equilibrium condition. The minimum time necessary to obtain equilibrium was determined by approaching the equilibrium condition from both directions for selected compositions in different composition ranges, instead of for each composition. Part of the specimen was heat treated at about 900°C to 950°C overnight to devitrify the specimen completely. These devitrified samples were then heat treated for different times. Some specimens of the same composition in the glass state were also heat treated for different times. Both sets of the specimen were examined for crystals. For most compositions, these two sets of specimens would yield the same liquidus temperature within experimental error after half an hour of heat treatment. This did not prove conclusively that these specimens had reached equilibrium because the amount of crystals present, which was not determined, in corresponding specimens might not be exactly the same. However, it was felt that the specimen used to establish the liquidus temperature should have reached equilibrium condition because they were held at temperatures for at least one hour and normally for six hours.

Although the work seemed to be routine, some experimental difficulties were encountered. One of which was due to the characteristics of the controller used. At the initial stage of the heat treatment, the temperature of the furnace dropped about 15°C, as soon as the specimen holder was inside the furnace. The temperature of the furnace normally overshot the control temperature for about 15°C, when the temperature was brought back to the control temperature from lower temperature. The temperature of the furnace would eventually be brought back to the control temperature at about one and half hours' time. This would subject the specimen to varying heat treatment. This difficulty was overcome by setting

the control temperature about 15°C higher than the desired control temperature before the specimen was heat treated. Immediately after the furnace was raised the control point was reset to the desired control temperature. The initial temperature of the specimen would be up to 5°C lower than the desired temperature but the specimens would attain the desired temperature in less than ten minutes without overshooting the control point. With suitable adjustment, the specimens would reach the desired temperature and maintain the steady state within two minutes after the beginning of heat treatment.

In some of the compositions with $Li_2O \cdot ZnO \cdot SiO_2$ or zinc orthosilicate as primary phase crystal, over a range of temperature, crystals were found to be at the bottom of the specimen with clear glass at the top. When these specimens were examined under a microscope, a secondary growth of crystal seemed to be present. These phenomena were found in large specimens heat treated for a long time. As this segregation of crystals might cause errors in the liquidus temperature, additional experiments were done on smaller specimens with successively shorter heat treatment time until the crystals in the specimen were distributed more or less uniformly. Some errors were found in the early liquidus temperature results, all these were redetermined. The segregation of crystal in the bottom of the specimen might be due to the high density of these crystals compared with that of the melt. At high temperature the melt was not very viscous, therefore the crystals formed would gradually sink to the bottom. This would cause inhomogenity and error in the determination of the liquidus temperature.

Surface devitrification possibly due to volatilization at the surface were found in some compositions with high silica. Redeterminations were done with shorter heat treatment time for all these compositions. Some errors were found in the early results in the identification of the primary phase crystals in the composition very near the primary phase boundary time.

4. Examination of heat treated specimen.

(1) Optical method.

The chilled specimen was crushed into smaller pieces in a percussion mortar. Pieces from a different part of the specimen were examined with a petrological microscope to find whether any crystalline phase was present. The distribution of the crystalline phase was also investigated to see if surface devitrification occurred and whether the crystalline phases segregated from the melt.

In the early stage of the work only X-ray diffraction was used to identify the crystalline phases present in the specimen. However, X-ray diffraction was not very sensitive to low percentages of crystals, especially tridymite. Therefore specimens heat treated at up to 50°C below the liquidus temperature had to be used to get identifiable amounts of crystal. When the composition being investigated was near the phase boundary line, secondary crystals were normally present in specimens heat treated much below the liquidus temperature. This made the identification of the primary phase crystal very difficult. Therefore a petrological microscope was also used in conjunction with the X-ray diffractometer.

In the petrological microscope examination, crushed pieces were immersed in liquids of known refractive indices. The growth habit and birefringence of crystals were noted. The crystal habits of some crystals changed with the composition of the specimen, therefore the refractive indices of the crystalline phases were determined by the Beche line technique. In this technique, an individual crystal in contact with the immersion liquid was focused accurately and the body of the microscope was raised slowly from the focused position. A line of light, called the Becke line, following the contours of the crystal would move from the medium of the lower refractive index to that of higher index. By using liquid of different refractive indices, the refractive indices of the crystal could be determined to an accuracy

of ± 0.003. The crystals present were normally very small, so accurate determination of refractive indices by Beche line technique was not easy. When the difference of refractive indices of two phases under examination increased, it was easier to see the Beche line. Therefore instead of using immersion liquid with refractive index very close to the crystals, liquids with refractive index in between the expected primary phases were used to differentiate the crystal in the specimen. From data in the previous experiment, it was normally possible to predict the crystalline phases. All the heat treated specimens were examined optically. The refractive indices of the primary phase in at least one specimen for each composition were measured accurately. The liquidus temperature of the secondary crystal was also determined in some compositions.

(2) X-ray diffraction.

To avoid any possible error in the identification of the crystalline phase and to confirm the results in the optical microscope determination, X-ray diffraction was used extensively. The X-ray instrument, manufactured by Solus-Schell Ltd., was equipped with a 9 cm. camera and a diffractometer. To obtain higher accuracy, the diffractometer was used. Throughout the present work, a copper target tube, giving nickel filtered copper k_α radiation was used. 50 kv 20 ma was used. A powdered quartz specimen was used to check the aligrment of the diffractometer periodically.

The crushed specimen was ground in an agate mortar into fine powder. An aluminium holder with a hole of 1 x 1½ x $\frac{1}{5}$ cm was used. A piece of microscopic slide glass was placed under the aluminium holder, and the powdered specimen was packed evenly in the hole. Another glass slide was stuck on top of the aluminium holder to give some support to the powdered sample. The glass slide under the aluminium holder was then removed and the surface of the powdered specimen originally in contact with this glass slide was used for X-ray diffraction work. This method of packing the powdered specimen

was preferred to that by rubbing flat the surface of the specimen with a glass slide, because rubbing the surface tended to encourage preferential orientation of the crystals in the specimen. With the present method of packing, a very smooth surface with more randomly orientated crystals could be obtained.

Specimens heat treated at about 30°C below the liquidus temperature were used. The powdered specimen was scanned at 1°/min from 5° - 45° θ automatically with a geiger counter. A trace was obtained from the recorder. These traces were compared with those obtained from specimens specially prepared as standards. If the amount of the crystal in the specimen was not high enough to permit conclusive identification, a different setting in the diffractometer was used. If it was still not possible to identify the crystalline phase, specimens heat treated at successively lower temperatures were used, until the primary phase was identified. On the other hand if two crystalline phases were found, then specimens heat treated at higher temperatures were used until only one crystalline phase was found to be present.

Not all the heat treated specimens were examined by X-ray diffraction. Normally when the result from one specimen identified the primary phase crystal conclusively, the other specimen of the same composition was not examined by X-ray diffraction. With compositions near the boundary line, it was not possible to identify conclusively the primary phase crystal by X-ray diffraction work, then reliance was placed on the result from the petrological microscopic examination alone.

During the course of the work, solid solution was found to be present in $Li_2O \cdot 2nO \cdot SiO_2$ crystals. All the X-ray diffraction traces were checked for shift of peak position. Whenever there was any doubt, the specimen was scanned minute by minute manually over the strong peaks to obtain conclusive results. This was found necessary, because the recorder drum in the recorder was driven by friction and

slight slipping would introduce error. Also the time constant of counter affected the peak position slightly. The relative intensities of the peaks were normally obtained from the trace.

The X-ray diffraction patterns of the specimens were compared with those of specially prepared standards. These standards were prepared from the same raw materials and melted by the same technique. However the homogeneous melts of the standardswere held at suitable temperatures to crystallise and then chilled rapidly to room temperature instead of pouring into rods and then annealing as the other compositions. The standards were examined under the microscope and no glassy phase was detected. Therefore these standards were pure. The melting temperature and the crystallization temperature were listed in Table I.

TABLE I

THERMAL HISTORIES OF VARIOUS STANDARDS.

STANDARD	MELTING TEMPERATURE	CRYSTALLIZATION TEMPERATURE	CRYSTALLIZATION TIME
Lithium disilicate	1300°C	1000°C	Four hours
Lithium metasilicate	1300°C	1150°C	Three hours
Lithium Orthosilicate	1400°C	1200°C	Seven hours
Zinc Orthosilicate	1550°C	1450°C	Six hours
$Li_2O \cdot ZnO \cdot SiO_2$	1550°C	1400°C	Six hours
$2\ Li_2O \cdot 4\ ZnO \cdot 3\ SiO_2$	1550°C	1350°C	Six hours

Attempts had been made to prepare pure tridymite from quartz or precipitated silica, but small amounts of either quartz or crystobalite was found in the specimen.

The X-ray diffraction patterns of the lithium orthosilicate standard and the zinc orthosilicate standard were found to agree with that in the X-ray Powder Data File. However, it was found that the data of lithium disilicate and lithium metasilicate in the X-ray

Powder Data File contained several lines which were not found in the X-ray pattern of the present standard. Later it was possible to identify these extraneous lines in the X-ray Powder Data File. More detailed information is given in the discussion section.

III. RESULTS AND DISCUSSION.

1. General.

About one hundred compositions were prepared and investigated. The calculated compositions in mole percent and weight percent were listed in Table II. The compositions were calculated to give the exact mole percent, and the weight percent data was given to two decimal places, because the actual compositions of the specimens did not warrant any higher accuracy. The refractive index of the chilled specimen which formed glasses were also listed in Table II against the corresponding compositions.

The investigated compositions were plotted in Fig. 4, with boundary curves and primary phase fields. The composition triangles and the glass forming region limits were plotted on Fig. 5. Fig. 9 was a plot of the isofracts in the glasses forming region. The isofracts were derived from data given in Table II.

In Fig. 6, isotherms had been added to the ternary system and the compositions had been omitted. The essential data from which Fig. 6 and 9 were drawn, was given in Table II. By employing the vertical gradient furnace, more than 2000 specimens were quenched. Not all of the data was listed in Table II, because most of it was not essential for the construction of the phase diagram.

Tridymite, lithium disilicate, lithium metasilicate, zinc orthosilicate and two new ternary compounds with the compositions of $Li_2O \cdot ZnO \cdot SiO_2$ and $2Li_2O \cdot 4ZnO \cdot 3SiO_2$ were found as primary phases. Although the high temperature form of silica, cristobalite were not found as primary phase crystal in the composition investigated, cristobalite would be the primary crystal in glasses having a high percentage of silica. Therefore it was added in the phase diagram.

FIG. 1.

THE SYSTEM Li_2O-ZnO-SiO_2
SHOWING CRITICAL COMPOSITIONS.

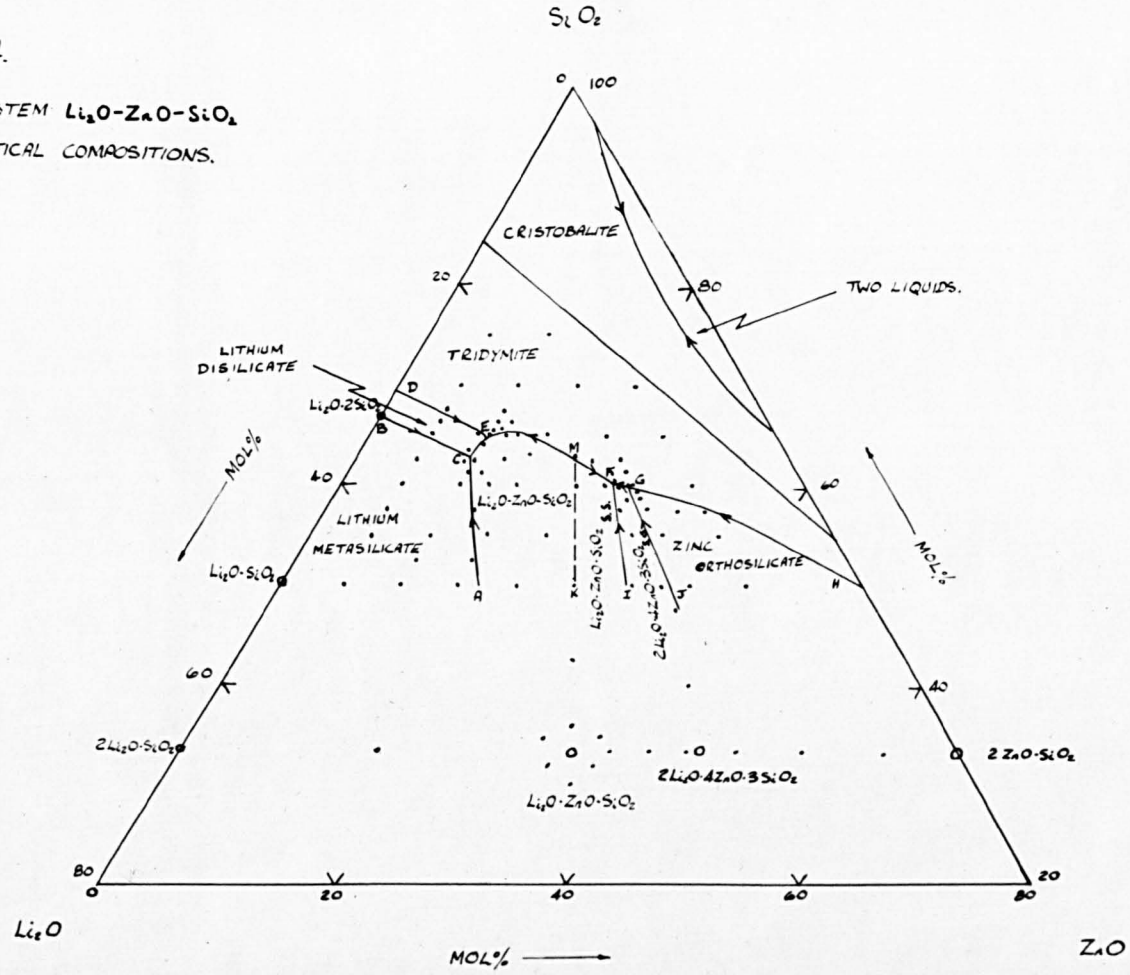

FIG 5

COMPOSITION TRIANGLES AND GLASS FORMING REGION LIMIT OF THE SYSTEM $Li_2O-ZnO-SiO_2$

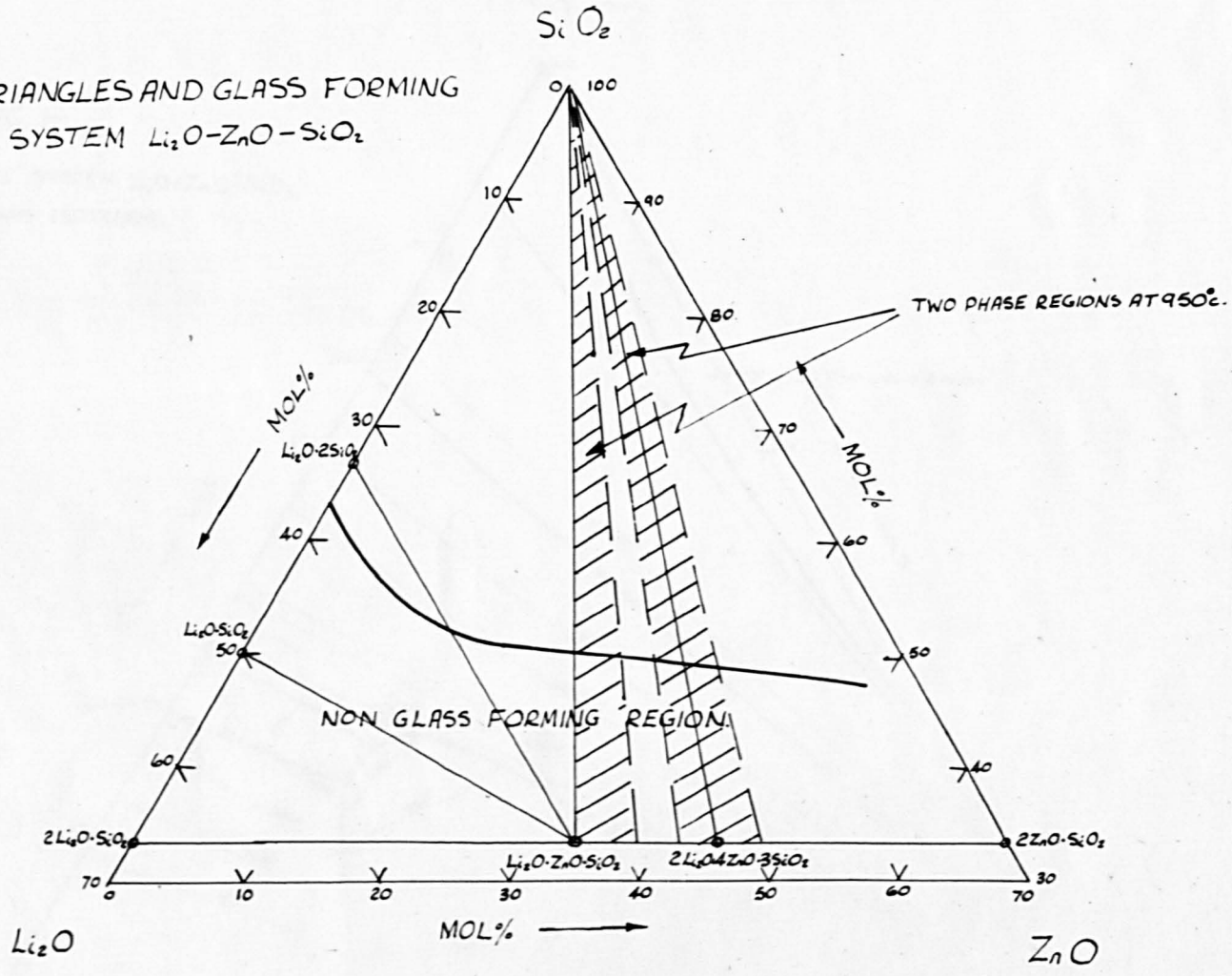

FIG. 6.

THE SYSTEM Li_2O-ZnO-SiO_2
SHOWING ISOTHERMS.

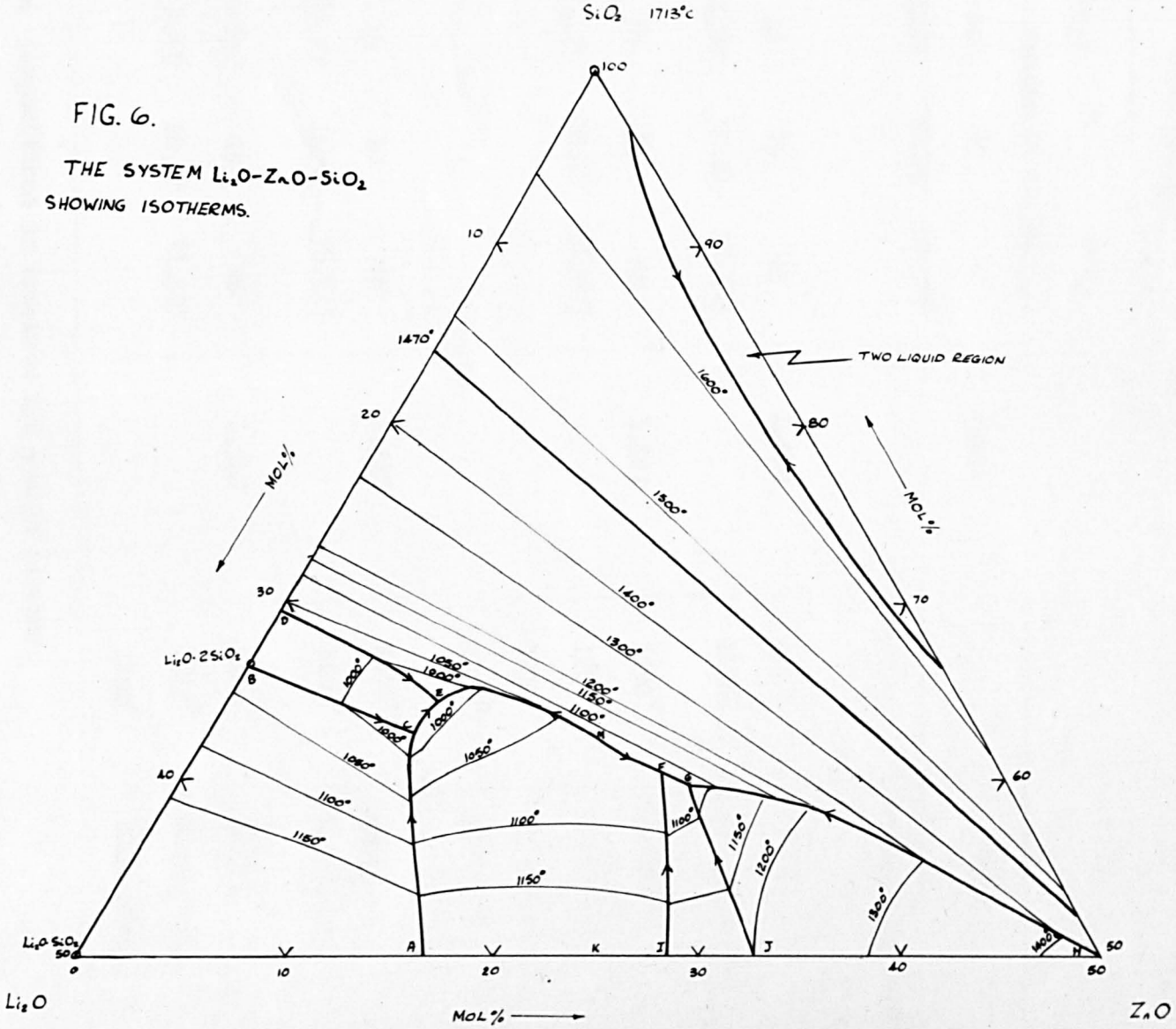

Table 2

Compositions and refractive indices of specimens investigated and quenching data

Composition ¥			Refractive Index of Glass	Temperature (°C)	Phases present ¥
Li_2O	ZnO	SiO_2			
Tridymite field.					
10	20	70	1.552	1415°	Glass
(4.87	26.54	68.59)		1390°	Glass, Trid.
				1200°	Glass, Trid.
10	25	65	1.570	1127°	Glass
(4.79	32.61	62.60)		1120°	Glass Trid.
10	30	60	1.587	1290°	Glass
(4.71	38.47	56.82)		1280°	Glass, Trid.
				1210°	Glass, Trid.
				1170°	Glass, Trid. & S.
15	10	75	1.533	1430°	Glass
(7.77	14.11	78.12)		1400°	Glass, Trid.
15	15	70	1.547	1360°	Glass.
(7.63	20.78	71.59)		1350°	Glass, Trid.
				1100°	Glass, Trid.

¥ Compositions in brackets are weight percent.

Trid. = Tridymite
LDS = Lithium disilicate
IMS = Lithium metasilicate
ZS = Zinc orthosilicate
A = $Li_2O \cdot ZnO \cdot SiO_2$
A_{ss} = $Li_2O \cdot ZnO \cdot SiO_2$ solid solution
B_{ss} = $2Li_2O \cdot 4ZnO \cdot 3\ SiO_2$ solid solution
NGF = non glass forming.

Composition			Refractive Index of Glass	Temperature (°C)	Phases present
15	20	65	1.560	1234°	Glass
(7.49	27.21	65.30		1228°	Glass, Trid.
				1138°	Glass, Trid.
15	22.5	62.5	1.570	1196°	Glass
(7.43	30.31	62.26		1182°	Glass, Trid.
				1074°	Glass, Trid.
				1060°	Glass, Trid, B_{ss}
15	23.75	61.25	1.577	1142°	Glass.
(7.39	31.87	60.74)		1137°	Glass, Trid.
				1104°	Glass, Trid.
				1086°	Glass, Trid, ZS.
15	25	60	1.580	1127°	Glass
(7.36	33.42	59.22)		1111°	Glass, Trid.
				1096°	Glass, Trid.
				1087°	Glass, Trid, ZS.
16.25	22.5	61.25	1.575	1130°	Glass.
(8.12	30.49	61.39)		1120°	Glass, Trid.
				1080°	Glass, Trid.
				1065°	Glass, Trid, B_{ss}
16.5	23	60.5	1.573	1060°	Glass
(8.24	31.25	60.52)		1050°	Glass, Trid.
				1040°	Trid, A_{ss}, B_{ss}

Composition			Refractive Index of Glass	Temperature (°C)	Phases present
17.5	20	62.5	1.570	1125°	Glass
(8.87	27.56	63.57)		1120°	Glass, Trid.
				1043°	Glass, Trid.
				1026°	Glass, Trid., A_{ss}
18.5	18.5	63	1.565	1111°	Glass
(9.46	25.76	64.78)		1105°	Glass, Trid.
				1090°	Glass, Trid.
20	5	75	1.525	1330°	Glass
(10.84	7.38	81.78		1320°	Glass, Trid.
				1125°	Glass, Trid.
20	10	70	1.537	1238°	Glass
(10.64	14.49	74.88)		1231°	Glass, Trid.
				1115°	Glass, Trid.
20	15	65	1.555	1126°	Glass
(10.44	21.33	68.23)		1114°	Glass, Trid.
				1030°	Glass, Trid.
				995°	Glass, Trid., A.
22.5	10	67.5	1.543	1133°	Glass
(12.15	14.69	73.16)		1122°	Glass, Trid..
				1005°	Glass, Trid.
22.5	11.25	66.25	1.550	1030°	Glass
(12.11	16.40	71.50)		1025°	Glass, Trid.
				985°	Glass, Trid.
				976°	Glass, Trid., A.

Composition			Refractive Index of Glass	Temperature (°C)	Phases present
23.75	10	66.25	1.548	1061°	Glass
(12.91	14.79	72.30)		1052°	Glass, Trid.
				1013°	Glass, Trid.
23.75	10.625	65.625	1.549	1047°	Glass
(12.86	15.67	71.47)		1025°	Glass, Trid.
				1015°	Glass, Trid.
				973°	Glass, Trid., A.
24.375	10	65.625	1.549	1036°	Glass
(13.28	14.84	71.89)		1027°	Glass, Trid.
				1005°	Glass, Trid.
25	5	70	1.532	1139°	Glass
(13.94	7.57	78.49)		1137°	Glass, Trid.
				1016°	Glass, Trid.
				991°	Glass, Trid., LDS.
25	10	65	1.549	1014°	Glass
(13.66	14.89	71.45)		1002°	Glass, Trid.
				997°	Glass, Trid.
27.5	5	67.5	1.540	1040°	Glass
(15.57	7.70	76.74)		1037°	Glass, Trid.
				1024°	Glass, Trid.
				1007°	Glass, Trid., LDS.

Composition			Refractive Index of Glass	Temperature (°C)	Phases present
Lithium disilicate field.					
26	9	65	1.550	984°	Glass
(14.35	13.53	72.13)		969°	Glass,LDS.
				960°	Glass,LDS,Trid.
27.5	9	63.5	1.552	980°	Glass
(15.35	13.65	71.00)		970°	Glass,LDS.
					Glass,LDS, A.
28.5	5	66.5	1.540	989°	Glass
(16.21	7.74	76.05)		984°	Glass,LDS.
				979°	Glass,LDS,Trid.
30	5	65	1.545	1012°	Glass
(17.21	7.81	74.98)		1008°	Glass,LDS.
				976°	Glass,LDS.
Lithium metasilicate field.					
28.5	9	62.5	1.552	980°	Glass
(15.95	13.72	70.34)		970°	Glass,LMS.
				960°	Glass,LDS,Trid.
28.75	10	61.25	1.556	1004°	Glass
(16.06	15.20	68.73)		995°	Glass,LMS.
				988°	Glass,LMS.
				970°	Glass,LMS, A.
30	10	60	1.560	1044°	Glass
(16.86	15.31	67.83)		1039°	Glass,LMS.
				1007°	Glass,LMS,A.
				970°	Glass,LDS,A.

Composition			Refractive Index of Glass	Temperature (°C)	Phases present
32.5	5	62.5	1.549	1041°	Glass
(18.94	7.93	73.13)		1037°	Glass,IMS.
				1004°	Glass,IMS.
				984°	Glass,IMS,LDS.
32.5	12.5	55	1.570	1157°	Glass
(18.39	19.14	62.47)		1146°	Glass,IMS.
				1003°	Glass,IMS, A.
32.5	15	52.5	1.580	1169@	Glass
(18.19	22.84	58.78)		1167°	Glass,IMS.
				1153°	Glass,IMS, A.
35	5	60	1.553	1096°	Glass
(20.68	8.05	71.28)		1079°	Glass,IMS.
				1005°	Glass,IMS.
35	10	55	1.567	1180°	Glass
(20.25	15.76	63.99)		1176°	Glass,IMS.
				1129°	Glass,IMS.
				1102°	Glass,IMS.
35	15	50	NGF	1170°	Glass
(19.84	23.16	57.00)		1150°	Glass,IMS.
37.5	5	57.5	NGF	1155°	Glass
(22.52	8.17	69.32)		1140°	Glass,IMS.
37.5	10	52.5	NGF	1180°	Glass
(22.05	15.99	61.96)		1170°	Glass,IMS.

Composition			Refractive Index of Glass	Temperature (°C)	Phases present
40	5	55	NGF	1160°	Glass
(24.36	8.29	67.35)		1150°	Glass,LMS.
40	10	50	NGF	1185°	Glass
(23.84	16.23	59.93		1170°	Glass,LMS.
45	5	50	NGF	1200°	Glass
(28.27	8.56	63.17)		1180°	Glass,LMS.
Zinc Orthosilicate Field.					
10	32.5	57.5	1.595	1267°	Glass
(4.67	41.33	54.00)		1259°	Glass,ZS.
				1200°	Glass,ZS,Trid.
10	35	55	1.601	1290°	Glass
(4.63	44.15	51.22)		1275°	Glass,ZS.
				1259°	Glass,ZS.
				1210°	Glass,ZS,Trid.
10	40	50	1.610	1330°	Glass
(4.56	49.63	45.81)		1310°	Glass,ZS.
12.5	30	57.5	1.590	1213°	Glass
(5.96	38.94	55.10)		1195°	Glass,ZS.
				1150°	Glass,ZS,Trid.
15	25.625	59.375	1.583	1103°	Glass
(7.35	34.18	58.48)		1099°	Glass,ZS.
				1078°	Glass,ZS.
				1059°	Glass,Trid., B_{ss}.

Composition			Refractive Index of Glass	Temperature (°C)	Phases present
15	26.25	58.75	1.583	1119°	Glass
(7.33	34.92	57.75)		1106°	Glass, ZS.
				1087°	Glass, ZS.
15	27.5	57.5	1.588	1140°	Glass
(7.30	36.42	56.29)		1127°	Glass, ZS.
				1088°	Glass, ZS.
15	30	55	1.593	1165°	Glass
(7.24	39.41	53.35)		1156°	Glass, ZS.
				1101°	Glass, ZS.
15	35	50	1.605	1251°	Glass
(7.12	45.20	47.68)		1248°	Glass, ZS.
				1185°	Glass, ZS.
15.625	25	59.375	1.580	1089°	Glass
(7.69	33.52	58.79)		1082°	Glass, ZS.
				1069°	Glass, ZS.
				1049°	Glass, Trid., B_{ss}.
$Li_2O \cdot ZnO \cdot SiO_2$ Field.					
17.5	22.5	60	1.577	1074°	Glass
(8.81	30.66	60.53)		1063°	Glass, A_{ss}.
				1045°	A_{ss}, B_{ss}, Trid.
20	20	60	1.575	1076°	Glass
(10.25	27.91	61.84)		1058°	Glass, A.
				1040°	Glass, A.
				988°	A, Trid.

Composition			Refractive Index of Glass	Temperature (°C)	Phases present
20	25	55	1.585	1141°	Glass
(10.06	34.27	55.67)		1138°	Glass, A_{ss}.
				1068°	Glass, A_{ss}.
22.5	12.5	65	1.552	997°	Glass
(12.05	18.11	69.84)		991°	Glass, A.
				985°	Glass, A, Trid.
22.5	15	62.5	1.565	1034°	Glass
(11.92	21.61	66.46)		1026°	Glass, A.
				1013°	Glass, A.
				980°	Glass, A, Trid.
23.75	11.25	65	1.554	986°	Glass
(12.86	16.50	70.65)		984°	Glass, A.
				977°	Glass, A.
				965°	Glass, A, Trid.
				955°	A, Trid., LDS.
25	12.5	62.5	1.560	998°	Glass
(13.53	18.40	68.07)		980°	Glass, A.
				973°	Glass, A, Trid.
25	15	60	1.569	1066°	Glass
(13.40	21.90	64.70)		1061°	Glass, A.
				1029°	Glass, A.
25	20	55	1.583	1136°	Glass
(13.15	28.64	58.20)		1125°	Glass, A.
				1085°	Glass, A.

Composition			Refractive Index of Glass	Temperature (°C)	Phases present
25	25	50	1.593	1210°	Glass
(12.91	35.16	51.93)		1185°	Glass,A.
26	10	64	1.552	955°	Glass
(14.29	14.97	70.74)		953°	Glass,A.
				951°	A,Trid.,LDS.
27.5	10	62.5	1.552	986°	Glass
(15.26	15.10	69.64)		972°	Glass,A.
				964°	Glass,A,LDS.
27.5	11.25	61.25	1.555	1009°	Glass
(15.20	16.85	67.95)		1006°	Glass,A.
				986°	Glass,A.
				968°	Glass,A,LDS.
27.5	12.5	60	1.562	1093°	Glass
(15.13	18.61	66.26)		1079°	Glass,A.
				1059°	Glass,A.
30	12.5	57.5	1.565	1075°	Glass
(16.70	18.95	64.36)		1053°	Glass,A.
				1030°	Glass,A,IMS.
30	15	55	1.572	1156°	Glass
(16.53	22.51	60.95		1148°	Glass,A.
				1141°	Glass,A.
				1137°	Glass,A,IMS.
				1085°	Glass,A,IMS.

Composition			Refractive Index of Glass	Temperature (°C)	Phases present
30	20	50	1.587	1208°	Glass
(16.21	29.44	54.35		1195°	Glass, A.
$2\ Li_2O \cdot 4\ ZnO \cdot 3\ SiO_2$ Field.					
16.25	23.75	60	1.579	1072°	Glass
(8.08	32.04	59.88)		1064°	Glass, B_{ss}.
				1058°	Glass, B_{ss}, Trid.
16.25	25	58.75	1.583	1089°	Glass
(8.04	33.63	58.33)		1078°	Glass, B_{ss}.
				1056°	Glass, B_{ss}.
16.5	28.5	55	1.590	1142°	Glass
(8.06	37.92	54.03)		1126°	Glass, B_{ss}.
17.5	25	57.5	1.586	1096°	Glass
(8.71	33.84	57.44)		1083°	Glass, B_{ss}.
				1064°	Glass, B_{ss}.
				1048°	Glass, B_{ss}, Trid.
17.5	27.5	55	1.590	1142°	Glass
(8.65	36.84	54.51)		1140°	Glass, B_{ss}.
				1091°	Glass, B_{ss}.
17.5	32.5	50	1.600	1205°	Glass
(8.50	42.80	48.70)		1195°	Glass, B_{ss}.
				1068°	Glass, B_{ss}.
17.5	35	47.5	1.605	1270°	Glass
(8.42	45.76	45.82)		1260°	Glass, B_{ss}.
				1075°	Glass, B_{ss}.

Composition			Refractive Index of Glass	Temperature (°C)	Phases present
20	30	50	1.597	1201°	Glass
(9.89	40.40	49.71)		1192°	Glass, B_{ss}.
				1158°	Glass, B_{ss}.

(2) Composition triangle.

The composition triangles were established with X-ray diffraction data of specimen heat treated specially below the solidus temperature. The compositions of the specimens and the X-ray diffraction results were listed in Table 3, and the composition triangles were shown in Fig. 5. Specimens of selected compositions were heat treated at 950°C for at least twenty four hours. Parts of the specimens were examined under the microscope for the glassy phase. With some compositions, heat treatments up to forty eight hours were done to ensure complete crystallization.

In this series of experiments, cristobalite was found in some specimens. Since tridymite was the stable form of silica in this heat treatment temperature, these specimens were not in equilibrium as far as the silica phase was concerned. One of the specimens with cristobalite present was heat treated again at 950°C for six days. Most of the silica was then found to be tridymite. Also another specimen with cristobalite present was heat treated again at 850°C for twenty-four hours, and quartz was found to be the only form of silica present. In both cases, the other crystals found in the specimens were not affected. Therefore, the presence of cristobalite did not affect the state of the other crystals present in the specimen. The existence of cristobalite in the specimen after long time heat treatment might be due to the sluggishness of the conversion of the cristobalite form to tridymite form. Therefore, the presence of cristobalite did not affect the conclusion of the composition triangles.

Table 3

X-ray data of specimen heat treated at 940° - 950°C.

Composition (mol %)					Phases Present. *
Li_2O	ZnO	SiO_2	Li_2O-ZnO-SiO_2	2 ZnO. SiO_2	
10	30	60			S, ZS, B_{ss}.
10	35	55			S, ZS, B_{ss}.
15	30	55			S, B_{ss}.
16.25	25	58.75			S, A_{ss}, B_{ss}.
17.5	22.5	60			S, A_{ss}.
17.5	27.5	55			S, A_{ss}.
17.5	35	47.5			S, B_{ss}.
20	15	65			S, A, IDS.
20	25	55			S, A_{ss}.
20	30	50			S, A_{ss}, B_{ss}.
25	15	60			S, A, IDS.
25	20	55			S, A, LDS.
30	10	60			S, A, LDS.
30	20	50			S, A, LDS.
32.5	15	52.5			S, A, LDS.
35	5	60			A, IDS, IMS.
45	5	50			A, IDS, LMS.
$6\frac{2}{3}$	60	$33\frac{1}{3}$	20	80	B_{ss}, ZS.
$13\frac{1}{3}$	$53\frac{1}{3}$	$33\frac{1}{3}$	40	60	B_{ss}, ZS.
19.04	47.62	$33\frac{1}{3}$	57	43	B_{ss}, ZS.
(4	10	7)			
22.22	44.44	$33\frac{1}{3}$	$66\frac{2}{3}$	$33\frac{1}{3}$	B
(2	4	3)			

Composition (mol %)					Phases Present.*
Li_2O	ZnO	SiO_2	$Li_2O \cdot ZnO \cdot SiO_2$	$2\ ZnO \cdot SiO_2$	
$23\frac{1}{3}$	$43\frac{1}{3}$	$33\frac{1}{3}$	70	30	B_{ss}.
$26\frac{2}{3}$	40	$33\frac{1}{3}$	80	20	B_{ss}, A_{ss}.
30	$36\frac{2}{3}$	$33\frac{1}{3}$	90	10	A_{ss}.

S = Quartz, tridymite or cristobalite

LMS = Lithium metasilicate

LDS = Lithium disilicate

ZS = Zinc orthosilicate

A = $Li_2O \cdot ZnO \cdot SiO_2$

A_{ss} = $Li_2O \cdot ZnO \cdot SiO_2$ solid solution (i.e. with peak shifts)

B = $2\ Li_2O \cdot 4\ ZnO \cdot 3\ SiO_2$

B_{ss} = $2\ Li_2O \cdot 4\ ZnO \cdot 3\ SiO_2$ solid solution (i.e. with peak shifts)

(3) Glass forming region.

The glass forming limit on the low silica side in the present system was noted during the determination of the liquidus temperature. The limit was found to be near the 50 mole percent silica line, being higher in silica at the lithium oxide rich side. Therefore lithium oxide imparted higher tendency of crystallization in the present system than zinc oxide did.

Glass formation is a kinetic problem. Whether a given composition will form a glass or not depends upon the rate of the cooling and thus the size of the specimen affects the limiting composition for glass formation. In the present investigation, specimens about 0.2 gramme in the form of cones were used. The specimen was held at a temperature slightly higher than the liquidus temperature, until a clear melt was obtained. The specimen was then withdrawn from the furnace rapidly and chilled in the air. A petrological microscope was used to examine for crystals. Any slight light scattering effect was regarded as an indication that the specimen was outside the glass forming region.

Bastress[13] investigated the glass forming region in the alkali silicate systems. He found that the limit was 37 mole percent lithium oxide in the lithium oxide - silica system, when specimen weighing 0.3 gramme was used. In the present investigation, a 40 mole percent lithium oxide, 60 mole percent silica specimen was prepared and examined. It was found that this composition was outside the glass forming region with the present procedure. Therefore, the result of Bastress was regarded as consistent with the present procedure and his result was used. The glass forming region was indicated in Fig. 5.

The glass forming region reported here is wider than it would have been if much bigger specimens were used. When forty or fifty grammes of compositions with 5 mole percent SiO_2 higher than the indicated limiting

compositions were poured from a platinum crucible after melting, devitrification was often found. Compositions near the indicated limit inevitably devitrified during pouring.

(4) Refractive index.

The refractive indices of the specimens within the glass forming region were measured by a microscope using the Beche line technique. The refractive indices of the matched immersion liquids were measured with a Leitz-Jelley Refractometer. Curves of the refractive indices against percentage of lithium oxide with constant silica content or percentage of silica with constant lithium oxide content were plotted. Data in the binary lithium silicate system was taken from Kracek's[8] work. A few of these curves were reproduced in Fig. 7 and 8. The refractive indices did not change linearly with mole percent composition with constant lithium oxide content but they changed linearly when zinc oxide was used to substitute lithium oxide. Compositions having various refractive indices were read off from the curves and plotted on the composition diagram, then the isofracts were constructed. The maximum experimental error of a single measurement with the Beche line technique is $\pm$ 0.003. With the present method of plotting the isofracts, the accuracy should be about $\pm$ 0.001. The results were given in Table 2 and Fig. 9.

(5) The tridymite field.

The field of tridymite was found to extend from 1470°C to the eutectic point E Li_2O 25.5 mol % ZnO 10 Mol %, SiO_2 64.5 Mol % at 955° $\pm$ 5°C and eutectic point F Li_2O 16.5 mol %, ZnO 23 mol %, SiO_2 60.5 mol % at 1050° $\pm$ 5°C in Fig. 6. In some very short time exploratory quenchings, meta stable cristobalite appeared in compositions of this field. In the actual determination of liquidus temperature, tridymite was found in every case, probably due to the long heat treatment time employed. The crystals obtained were small lath like, sometimes round with very low birefringence and refractive index, actually lower than the surrounding glass. These characteristics were used for

FIG. 7 REFRACTIVE INDICES OF GLASSES WITH CONSTANT SILICA CONTENT.

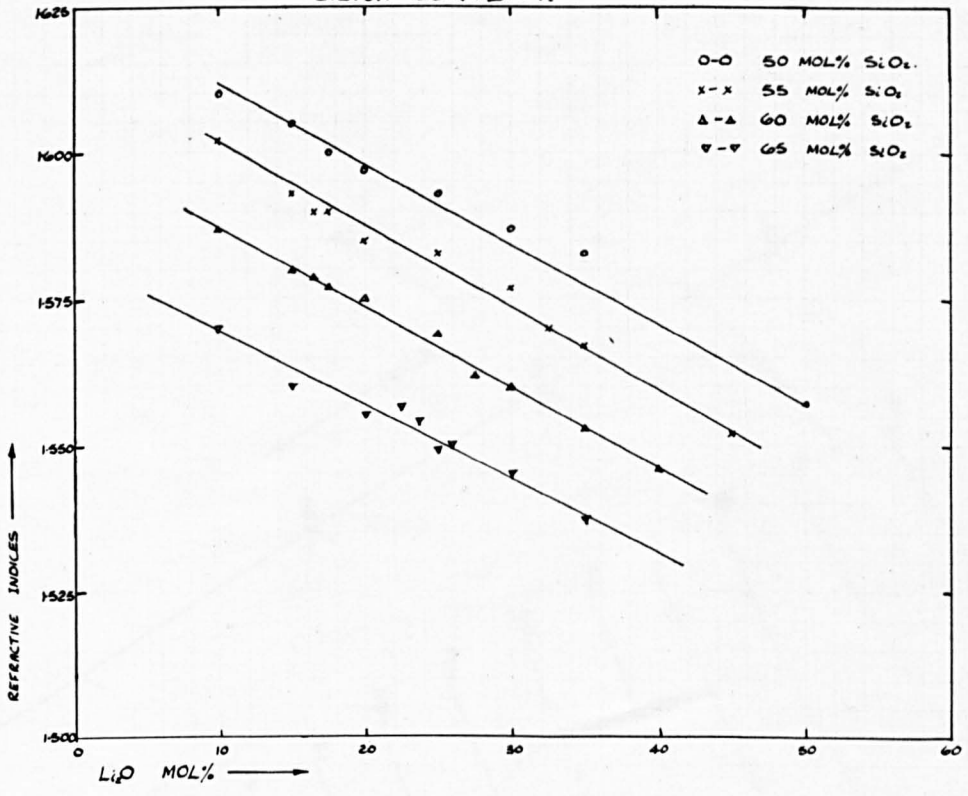

FIG. 8. REFRACTIVE INDICES OF GLASSES WITH CONSTANT LITHIUM OXIDE CONTENT.

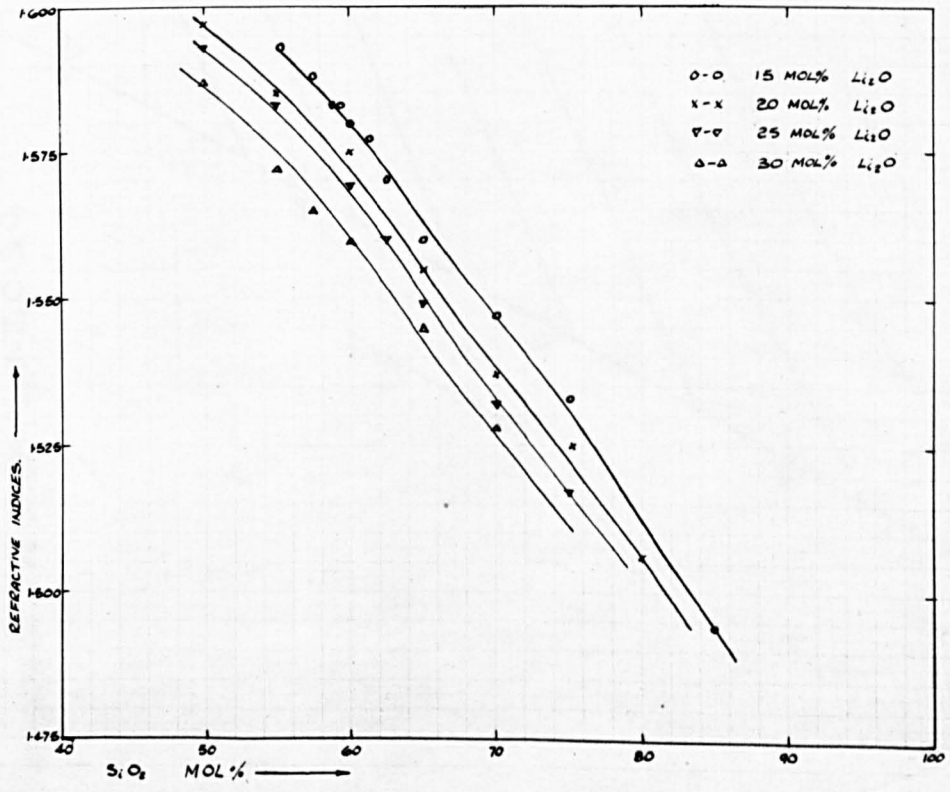

FIG. 9.

ISOFRACTS FOR THE GLASS FORMING REGION OF THE SYSTEM Li_2O-ZnO-SiO_2

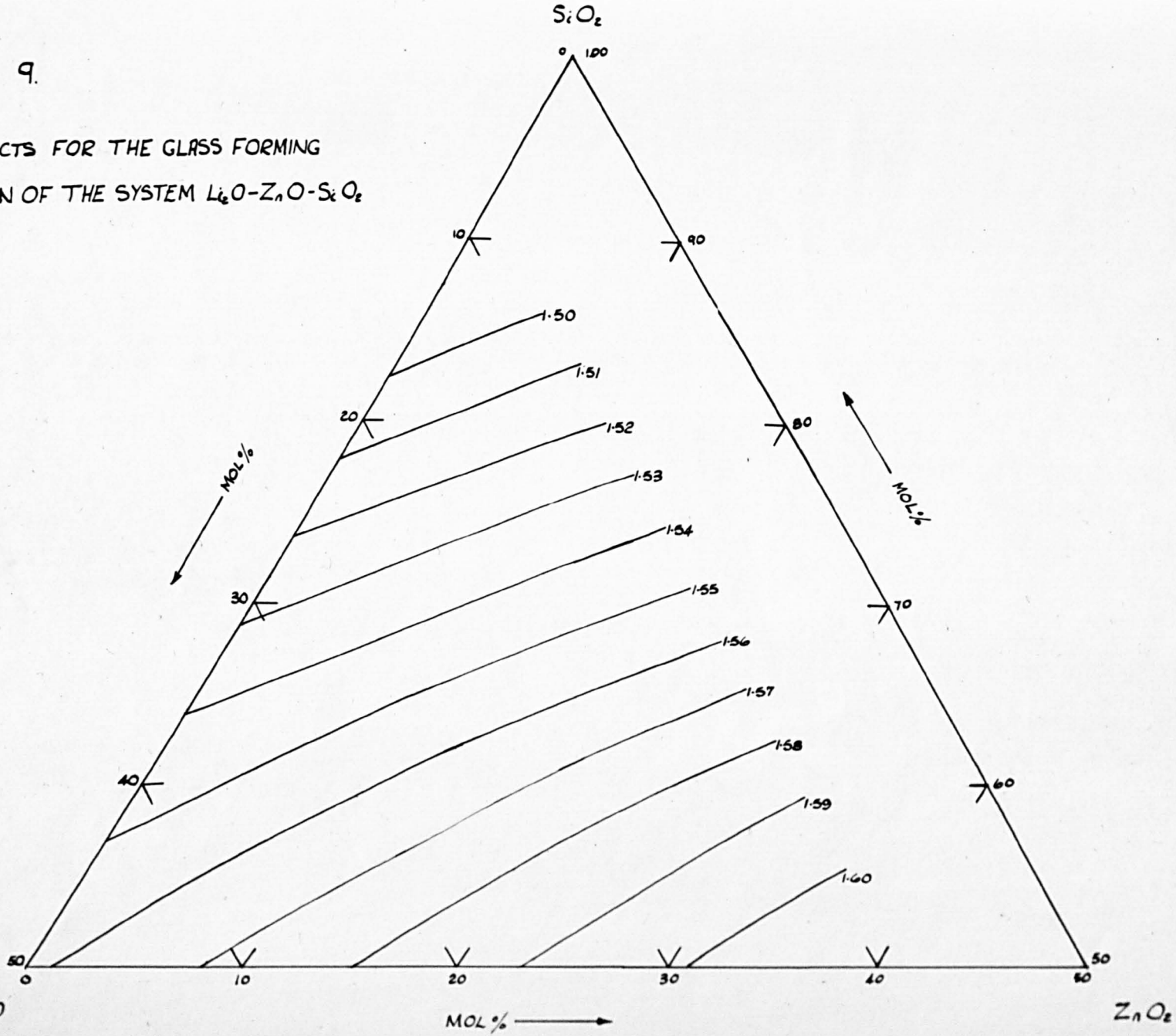

optical identification. The familiar sixty degrees branching needle crystal of tridymite was not found in the present study. This crystal gave a very weak X-ray diffraction pattern. Therefore, it was sometimes difficult to use X-ray diffraction for identification. However, the optical characteristics of this crystal were so different from the other primary phase crystal, that, it presented no problem in identification. The X-ray diffraction pattern found was the same as published in the X-ray Powder Data File. (A. S. T. M. Card).

The point M was found to be the minimum point on the join SiO_2 - $Li_2O \cdot ZnO \cdot SiO_2$ and the maximum point of on the boundary curve.

The system SiO_2 - $Li_2O \cdot ZnO \cdot SiO_2$ - $2\ Li_2O \cdot 4\ ZnO \cdot 3\ SiO_2$ is not completely ternary owing to an encroachment of the zinc orthosilicate field. The eutectic point of this system was found to be Li_2O 16.5 mol %, ZnO 23 mol % and SiO_2 60.5 mol % at 1050 ± 5°C. The reaction point between the silica, zinc orthosilicate and $2\ Li_2O \cdot 4\ ZnO \cdot 3\ SiO_2$ is located in this composition triangle at Li_2O 15.7 mol %, ZnO 24.6 mol % SiO_2 59.7 mol % at 1068° ± 5°C.

The system SiO_2 - $Li_2O \cdot 2\ SiO_2$ - $Li_2O \cdot ZnO \cdot SiO_2$ is not completely ternary owing to an encroachment of the lithium metasilicate field. The eutectic point was found to be Li_2O 25.5 mol % ZnO 10 Mol % SiO_2 64.5 Mol % at 955° ± 5°C. A second invariant point between lithium disilicate, lithium metasilicate and $Li_2O \cdot ZnO \cdot SiO_2$ is located in this composition triangle at Li_2O 27.5 mol % ZnO 9.8 mol % SiO_2 63.7 mol % at 976° ± 5°C.

Cristobalite was not found as primary phase crystal in the compositions investigated, because the high silica field was not investigated. However, this field was expected from the data in the binary systems. In Fig. 4 and 6 the cristobalite - tridymite boundary was drawn tentatively to confirm with the accepted 1470°C inversion temperature.

(6) The Lithium Disilicate Field.

The field of lithium disilicate is very small and is outlined by the area BCDE. This compound was found to be fairly big rectangular lath crystal with fairly sharp corners. The refractive indices of this crystal are very near to that of glasses in this field. Consequently the profile of the crystal is not very distinct, when examined under ordinary light. Under polarized light, this crystall appeared to be typical lath like, positive elongated crystal with parallel extinction, and could be fairly easily recognised. The optical properties of this crystal were listed in Table 4.

Table 4

Optical properties of lithium disilicate crystal

Authors	Refractive Indices			Mineral Group	Crystal System	Crystal Habit	Extinction	Elongation
	α	β	γ					
A.E.Austin[14]	1.54*	1.55	1.56	Biaxial positive				
R.Roy and E.F. Osborn[16]	1.546		1.558	Biaxial positive	ortho-rhombic	prism	parallel	
F.C.Kracek[6]	1.547	1.550	1.558	Biaxial positive	ortho-rhombic		parallel	
Present Study	1.547	1.550	1.560	Biaxial positive	ortho-rhombic	prism	parallel	positive

Specimens of pure lithium disilicate were specially prepared to be used as standards. When the X-ray diffraction data of the standard was compared with that in the X-ray Powder Data File, it was found that several extraneous lines were included in the X-ray Powder Data File. Other data of this crystal was then collected from the literature, and the present data was indexed.

The data in the X-ray Powder Data File is due to A. E. Austin[14]. Relative intensities and d-spacings were given but no Millor Index was given. Several extraneous lines in this data were due to lithium meta-

silicate. These might be due to the inhomogenities in A. E. Austin's specimen.

G. Donnay and J. D. H. Dannay[15] measured the cell parameter of this crystal with Weissenberg single crystal technique. This crystal was found to be orthorhombic with parameter ^{a}o = 5.80 Å , ^{b}o = 14.66 Å and ^{c}o = 4.806 Å. No diffraction data was given.

R. Roy and E. F. Osborn[16] gave the powder data of this crystal but no Millor Index was given. Using Donnay's parameter data G. Rindone[17] gave the Millor Index of his powder data. The d-spacings published seemed to be the calculated value instead of the observed value.

The present powder data was indexed as orthorhombic crystals with cell parameter ^{a}o = 5.80 Å , ^{b}o = 14.66 Å , and ^{c}o = 4.806 Å . With four formulae weight per unit cell, the calculated density was 2.438 gm/cm^3 and agreed with the observed density of 2.447 gm/cm^3.

The relative intensities of these crystals can easily be affected by preferential orientation in the powder specimen. The intensities of 111 and 002 increased greatly when coarse particles were present in the specimen. The intensities of these lines decreased with further grinding and careful preparation of the powder specimen. R. Roy[16] and G. Rindone's[17] data seems to indicate that preferential orientation occurred in their specimens. The calculated and observed powder data was listed in Table 5, together with other data in the literature.

Table 5.

X-ray Data of Lithium Disilicate

Present Study				A.E.Austin's[14] Data(X-ray Powder Data		R.Roy's and E.F.Osborn's[16] Data		G.Rindone's[17] Data		
hkl	$d_{(cal)}$	$d_{(ob)}$	I/I_o	d	I/I_o	d	I/I_o	d	I/I_o	hkl
020	7.332	7.31	12	7.32		7.35	4	7.332	4	020
110	5.392	5.41	6			5.39	12	5.392	8	110
				*4.70	11					
021	4.007	4.02	1	4.08	4	4.10	4			
130	3.738	3.75	45	3.75	33	3.73	80	3.738	58	130
040	3.665	3.66	100	3.67	100	3.64	65	3.666	52	040
111	3.589	3.61	30			3.58	100	3.588	100	111
				*3.34	3					
								2.950	5	131
200	2.900	2.91	2			2.93	10	2.900	12	200
				*2.72	11					
002	2.403	2.39	4	2.40	3	2.385	30	2.403	29	002
221	2.353	2.35	4	2.37	4	2.36	10	2.352	8	221
151	2.298	2.295	4	2.31	2	2.30	5	2.299	14	151
241	2.055	2.054	2			2.06	7	2.056	7	241
042	2.010	2.012	2			2.00	5	2.010	5	042
170	1.970	1.966	30	1.98	24	1.96	15	1.970	12	170
202	1.850	1.847	2	1.84	2	1.84	4	1.850	5	202
080	1.832	1.833	2							
222	1.794	1.796	2			1.81	6			
				*1.57	4					
113	1.536	1.533	2							
033	1.522	1.521	2	1.50	4	1.528	6			
133	1.473	1.473	2			1.47	4			
042	1.468	1.468	16	1.47	18	1.46	4			
332	1.440	1.442	2			1.44	4			
420	1.422	1.423	4			1.425	4			
				1.41	3					
223	1.378	1.376	2			1.37	3			
				*1.30	3					
451	1.255	1.251	6	1.26	6	1.25	3			
372	1.225	1.224	2			1.22	2			

* Due to lithium metasilicate

The $Li_2O \cdot 2\ SiO_2 - Li_2O \cdot ZnO \cdot SiO_2$ join is not a true binary system owing to the presence of lithium metasilicate. The compounds, lithium disilicate, lithium metasilicate and $Li_2O \cdot ZnO \cdot SiO_2$ form a composition triangle. The invariant point of this composition triangle is a reaction point which is Li_2O 27.5 mol % ZnO 9.8 mol % SiO_2 63.7 mol % at $976^\circ \pm 5^\circ C$ in the lithium disilicate, silica and $Li_2O \cdot ZnO \cdot SiO_2$ composition triangle.

(7) The lithium metasilicate field.

The lithium metasilicate field above the fifty mole percent silica line is outlined by the area ABC.

The lithium metasilicate crystals generally appeared in the glass as lath like positive elongated crystals with parallel extinction. The crystal habit changed considerably. When the compositions were near the lithium metasilicate compositions, the crystals were found to be well formed laths with rounded corners. When the compositions approached the $Li_2O \cdot SiO_2 - Li_2O \cdot ZnO \cdot SiO_2$ boundary, the crystals tended to become rounded triangles. The specially prepared lithium metasilicate standards were well developed triangular prisms which could be easily broken into tiny needle-shaped crystals. When it was examined with the needles lying flat, they appeared to be uniaxial. Since this crystal was reported in the literature to be pseudo-hexagonal orthorhombic, a specimen was specially prepared to examine the crystal along the axis of this needle. Several crystal prisms were mounted vertically in Paris plaster reinforced by Canadian balsam. This specimen was so ground that the axis of these prisms were parallel to the light path of the petrological microscope well developed biaxial interference figure was obtained from this specimen. Therefore it had proved conclusively that this crystal is actually biaxial. The optical properties of this crystal were listed in Table 6.

Table 6

Optical properties of lithium metasilicate crystal.

Authors	Refractive Indices			Mineral Group	Crystal System	Crystal Habit	Extinction	Elongation
	α	β	γ					
A.E.Austin[14]	1.59+		1.61+	Uniaxial positive				
R.Roy and E.F.Osborn[16]	1.590		1.610	Uniaxial positive		prism	parallel	negative
F.C.Kraeck[8]	1.591		1.611	Uniaxial		prism	parallel	negative
G.Donney and J.D.H. Donney[15]	1.584		1.609	Biaxial positive	ortho-rhombic	lath	parallel	positive
Present Study	1.585	1.593	1.611	Biaxial positive	ortho-rhombic	lath	parallel	positive

Several extraneous lines were also found in the data in the X-ray Powder Data File when they were compared with that obtained from the standard prepared in the present study. The data in the X-ray Powder Data File is also due to A. E. Austin[14]. Relative intensities and d-spacings were given but not the Miller Index. These extraneous lines were later identified to be due to lithium orthosilicate.

The cell parameters were measured by G. Donnay and J. D. H. Donnay[15] with Weisenberg single crystal technique. No diffraction data was given. They indexed these crystals as pseudo-hexagonal orthorhombic with ^{a}o = 5.43 Å , ^{b}o = 9.41 Å , and ^{c}o = 4.660 Å .

The present powder data was indexed as pseudo-hexagonal orthorhombic based on Donnay's cell parameter. Since $^{a}/_{b}$ = 0.577, this crystal was hexagonal within the experimental accuracy, if dimensions alone were considered. However, results from the optical examination have proved conclusively that this crystal is biaxial. Therefore, the data was indexed as an orthorhombic crystal. With four formulae weight per unit cell, the calculated density is 2.51 gm/cm^3 in agreement with the observed

density of 2.520 gm/cm^3. The calculated and observed powder data was listed in Table 7 together with A. E. Austin's[14] data.

Table 7

X-ray Data of Lithium Metasilicate

Present Study				A. E. Austin's[14] Data (X-ray Powder Data File)	
hkl	$d_{(cal)}$	$d_{(ob)}$	I/I_o	d	I/I_o
				*5.32	2
110,020	4.705	4.70	100	4.70	100
				*4.02	10
111,021	3.311	3.31	22	3.32	22
				*3.20	2
130,200	2.716	2.71	92	2.72	74
				*2.66	13
				*2.59	4
131,201	2.347	2.34	17	2.35	19
002	2.330				
112,022	2.088	2.09	3	2.10	5
132,202	1.769	1.773	8	1.78	10
150,240	1.779				
222,042	1.655	1.655	7	1.66	12
060,330	1.568	1.567	40	1.57	30
003	1.553	1.560	40		
				*1.53	4
312,242	1.413	1.412	3	1.40	2
260,400	1.357	1.355	4	1.36	6
133,203	1.348	1.349	4		12
062,332	1.300	1.299	7	1.30	12
351,421	1.256	1.255	6	1.26	8
313,243	1.170	1.170	3	1.18	5
422,352	1.138	1.138	3	1.14	5

* Due to lithium orthosilicate

(8) The zinc orthosilicate fluid.

The zinc orthosilicate field above the fifty mole percent silica line is fairly big and is outlined by the area GHJ.

The zinc orthosilicate crystals generally appeared in the glass as well developed hexagonal long prisms with high refractive indices and birefringence. Sometimes this crystal was found to be irregular grain with no characteristic crystal habit. The X-ray diffraction pattern was found to be the same as published in the X-ray Powder Data File (A.S.T.M. Cards).

Zinc orthosilicate forms a composition triangle with silica and $2\ Li_2O \cdot 4\ ZnO \cdot 3\ SiO_2$. The invariant point of this composition triangle is a reaction point at Li_2O 15.7 mol %, ZnO 24.5 mol % and SiO_2 59.7 mol % and $1068^\circ \pm 5^\circ C$ in the $2\ Li_2O \cdot 4\ ZnO \cdot 3\ SiO_2$, silica and $Li_2O \cdot ZnO \cdot SiO_2$ composition triangle. Zinc orthosilicate dissolves in $2\ Li_2O \cdot 4\ ZnO \cdot 3\ SiO_2$ to form solid solution.

(9) The $Li_2O \cdot ZnO \cdot SiO_2$ field.

The $Li_2O \cdot ZnO \cdot SiO_2$ field above the fifty mole percent silica is outsided by the area ACEMFIK. The primary phase crystal of the compositions in the area ACEMK is pure $Li_2O \cdot ZnO \cdot SiO_2$, because it does not form solid solution with lithium disilicate, lithium metasilicate or silica. However it forms partial solid solution with $2\ Li_2O \cdot 4\ ZnO \cdot 3\ SiO_2$, and two phase regions were found on the right of the line KM.

The composition of this primary crystal A was fully investigated. Several compositions with simple oxide ratio were prepared by repeated grinding and sintering or by melting with mechanical stirring. These specimens were then completely devitrified. The results were shown in Table 8.

Table 8

Compositions with simple oxide ratio.

Composition (mol %)					X-ray results
Li_2O		ZnO		SiO_2	
1	:	1	:	3	A + SiO_2
1	:	1	:	2	A + SiO_2
2	:	2	:	3	A + SiO_2
1	:	1	:	1	A
1	:	2	:	2	~~$2ZnO \cdot SiO_2$~~ + SiO_2 + B_{ss}.

Note: SiO_2 includes quartz, tridymite, and cristobalite.

Six compositions around $Li_2O \cdot ZnO \cdot SiO_2$ were investigated by X-ray diffraction. All the specimens were heat treated at 950°C for one or two days. The results were listed in Table 9.

Table 9

Compositions around $Li_2O \cdot ZnO \cdot SiO_2$.

	Compositions (mol %)			X-ray results
	Li_2O	ZnO	SiO_2	
1	35	30	35	A + $Li_2O \cdot SiO_2$
2	35	35	30	A + ZnO
3	30	35	35	A (with peak shift) + SiO_2
4	32	32	36	A + SiO_2
5	32	36	32	A + ZnO
6	36	32	32	A

Assuming that the composition of this primary phase crystal A is $Li_2O \cdot ZnO \cdot SiO_2$, the excess Li_2O in No. 2 and No. 6 compositions could not be found. This may be due to the low atomic number of lithium. The other four compositions indicated that this primary phase crystal A does not form an appreciable solid solution with zinc oxide, lithium metasilicate or silica.

The phase relationships at 950°C were investigated to establish the composition triangles. The results were presented and discussed in the section concerning the composition triangles. From this data and that in the preceding two sections, the composition of this primary crystal A is certain to be $Li_2O \cdot ZnO \cdot SiO_2$. Although the presence of solid solution may cause error in interpretation, the data on the left of the $Li_2O \cdot ZnO \cdot SiO_2 - SiO_2$ join clearly indicates that the conclusion is correct.

Two specimens of $Li_2O \cdot ZnO \cdot SiO_2$ were prepared - one by repeated grinding and sintering and the other by melting. Both specimens showed peaks corresponding to those of the primary crystal A. There are some discrepancies in the ratio of intensities between the $Li_2O \cdot ZnO \cdot SiO_2$ specimen and those of the primary crystal A. However, it was found that the intensity ratios are not as reproducible as with other compounds. This was found both in the $Li_2O \cdot ZnO \cdot SiO_2$ and in the primary phase crystal A. I. M. Stewart and G. J. P. Buchi[12] had also identified this composition as $Li_2O \cdot ZnO \cdot SiO_2$ in their work on the phase relationship of $Li_2O - ZnO - SiO_2$ system. They had indexed their powder data on the basis of primitive tetragonal cell with parameter a_o = 11.47 Å and c_o = 10.78 Å. It was found in the present study that the powder data could also be indexed on the basis of hexagonal cell with parameter a_o = 18.7 Å and c_o = 8.2 Å. Discrepancies were found in several lines between the calculated and observed value in the basis of both unit cells, with slightly better agreement with the hexagonal cells. The discrepancies were slightly bigger than the maximum experimental error. These two unit cells were not transformable, therefore they are incompatible. The apparent fit with these unit cells may be due to the big unit cells

used and the large maximum error assumed. The density of this crystal was found to be 3.39 $^{gm}/_{c.c.}$ by displacement technique. Therefore each hexagonal cell contains thirty formula units and the tetragonal unit cell contains seventeen formula units, so that both unit cells seem to be far too big. It may be possible that the true unit cell of $Li_2O \cdot ZnO \cdot SiO_2$ is only very close to the hexagonal cell. The X-ray diffraction dat was shown in Table 10.

Table 10.

X-ray powder data of $Li_2O \cdot ZnO \cdot SiO_2$

Present study		I. M. Steward and G.J.P. Buchi.(12)	
d	I/I_o	d	I/I_o
5.40	70	5.405	5
4.05	60	4.059	md
3.93	50	3.941	md
3.64	100	3.665	vs
3.12	10		
3.08	90	3.099	m+ bd
		2.991	vvw
2.88	10	2.888	vw
		2.815	vvw
2.70	100	2.696	s+
2.65	90	2.643	w+
2.56	8	2.578	vwd
2.51	70	2.508	s
2.44	10	2.431	vvwd
2.36	20	2.351	vvwd
2.34	20		
2.26	5	2.266	vvwd
2.190	5	2.199	vvwd
2.120	40	2.123	vw
2.020	5	2.019	vvwdb
1.940	10	1.942	w
1.901	10	1.889	w
1.865	20	1.865	w
1.816	10	1.820	w
1.796	8	1.794	w
1.757	5	1.748	vvwd
		1.692	vvwd
1.610	10	1.615	vw
		1.592	vvw
1.564	20	1.563	w+
1.540	50	1.536	5
1.509	5	1.511	w

d	I/I_o	d	I/I_o
		1.488	vvw$^-$
1.466	10	1.468	wd
1.446	8	1.453	vw
		1.438	vvw$^-$
		1.423	vvw$^+$
1.410	10	1.409	vvw$^-$
		1.364	vvw$^-$d
		1.354	vvwd
1.310	25		

The $Li_2O \cdot ZnO \cdot SiO_2$ crystals were normally found to be rectangular tablets with rounded corners in the glass. The $Li_2O \cdot ZnO \cdot SiO_2$ standard prepared for X-ray work was found to be irregular grains with no characteristic crystal form or habit and with no good cleavage. Also multiple twinning in all directions seemed to be present in these samples. Therefore it was very difficult to obtain accurate refractive indices. The maximum and minimum refractive indices were determined and found to be 1.635 and 1.664.

(10) The $2\ Li_2O \cdot 4\ ZnO \cdot 3\ SiO_2$ field.

The $2\ Li_2O \cdot 4\ ZnO \cdot 3\ SiO_2$ field above the fifty mole percent silica is outlined in the area FGJI. The refractive indices and the X-ray data of this crystal are very similar to that of $Li_2O \cdot ZnO \cdot SiO_2$. Also solid solutions were found between these two compounds. Therefore these made it difficult to locate very accurately the eutectic point F in the SiO_2 - $Li_2O \cdot ZnO \cdot SiO_2$ - $2\ Li_2O \cdot 4\ ZnO \cdot 3\ SiO_2$ composition triangle. Liquidus temperatures of compositions around the point F were used for locating F. The present data of point F is Li_2O 16.5 mol %, ZnO 23 mol % SiO_2 60.5 mol % at $1050^o \pm 5^oC$.

During the early stage of the investigation of liquidus temperatures of the compositions in the glass forming region, the primary phase field of the crystal B was mistaken as that of the crystal $Li_2O \cdot ZnO \cdot SiO_2$. After I. M. Stewart and G. J. P. Burchi[12] had reported the existence of the ternary compounds $Li_2O \cdot ZnO \cdot SiO_2$ and $4\ Li_2O \cdot 10\ ZnO \cdot 7\ SiO_2$; the X-ray diffraction data of all compositions with $Li_2O \cdot ZnO \cdot SiO_2$ as primary phase crystal were re-examined. It was found that the X-ray data of seven compositions near the zinc orthosilicate field showed slight shifts of peak positions. Owing to the close similarity between the X-ray pattern of crystal B and that of $Li_2O \cdot ZnO \cdot SiO_2$ and the ill-defined pattern obtained from the small amount of crystal in the X-ray specimen, these differences were overlooked at the time of the experiment. Specimens of these compositions, heat treated at lower temperature, but above 1000^oC were then examined by X-ray diffraction and the peak shifts

were confirmed. After the investigation of the $Li_2O \cdot ZnO \cdot SiO_2$ - $2\ ZnO \cdot SiO_2$ join, the existence of the primary phase crystal B and its primary phase field inside the glass forming region were confirmed. Also data in the zinc orthosilicate primary phase field supported the existence of another ternary compound.

The composition of this primary phase crystal B was not investigated as conslusively as that of $Li_2O \cdot ZnO \cdot SiO_2$, but $2\ Li_2O \cdot 4\ ZnO \cdot 3\ SiO_2$ seems to be the most likely composition for this primary phase crystal B. This point was discussed in more detail in the following section concerning the $Li_2O \cdot ZnO \cdot SiO_2$ - $2\ ZnO \cdot SiO_2$ join. The X-ray data of $2\ Li_2O \cdot 4\ ZnO \cdot 3\ SiO_2$ were shown in Table 11.

Table 11.

X-ray powder data of $2\,Li_2O \cdot 4\,ZnO \cdot 3\,SiO_2$

d	I/I.
5.47	25
5.24	10
4.07	75
3.97	45
3.69	40
3.63	35
3.21	20
3.15	5
3.07	25
2.86	25
2.74	100
2.63	80
2.51	80
2.44	5
2.40	25
2.319	5
2.135	25
2.026	15
1.936	20
1.879	5
1.850	20
1.816	5
1.742	5
1.601	30
1.536	40
1.470	15
1.438	10
1.369	15
1.307	20

(11) The $Li_2O \cdot ZnO \cdot SiO_2$ - $2\,ZnO \cdot SiO_2$ join.

Four compositions in this join were prepared by repeated grinding and sintering at 1400°C. The results obtained were not reproducible. Therefore new specimens were prepared by melting at 1500 - 1580°C in a Pt/Rh winding furnace and these specimens were used for subsequent heat treatment experiments. Finally nine compositions were prepared.

The melted specimens chilled from the melting temperature were examined by X-ray diffraction. Gradual changes of the peak positions and intensities with composition were found. The peak shifts were not constant and also not in the same direction for all peaks. The biggest shifts were in the two strong peaks from 2.70 Å to 2.76 Å and from 2.65 Å to 2.61 Å. Also the peak of $Li_2O \cdot ZnO \cdot SiO_2$ at 3.64 Å split into a double peak. Compositions containing up to 60% of zinc orthosilicate gave one phase with an X-ray pattern similar to $Li_2O \cdot ZnO \cdot SiO_2$, and no zinc orthosilicate was detected. This indicates the existence of a continuous series of solid solution in the $Li_2O \cdot ZnO \cdot SiO_2$ - $2\,ZnO \cdot SiO_2$ join up to 60% of zinc orthosilicate in $Li_2O \cdot ZnO \cdot SiO_2$ in specimen chilled from higher than 1500°C. Attempts were made to index the powder data of this series of solid solution on the basis of a hexagonal cell with parameter a_o = 18.7 Å and c_o = 8.2 Å for the $Li_2O \cdot ZnO \cdot SiO_2$ crystal, with increasing a_o and decreasing c_o for this series of solid solution. Higher discrepancies were found between the calculated and the observed values than that in the $Li_2O \cdot ZnO \cdot SiO_2$ crystal. This may be due to the wrong unit cell used for the $Li_2O \cdot ZnO \cdot SiO_2$ crystal.

These compositions were also heat treated at various temperatures in the range of 950° - 1500°C. The X-ray data was fairly difficult to interpret due to the close similarities of the X-ray pattern of the crystal B and $Li_2O \cdot ZnO \cdot SiO_2$. However the presence of zinc orthosilicate could easily be identified. Compositions containing higher than

40% 2 ZnO • SiO_2 and heat treated at low temperatures gave the X-ray pattern of zinc orthosilicate and an X-ray pattern similar to Li_2O • ZnO • SiO_2. In the specimen corresponding to the composition of 4 Li_2O • 10 ZnO • 7 SiO_2 only one phase with an X-ray pattern similar to Li_2O • ZnO • SiO_2 was found, when the specimen was quenched from above 1050°C; below that temperature zinc orthosilicate precipitated out and the X-ray pattern of the other crystal shifted toward that of Li_2O • ZnO • SiO_2. This data proved conclusively that the "compound" 4 Li_2O • 10 ZnO • 7 SiO_2 reported by I. M. Steward and G. J. P. Buchi[12] is not a true compound, but a solid solution of zinc orthosilicate in a compound with composition situated on the left of the 4 Li_2O • 10 ZnO • 7 SiO_2 composition along the Li_2O • ZnO • SiO_2 - 2 ZnO • SiO_2 join.

Zinc orthosilicate was not found in specimens containing less than 35% of 2 ZnO • SiO_2. In the region between Li_2O • ZnO • SiO_2 and 33⅓% 2 ZnO • SiO_2, only one X-ray pattern similar to Li_2O • ZnO • SiO_2, was found, except in compositions near 20% 2 ZnO • SiO_2. The X-ray pattern of the specimen containing 20% 2 ZnO SiO_2 heat treated at low temperature were the same as in the specimen chilled from above the liquidus temperature except the two strong peaks at 2.61 Å and 3.64 Å which split into double peaks. If these double peaks are interpreted as from two different compounds with very close X-ray diffraction patterns then there is a ternary compound in the region of 20 - 35% 2 ZnO • SiO_2. Within this region, the only simple oxide ratio compound is 2 Li_2O • 4 ZnO • 3 SiO_2. It should be pointed out here that the peak shifts of these two peaks are much bigger than those of the other peaks, when solid solutions were found in the specimens chilled from above the liquidus temperature. If the specimen containing 20% 2 ZnO • SiO_2 broke down from one phase at the high temperature into two phases at the lower temperature, the strong peaks would split but the other peaks would just become broader peaks, owing to the small peak shifts. Therefore, it is reasonable to assume the existence of another ternary compound in this join.

During the investigation of phase relationships at 950°C, it was thought that only two phases, silica and $Li_2O \cdot ZnO \cdot SiO_2$ solid solution, were found in the area outlined by KMGJ, but on closer examination some specimens also showed the split of these two strong peaks in their X-ray patterns. Therefore two two-phase regions separated by a three phase region were shown in the composition triangle diagram.

Several compositions in the $2\ ZnO \cdot SiO_2$ primary phase field were found to contain tridymite and crystals similar to $Li_2O \cdot ZnO \cdot SiO_2$ only and $2\ ZnO \cdot SiO_2$ was not present in specimens heat treated at temperature lower than 1070°C. This indicated that the point G is only a reaction point and another compound is present with composition in the $Li_2O \cdot ZnO \cdot SiO_2 - 2\ ZnO \cdot SiO_2$ join.

Attempts to determine the liquidus temperature along this join by quenching technique were not successful, because it was not possible to differentiate the small amount of the crystal B from $Li_2O \cdot ZnO \cdot SiO_2$ by X-ray diffraction due to the close similarity of these two X-ray patterns and the existence of solid solutions between them. Identification by optical methods were not successful, because the optical properties of these two compounds are very similar and the size of crystals formed during the high temperature heat treatment was similar to those formed during the quenching from high temperature to low temperature.

At the moment, no differential thermal analysis apparatus capable of reading 1500°C was available, so the quenching furnace was used for thermal analysis. Two alumina specimens were put in two adjacent specimen cones. Temperature difference between these two cones were deduced from the temperature measurement of alternate cone at half a minute intervals. Lithium metasilicate was used to find if some thermal effect could be detected. The temperature difference of these two cones over and above that found in the alumina run were regarded as thermal effect of the lithium metasilicate. The same heat up schedule was used. At 1205°C (liquidus temperature of lithium metasilicate is

1201° ± 1°C) a temperature drop of about 5°C was found. The specimens of other compositions were investigated with the same procedure. A temperature drop of about 4°C was found at 1480°C with $Li_2O \cdot ZnO \cdot SiO_2$, and a temperature drop of about 3°C was also found at 1430°C. Unfortunately, no significant thermal effect was found with other composition. Obviously this was due to the insensitivity of the arrangement of the apparatus, because the thermocouples were outside the specimen cones instead of embedded in the specimen. Although the composition of the primary phase crystals B was not proved to be $2\ Li_2O \cdot 4\ ZnO \cdot 3\ SiO_2$ conclusively by the liquidus curve in the $Li_2O \cdot ZnO \cdot SiO_2 - 2\ ZnO \cdot SiO_2$ join, it is tentatively identified as $2\ Li_2O \cdot 4\ ZnO \cdot 3\ SiO_2$ on the evidence discussed above.

PART B. MECHANISM OF CRYSTALLIZATION

I. LITERATURE SURVEY.

1. Explanation of terms.

In the literature, different terms have been used by various workers to refer to the same processes. For the convenience of discussion, the terms used in this thesis will be explained here to avoid confusion.

When nucleation takes place anywhere in a structure, the process is called homogeneous nucleation. Generally, the rate of nucleation does not change with time. If nucleation takes place at prepared sites, the process is called heterogeneous nucleation. The rate of such nucleation decreases with time as the preferred nucleation sites are exhausted.

If the concentration of crystals at the surface of a specimen is much higher than that of the whole body, the process is called surface crystallization. When there is not much difference between the concentrations of crystals on the surface and in the body, the process is called uniform crystallization.

The mechanisms of crystallization are classified according to the behaviour of the specimen in the nucleation stage. The crystallization processes generally refer to the microstructure of the specimen.

2. Nucleation.

(1) Classical nucleation theory.

G. Tammann[18] considered the free energy change in the crystallization processes of undercooled liquids. Classical nucleation theory is based mainly on his arguments and experimental results. In an undercooled liquid system, the liquid phase has a higher free energy than that of the stable crystalline phase. Therefore there is a decrease in free energy during the trans-

formation of the liquid phase into the crystalline phase. However, in the formation of the crystalline phase, a new boundary is formed, and this increases the total free energy of the whole system in the form of surface energy. During the initial stage of the formation of the crystalline phase, the total free energy of the whole system increases, while the crystal grows, because the increase of the surface energy of the boundary, due to the newly formed crystal, is higher than the decrease of free energy owing to the difference between the free energy of the crystal and that of the undercooled liquid. The net result is an increase of free energy for the whole system arising from the high surface to volume ratio of a small particle. Therefore nucleation has an energy barrier. If the crystal is bigger than a certain size, the total energy of the system decreases while the crystal grows, because the increase of surface energy as a result of the larger surface of the crystal is lower than the decrease of free energy due to the difference between the free energy of the crystal and that of the undercooled liquid. Therefore, in these conditions, the total free energy of the system decreases, during the growth of the crystal and the crystal is stable. The minimum size of the stable crystal depends both on the surface energy of the boundary and the difference of free energy of the liquid and the crystal. This minimum size is called the critical size and it changes with temperature. As a result, nuclei above the critical size will grow and those below the critical size will be dissolved. The homogeneous formation of nuclei is instantaneous and can only arise from thermodynamic fluctuations of sufficient magnitude.

After the formation of the stable nuclei, the growth of the crystals will decrease the total free energy of the system. Therefore, there is no energy barrier in the steady state crystal growth. Owing to the different nature of these two stages of crystallization, Tammann[18] divided the mechanism of crystallization into two separate processes, the formation of stable nuclei and the steady state crystal growth.

He considered that the ability of a liquid to be undercooled depends both on the rate of formation of stable nuclei and the rate of steady state crystal growth. The rate of nucleus formation increases with the degree of undercooling and then decreases after reaching a maximum. The rate of nucleus formation versus degree of undercooling curve is in the form of a random distribution curve. He also predicted that the shape of the growth rate versus degree of undercooling curve would be of the same form.

He verified his theory by experimental work on organic liquids, mainly pure compounds. In the absence of accurate data on the surface energy of the crystal and liquid interface, he predicted that the critical size of nuclei was very small. He undercooled organic liquids for a certain time interval at constant temperature and then held them at higher temperature to grow the nuclei. By assuming that no new nuclei were formed at the higher temperature, he counted the crystals and obtained the rate of nucleus formation. The number of crystals was not constant but followed the law of probability. He found that the rate of nucleus formation at each temperature decreased with successive undercooling. Also holding for a long time at higher temperatures decreased the rate. However, the shape of the rate versus temperature curve assumed the predicted form and the maximum rate temperature was not affected by repeated heating.

R. T. Jacobdine[19] studied the rate of nucleus formation in a binary lithium silicate glass containing 30 mol % of lithium oxide. The specimens were heat treated at 520°, 560° or 600°C for up to three days. After acid etching, the specimens were examined under microscope. Lithium disilicate was found to be the crystalline phase. The size of the crystals was not uniform indicating that they did not start to grow at the same time. The number of crystals per unit area was found to increase linearly with time at the three temperatures investigated. The rate of nucleus formation was higher at higher temperature. However not enough data was obtained to enable conclusions to be drawn about the rate of nucleus formation over a wide temperature range.

O. Kapp[20] studied the nucleation of a lead glass and a magnesia glass by holding the specimen at constant temperature. In the specimen of the magnesia glass heat treated at 700°C for various time intervals from thirty minutes to three hours, all crystals were of the same size indicating simultaneous growth. In the specimens of the lead glass, some small crystals were found suggesting the formation of new nuclei at later stages of heat treatment. In another series of experiment, he heat treated seven specimens of magnesia glass and lead glasses at 750°C for a half of an hour, and photographs were taken. The number of crystals in one sixth of the photograph were counted. Very widely scattered results were obtained. The standard deviation for each specimen was found to be as high as twenty five percent of the mean. By using Graf's statistical analysis, he concluded that the variation in the rate of nucleus formation was due to chance. Also he found that each glass had its own range of rate of nuclei formation.

During the investigation of titania white enamel, T. B. Yee and A. I. Andrews[21] studied the number of crystals formed during the heat treatment. Thin films of the enamel were supported on

quartz slides and heat treated at temperature range from 700° to 1100°C for two to eight minutes. The number of crystals in unit area were counted in the enlarged photomicrographs. The rate of nucleus formation increased with increasing temperature up to 850° - 900°C and decreased at higher temperature. However a very high scatter was found and the curve was not symmetrical. Both anatase and rutile were found as crystalline phases in the enamel.

R. D. Maurer[22] studied the nucleation process of a photosensitive glass. The specimens were exposed to high energy radiation of varying intensities and for various lengths of time and then heat treated. Light scattering and light absorption measurements were used to deduce the number and size of the stable gold nuclei. He concluded that the number of stable nuclei in the specimen depended solely on the intensity and length of irradiation but not heat treatment. The smallest stable gold nuclei was only one to three atoms big and the growth of the gold crystal obeyed a simple diffusion law.

(2) Heterogeneous nucleation.

a. Glass ceramic process.

S. M. Ohlberg, A. R. Golob and D. W. Strickler[23] studied the mechanism of crystallization in three quaternary system. Electronic microscope, optical microscope and an X-ray diffractometer were used.

In the magnesia - alumina - silica - titania system, a series of specimens was heat treated at 1000°C for different times. The crystalline phase was identified. Silica - O crystals were found first. Cordierite crystals were identified later. Rutile was found only after a long heat treatment. In another series of experiments, the specimen was heat treated at 900°C at different times. After twenty-five minutes of heat treatment, about eighty percent of crystalline phases was found, but these crystalline phases were not identified. They concluded that when the specimen was chilled during

casting, glass-in-glass phase separation occurred. During the heat treatment, droplets of glass of different composition from the main body of the glass increased in size. Later, magnesium ditatanate was formed which nucleated the silica-O crystals heterogeneously. Cordierite and rutile were developed later, by the reaction of the intermediate crystalline phases and the glass matrix.

In the lithia - lime - silica - titania system, the specimens were heat treated at different temperature for different times. When the heat treatment temperature was below 600°C, no crystalline phase was identified by X-ray diffraction, but small droplets were found in the electron micrographs. At higher temperature heat treatment, crystalline phases were found, and the appearance of the boundary of the droplets changed during crystallization. In the specimen heat treated for a long time, quartz, lithium disilicate and an unknown crystalline phase with a total crystalline content of 90% was found. They concluded that, glass in glass phase separation occurred when the specimen was cast. During the heat treatment more glass droplets were formed and these heterogeneously nucleated the minor crystals which then grew from the boundary. In the final stage, the minor crystals nucleated the major crystals heterogenously.

In the lithia - magnesia - alumina - silicate system, the specimens were heat treated at lower temperature and then at higher temperature. Droplets were found in the electron micrographs. Later, the crystallization started at the interfaces of the droplets and the crystal grew into the droplet. In the specimen heat treated at high temperature for a long time, 85% of β-spodumene and silica-O crystals were found. They concluded that in this system, glass in glass phase separation also occurred.

W. Vegel and K. Gerth[23] studied two glasses, one of which was mainly a lithia - alumina - silica - titania glass with minor constituents and the other was a lithia - beryllia fluoride glass. In both glasses, phase separation droplets were clearly demonstrated in the electron micrographs. In the aluminosilicate glass, the droplets crystallized first and then the glass matrix crystallized. In the fluoride glass, the glass matrix crystallized first and then the droplets crystallized. They concluded that catalysts (i.e. titania and cerium oxide) promoted phase separation. During the phase separation, network former oxides would concentrate in one phase and the other phase which contained a high percentage of network modifier oxide would devitrify first and then this crystalline phase heterogenously nucleated the other phase.

R. D. Maurer[24] studied the crystallization of a titania nucleated glass. Results from light scattering and X-ray diffraction were used to deduce the size and number of crystals. At the initial stage, isotropic regions were found which became anisotropic with time. Higher temperatures favour this transformation. It was concluded that liquid in liquid phase separation occurred at the early stage of heat treatment, and the phase separation promoted the crystallization of magnesium dititanate. With about ten percent of total crystalline phase the sizes of the crystals were found to range from 57 Å to 211 Å in specimens heat treated at different temperature for different time. The numbers of crystals in these specimens were found to be $10 - 1000 \times 10^{15}$ crystal/cm^3.

J. P. Williams and G. B. Carrier[25] investigated the crystallization processes in two glasses. In the lithia - alumina - silica - titania glass, the specimens were heat treated at 800°C for one hour and then at higher temperature for one or four hours. β-eucryptite was found in the specimen heat treated at 800°C only. Prolonged heat treatment at this temperature did not affect the size and number

of crystals significantly.. If the specimen was heat treated at 800°C and then at 930°C for one hour, the crystals grew slightly. If the heat treatment temperature was raised to higher than 940°C, the crystals grew much faster, and changed from hexagonal β-eucryptite to tetragonal β-spodumane. In the fully heat treated specimen, only β-spodumane solid solution crystals, aluminium titanate and glass matrix were found.

In the barium aluminosilicate glass, the specimens were heat treated at 950°C for two hours and then at different higher temperature for ten hours. Only mullite crystals were found. Bigger crystals and lower crystal content were found in specimens heat treated at higher temperature. The acid resistance of the specimen changed with the final heat treatment temperature.

R. Roy[26] discussed the phenomena in the crystallization of glasses in the lithia - alumina - silica and magnesia - alumina - silica - titania systems. In the early stage of heat treatment, silica-O crystals were identified always. Later β-eucryptite solid solution, β-spodumane solid solution or cordierite crystals were found. Also different crystals were found simultaneously, indicating the precipitation of different crystals from phases of different compositions. The "catalyst" crystals (i.e. titania and lithium disilicate in these cases) were found only at a very late stage of the heat treatment, so phase separation was the initial step of crystallization. Metastable phase separation was favoured by a stable two liquid region at high temperature and a flattened liquidus curve.

He suggested that the structure of a liquid"would be described as random, and that of glass as possessing short range order". During isothermal crystallization, the structure of glass changed, and metastable two liquids, or a metastable crystal might form before the appearance of the final stable crystals. In the original liquid, sub-critical nuclei existed in large numbers. These nuclei were

simply regions of different compositions, still having only short-range order and were in dynamic equilibrium with each other with no surface separating the areas. On quenching and reheating, such nuclei grew as a result of a very low activation energy process, since the structural demands of the short range order were minimal. Therefore uniform crystallization could most easily be accomplished by the separation of a second short range order phase. This would imply the formation of meta stable phase separation or the crystallization of a meta stable crystals capable of forming solid solution.

W. B. Hillig[27] discussed theoretically the effects of liquidus temperature, time, surface free energy and diffusion coefficient on the rate of nucleus formation. The barium oxide - silica - titania and the barium oxide - alumina - silica - titania systems were investigated./ The liquidus temperature, the critical homogeneous nucleation temperature, critical nucleation temperature on platinum, and lower cut off to homogeneous nucleation were measured. He concluded that for the system investigated, a nucleation catalyst was not necessary to produce glass - ceramic.

F. P. H. Chen[28] studied the crystallization of a synthetic mica glass. The specimens were heat treated at different temperatures for different time intervals. The carbon replica technique was used in an electron microscope to investigate the microstructure of the specimen. The number of crystals per unit area was obtained by counting the particles in the electron micrographs. An unidentified intermediate phase was found in the crystallization of mica crystals. Nucleation of the intermediate phase was affected by the heat treatment temperature. The rate of nuclei formation was higher when the specimens were heat treated at the lower temperature. Also the rate at constant temperature decreased with increasing time of heat treatment. The final stable mica crystal is formed from the transformation of the intermediate unstable crystalline phase. He concluded that the formation of the intermediate phase was a hetero-

geneous nucleation process and the decrease of the rate of the nuclei formation was due to the exhaustion of preferred nucleation site.

b. Photosensitive glass process.

The final microstructure of the article made by the glass-ceramic process is very similar to that made by the photosensitive glass process. Both of them are mainly polycrystalline materials with extremely small crystals and zero porosity. They differ in the processes by which they are formed. In the photosensitive glass process, the articles are irradiated by high energy radiation and then heat treated to convert the exposed glass into polycrystalline material. Therefore the glass is "nucleated" by irradiation. In the glass ceramic process, heat treatment is used to "nucleate" the article. As it is difficult, if not impossible, to heat treat accurately a part of the article, the final microstructure of the whole article made by the glass ceramic process is substantially the same. In the photosensitive glass process, part of the article can be exposed to radiation, while the other parts are shielded from the radiation. After heat treatment part of the article will be mainly in the crystalline state and the other parts will be mainly in glassy state.

These two processes are also different in their mechanisms of crystallization. Although they are both heterogeneous nucleation processes, their paths are different. In the glass ceramic process, all the experimental evidence points to the initial stage of liquid in liquid phase separation, then the formation of the intermediate unstable crystalline phases on the phase boundary of the liquids and finally the transformation of the unstable crystalline phases to the stable crystalline phase. Although in some experiments, the liquid in liquid phase separation was not apparent, on the evidence of other researches, it would be reasonable to assume that the specimen, with the shortest heat treatment that they examined, had passed the liquid in

liquid phase separation stage. In the photosensitive glass process, metallic particles are precipitated homogeneously in the glass body, during the early stage of the heat treatment. These particles grow to a size big enough to act as nuclei to provide nucleation sites for the stable crystalline phase. In other words, the stable crystalline phase precipitated directly from the glassy phase onto the metallic particles without the intermediate step of liquid in liquid phase separation or the step of the transformation of unstable crystalline phase into the stable crystalline phase.

Not much work about the photosensitive glass process had been published. S. D. Stookey[29] had described the path of crystallization of photosensitive glass as part of his discussion on catalyzed crystallization of glass. R. D. Maurer[22] had shown from his work in light scattering and light absorption that the gold particles were precipitated homogeneously from the glass phase. The growth of the gold crystals obeyed a simple diffusion law. The smallest stable nuclei was only one to three atoms. For catalyzing the crystallization of lithium metasilicate, the minimum size of the gold particles was about 80 Å (i.e. about ten thousand gold atoms). He suggested that this requirement was due to the stress on the nuclei of lithium metasilicate arising from the slight misfit between the lattice spacings of the gold crystals and that of the lithium metasilicate.

3. Steady state crystal growth.

(1) Crystal growth in pure compounds.

G. Tammann[18] also investigated the rate of crystal growth in the undercooled organic liquids by observing the advance of the crystal liquid interface. The organic liquids investigated were pure compounds. He nucleated the undercooled liquids by putting the corresponding crystals on the surface of the liquid. The growth was found to be linear with time and the usual hump shaped growth rate versus temperature curves were obtained. The maximum rate was found

at a temperature higher than that of the maximum rate of nuclei formation. When the rate was higher than 5 mm/min, the relationship was very complicated.

W. D. Scott and J. A. Pack[30] studied the crystal growth of sodium disilicate from its own melt with a hot stage microscope. No homogeneous nucleation was observed. All the crystallization started at the interface with the platinum wire or with air. Both α and β sodium disilicate were found depending on the nucleating temperature. Sometimes both types of crystals were found to grow simultaneously. The growth rate followed the equation

$$U = A T^{1.75 \pm 0.05}$$

where U = growth rate

A = fluidity

T = undercooling.

Using existing viscosity data, the empirical equation fitted the data quite well.

N. G. Hinslie, C. R. Morelock and D. Turnbell[31] studied the crystallization of fused silica. Heterogeneous nucleation by "dirt" on the surface was demonstrated. It was found that fire finish could prevent this nucleation effectively. Ordinary specimens without fire finish were heat treated at different temperature from 1356° to 1678°C for time up to six days in electric furnace. Crystallization started from the surface, and the thickness of the crystalline layer was measured at room temperature with a microscope. Different atmospheres were used. With water vapour and oxygen in the sealed capsules containing the specimen the crystal rate was the same as that in air. With dry argon or nitrogen atmosphere, the crystal layer was only about one tenth of that in air. The growth of the crystalline layer was found to be proportional to the square root of time instead of linear with time. When graphite, chromium or germanium was put on the surface of

the specimen heat treated in water vapour atmosphere, the crystalline layer was much thinner and seemed to increase linearly with time. Internal crystallization was observed occasionally. The growth rate increased with temperature up to nearly the melting point of cristobalite. Also the growth rate was found to be much higher than that derived theoretically. They concluded that the growth of cristobalite was influenced greatly by impurities, and the impurities diffused from the surface through the crystalline layer to the crystal and glass interface. Therefore the growth was diffusion controlled.

S. D. Brown and S. S. Kistle[32] studied the devitrification of fused silica containing 0.005 - 0.5 mol % of alumina. Great care was taken in the selection of batch material and the preparation of the specimens to obtain homogeneous specimens. The specimens were nucleated by immersion in water and heat treatment at low temperature. The growth rate was obtained by observing the advance of the crystal and glass interface in a rod at different time intervals until about ninety percent of the specimen was crystallized. The growth versus time curves for different temperatures were found to be straight lines. The log growth rate versus $^1/_T$ curve were also straight lines. The growth rate was found to increase with increasing temperature. Over the temperature range from 1280° to 1460°C. the experimental data fitted the equation

$$U = A\,T^{-B/T}$$

Where U = growth rate

T = absolute temperature

A,B = constant

Log A decreased with increasing amount of alumina but a minimum was found. B also decreased with increasing amount of alumina, ranging from 55 to 34 K Cal/Mol. The growth rate at different temperature was plotted against composition. At the same temperature, the growth rate

increased generally with addition of alumina. The viscosity over the same temperature range was found to increase with increasing amount of alumina. Cristobalite was found to be the only crystalline phase.

(2) Crystal growth in complex glass.

E. Preston[33] heat treated a commercial sheet glass in a gradient furnace for different time and at various temperatures to study crystal growth. The linear growth rate was obtained from the half length of the crystals measured under a microscope at room temperature. It was found that the crystal size on the surface was different from that inside the glass. The primary phase crystal was devitrite. The usual hump shaped curves for the rate of growth versus temperature were obtained. It was found that the experimental data fitted the following formula quite well.

$$U = Ce^{-A/T_{ab}(T_{liq} - T)}$$

Where A, C = constant

U = growth rate

T = heat treatment temperature

T_{liq} = liquidus temperature.

G. O. Jones[33] gave the figure of 15 $^{k\ Cal}/_{mol}$ as the typical value for A. The length of the crystal versus time curves were straight lines at short time interval but tailing off afterwards.

A. T. Milne[34] studied a soda lime silica glass with heat treatment at different temperature for different time. Above the maximum growth rate temperature, the linear growth rate varied inversely proportional to the degree of undercooling. The log rate of growth versus $^{1}/_{T_{ab}}$ curve was a straight line at low temperature range. The calculated activation energy was about 10 $^{K\ cal}/_{mol}$.

H. R. Swift[35] studied the effect of magnesia and alumina on the rate of crystal growth. Heat treated specimens were examined under a microscope at room temperature. The longest crystal was taken for

measurement, but sometimes, the same crystal was measured at different time interval of heat treatment. The crystals were found to originate from the surface. All the crystal length verus time curves were straight lines and the solution rate joined continuously to the growth rate versus temperature cruve. The primary phase crystal and the secondary crystal were all investigated. The maximum growth rate of the secondary phase crystal might be higher than that of the primary phase crystal. The inflexion point in the maximum growth rate versus composition curve corresponded to the entectic point in the phase diagram. The usual hump shaped rate of crystal growth versus temperature curves were obtained. The experimental data were found to be close to the formula

$$R = \frac{2\rho}{\eta} (T_{liq} - T)$$

Where R = growth rate
η = viscosity
T = heat treatment temperature
T_{liq} = liquidus temperature.

O. N. Grauer and E. H. Hamilton[36] studied the liquidus temperature and crystal growth of a soda lime silica glass with a gradient furnace. The usual hump shapedcurves were obtained for crystal size versus temperature. All the crystal length versus time curves were straight lines passing through origin.

J. T. Littleton[37] reviewed Dietzel's work on crystallization of soda lime silica glass. The rate of growth was determined by the time taken for a crystal to reach a length of three hundred microns. The usual hump shaped curves were obtained. The maximum growth rate temperature changed with glass and also this temperature did not correspond to any specific viscosity value. A straight line was obtained for the maximum growth rate versus fluidity. When the product of growth rate time viscosity was plotted against the temperature, the

straight line of the high temperature side extended far beyond the maximum growth rate point into the low temperature range.

T. B. Yee and A. I. Andrews[21] also investigated the growth rate of titania crystals in the enamel. Data was obtained from both photo and electron micrographs. The replica technique was used in the electron microscope. The growth rate was found to increase with temperature over the temperature range studied.

J. G. Morley[38] studied the crystal growth rate of five binary lithium silicate glasses with a microfurnace type hot stage microscope. Cristobalite, tridymite, lithium disilicate and lithium metasilicate were found to be the crystalline phases by X-ray diffraction. The growth of the crystals was found to be linear with time. The usual hump shaped growth rate versus temperature curves were obtained. The maximum growth rate of silica was about 340 microns per minute. The maximum growth rate of one lithium silicate was found to be about 850 micron per minute and that of the other was about 200 micron per minute. It was not possible to make positive identification as to which of these lithium silicates showed the very high growth rate. The maximum growth rate of the lithium silicate with a high growth rate increased with higher lithium oxide content at first and then levelled off at about 850 micron per minute at still higher lithium oxide content. Morley suggested that the growth rate might be limited by the rate of heat transfer during the crystal growth process.

G. E. Rindone[39] studied the influence of platinum on the crystallization in a binary lithium silicate glass containing twenty mole percent of lithium oxide. The rate of crystallization was increased with platinum content. Platinum precipitated out before heat treatment, because the glass was grey in colour. X-ray diffraction was used to measure the percentage of crystal in the specimen. The percentage of crystal versus time curves were all straight lines for short time periods but tailed off at longer time. When the activation energy was calculated, it was found that the original value of 120 $^{K\ cal}/_{mol}$

without platinum decreased to 50 K cal/mol at higher concentration and maintained this value. Lithium oxide rich regions were said to be found in the electron micrograph. These regions increased from 250 to 500 Å after platinum was added.

II. NUCLEATION.

The crystallization characteristics of the glasses in this Li_2O - ZnO - SiO_2 ternary system were compared with a commercial soda lime silicate glass. The glass used was G.E.C. Wembly X-8. It is a complex glass and its liquidus temperature is given at 850°C. Specimen rods were heat treated individually at about 50°C intervals in the temperature range from 390°to 650°C for one or two days. After the heat treatment, the specimens remained clear, and no change could be detected with a microscope. These specimens were then further heat treated at 750°C for one or two days. These specimens deformed and their surface became cloudy. When they were examined with a microscope, islands of crystals were found on the surface, but no crystals were found in the interiors of the rods. Other specimens were heat treated at 750°C for two or three days without previous heat treatment, and again only surface devitrification was observed. When the specimens which had been heat treated at 750°C for two days were compared, no significant difference was found between those with previous low temperature heat treatment and those without.

Two series of experiments were done on specimens of glasses in this ternary system. In one series, the effect of temperature was investigated. In the other series, the effect of time was investigated.

The specimens of five glasses were investigated. Their compositions, liquidus temperatures and primary phase crystals were listed in Table 12.

Table 12

Glasses used in the nucleation experiment

Glass number	Composition (mol %) Li_2O	ZnO	SiO_2	Liquidus temperature	Primary phase crystals
1	25	10	65	1008 ± 5°C	tridymite
2	23.75	10	66.25	1056° ± 5°C	tridymite
3	23.75	11.25	65	985° ± 5°C	$Li_2O \cdot ZnO \cdot SiO_2$
4	20	15	65	1120° ± 5°C	tridymite
5	15	20	65	1230° ± 5°C	tridymite

1. Effect of temperature.

(1) Experimental work.

The specimens in the form of triangular rods of the first three compositions were heat treated individually in a horizontal gradient furnace in the temperature range of 400° - 550°C for twenty four hours. They wereexamined at room temperature visually and under the microscope. After the examinations, one side of each rod was ground and polished and the whole specimens were immersed in 1% hydrofluoric acid for ten minutes. The ground and polished surfaces were examined under a microscope with reflected light. Freshly broken surfaces of the high temperature and low temperature end of the specimen of glass No. 1 were examined with an electron microscope with replica technique. Also the high temperature zone of this specimen was examined by X-ray diffraction.

These specimens were then subjected to further heat treatment. The temperature of the furnace was raised from 550°C to 750°C in one hour. These specimens were then examined under a microscope before they were held at 750°C for half an hour.

Table 12

Glasses used in the nucleation experiment

Glass number	Composition (mol %) Li_2O	ZnO	SiO_2	Liquidus temperature	Primary phase crystals
1	25	10	65	1008 ± 5°C	tridymite
2	23.75	10	66.25	1056° ± 5°C	tridymite
3	23.75	11.25	65	985° ± 5°C	$Li_2O \cdot ZnO \cdot SiO_2$
4	20	15	65	1120° ± 5°C	tridymite
5	15	20	65	1230° ± 5°C	tridymite

1. Effect of temperature.

(1) Experimental work.

The specimens in the form of triangular rods of the first three compositions were heat treated individually in a horizontal gradient furnace in the temperature range of 400° - 550°C for twenty four hours. They wereexamined at room temperature visually and under the microscope. After the examinations, one side of each rod was ground and polished and the whole specimens were immersed in 1% hydrofluoric acid for ten minutes. The ground and polished surfaces were examined under a microscope with reflected light. Freshly broken surfaces of the high temperature and low temperature end of the specimen of glass No. 1 were examined with an electron microscope with replica technique. Also the high temperature zone of this specimen was examined by X-ray diffraction.

These specimens were then subjected to further heat treatment. The temperature of the furnace was raised from 550°C to 750°C in one hour. These specimens were then examined under a microscope before they were held at 750°C for half an hour.

(2) Results.

In contrast to the commercial soda lime silicate glass investigated previously, all specimens were pale opal in colour at the high temperature zone, but remained clear at the low temperature zone, after the initial heat treatment at the lower temperature. When the specimens were viewed with transmitted light, the colour changed gradually along the rod indicating the change in size of the light scattering particles. The lengths of the specimens which gave light scattering effect varied slightly, but the temperature range was approximately from 500° - 550°C.

Small broken pieces from the high temperature end of the specimens were examined under a microscope with transmitted light. Small spheres of crystals were found. The crystals at the same temperature were found to be very uniform in size. They were about seventy microns at sections heat treated at 550°C and about thirty five microns at 520°C. Below 500°C, no crystals were detected. In these broken pieces, half spheres of crystals were found to be at the edges with the edges passing through the centres of the crystals. Sometimes sectors of crystals were found to lie with the centres of the crystals at the corners of the broken pieces. These seemed to suggest that the specimens broke along the cleavage planes of the crystals and that these cleavage planes were radiating from the centres of the crystals. Owing to the uncertainty of the thickness of the broken pieces, it was found difficult to estimate the number of crystals at different temperature.

By the Beche line technique, all these spherical crystals were found to be lithium disilicate. This result was confirmed by X-ray diffraction on the specimen of glass No. 1, and no other crystals were identified. The concentration of the lithium disilicate was about three percent. Calculated from the size and concentration of the lithium disilicate crystals, the number of crystals was about 10^{5} per cubic centimeter, compared with 10^{15} per cubic centimeter in the commercial glass ceramic.

Besides the big spherical crystals described above, there were a lot of tiny crystals in the glass matrix of the high temperature zone of the specimens. These tiny crystals were just visible with 350 X magnification, so they should be smaller than one micron. When these broken pieces were examined with light perpendicular to the optical axis of the microscope, a cloudy appearance was observed. Some specimens without heat treatment were examined under the same conditions and no light scattering effect was observed.

Some electron micrographs were taken on the broken surfaces of the high temperature end and the low temperature end of the specimen of glass No. 1 by Mr. J. Lewins of the Department of Glass Technology. Some electron micrographs were reproduced as Fig. 10, 11 and 12. The carbon replica technique was used. Unfortunately, the micrographs were not very clear due to the low contrast of the replica with this technique. A platinum preshadowed carbon replica will provide much more detail, but this technique on glass specimen was not yet acquired into perfection by Mr. J. Lewins. However, the present micrographs did show up the difference between the section at the high temperature zone and that at the low temperature zone. Some particles of the size of 0.4 micron were found on the micrograph of the high temperature zone specimens only. This corresponded fairly well with the observation under the microscope. Therefore there were two sizes of crystals present in the heat treated specimen. The size of the big crystals was too big and their number was too few to give the light scattering effect. Therefore the light scattering effect might be mainly due to the small crystals.

Electron Micrographs.

Magnification 40,000 X.

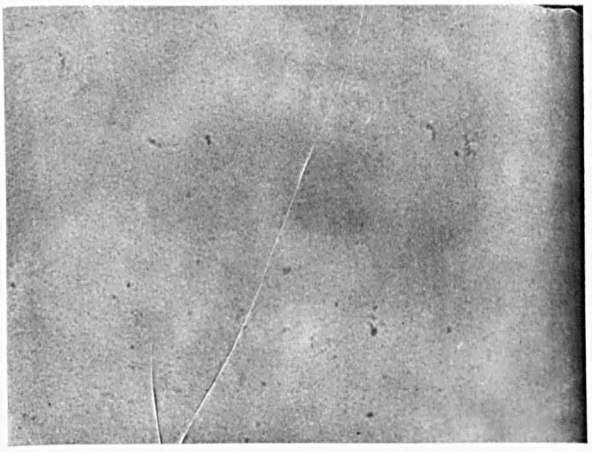

Fig.10

Unheat treated soda lime silicate X-8 glass.

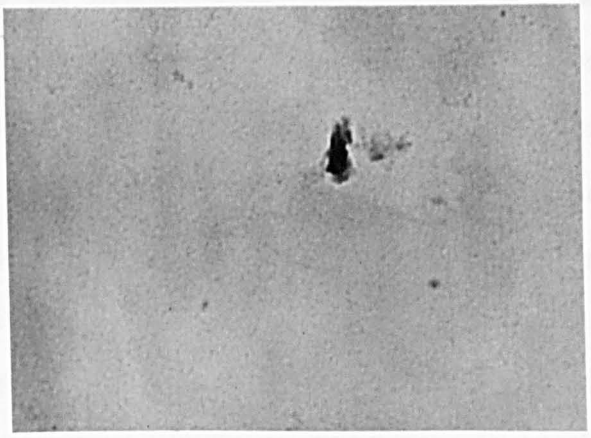

Fig.11

Glass No. 1 heat treated at about 430 °C for 24 hours.

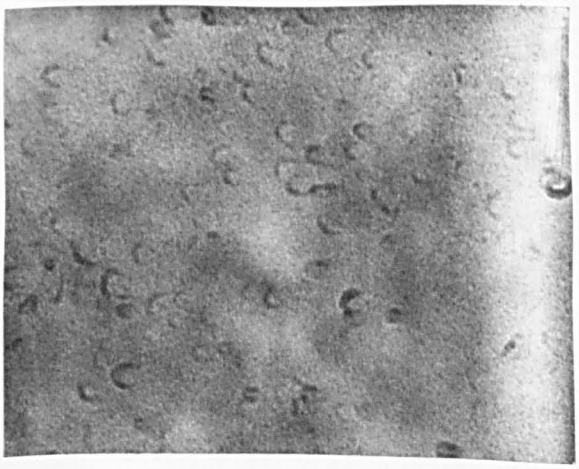

Fig.12

Glass No. 1 heat treated at 550 °C for 24 hours.

After the hydrofluoric acid treatment, some small pits were found on the polished surface. On examination under the microscope with reflected light, these pits were found to be of the shape and size of the well developed spherical big crystals observed with transmitted light. Therefore these pits were the sites of these crystals preferentially attacked by the acid. More pits were found at the higher temperature zone.

The polished surface seemed to be smooth except for the pits, after the acid etching, but the original surface of the whole rod was not smooth. This indicated that the properties of the surface were significantly different from that of the bulk of the glass. One specimen without heat treatment was also acid treated at the same time, and the surface remained bright and clear. This suggested that heat treatment had produced regions on the surface which caused the etched effect on the surface due to differential acid resistance, and that the structure of the low temperature zone was not as random as that of the non heat treated specimen, although it did not have any light scattering effect.

After the heat treatment from 550° to 750°C, the lithium disilicate crystals at the high temperature zone had grown to 125 micros. The size of the crystals in the same temperature zone was found to be as uniform as before. Small lithium disilicate crystals were found to extend to the lower temperature zone. The tiny crystals were bigger and easier to be seen, but they were still too small to be measured with a microscope.

After the specimens were held at 750°C, they were examined under a microscope with transmitted light. The lithium disilicate spherical crystals were found to merge into each other at the high temperature zone. Some small lithium disilicate crystals seemed to have developed

at the high temperature zone indicating that new crystals were formed at the heat treatment at 750°C. The tiny crystals could be seen in the gaps of the big spherical crystals.

2. Effect of time.

(1) Experimental work.

Glasses No. 1, 4 and 5 were investigated in this series. The heat treatment consisted of holding at 550°C for twenty four hours, raising the temperature to 750°C and holding at 750°C for eight hours.

Eleven specimens of glass No. 1 were heat treated. One specimen was taken out at the end of the heat treatment at 550°C for ½, 1, 2, 4, 8, 16 and 24 hours; when the heat treatment had reached 750°C; and after the heat treatment at 750°C for 2, 4 and 8 hours. Five specimens of glass No. 4 and 5 were heat treated. The effect of time in heat treatment at 550°C for less than twenty four hours was not investigated, so they were all heat treated at 550°C for twenty four hours before they were heat treated at higher temperature.

(2) Results.

The specimens were intended for examination in the electron microscope. Owing to the experimental difficulties of the replica technique, only visual and microscopic examinations were done. The results of the examinations were present in Tables 13-15. All the specimens were found to retain their original shapes, and no deformation was noticed.

Table 13

Results of heat treatment of glass No.1

Heat treatment			Result	
550°C	550° - 750°C	750°C	Appearance	Crystalline phases
½ hr.	-	-	Transparent	None
1 hr.	-	-	"	"
2 hrs.	-	-	"	"
4 hrs.	-	-	"	"
8 hrs.	-	-	Slight light scattering.	"
16 hrs.	-	-	Light scattering increased.	Spherical lithium disilicate 40 μ and tiny crystals.
24 hrs.	-	-	Light scattering further increase.	Spherical lithium disilicate 65 μ and tiny crystals.
24 hrs.	1 hr.	-	Slight opal	Spherical lithium disilicate 120 μ and slightly bigger tiny crystals.
24 hrs.	1 hr.	2 hrs.	Light opal.	Spherical lithium disilicate 50 - 180 μ and bigger tiny crystals.
24 hrs.	1 hr.	4 hrs.	Opal.	Lithium disilicate size varied but could not be measured because crystal merged.
24 hrs.	1 hr.	8 hrs.	Opal.	Same as above.

Table 14

Results of heat treatment of glass No.4.

Heat treatment			Result	
550°C	550° - 750°C	750°C	Appearance	Crystalline phases
24 hrs.	-	-	Light scattering.	Spherical lithium disilicate 25 μ much less in number. Higher concentration of tiny crystals.
24 hrs.	1 hr.	-	Light opal.	Lithium disilicate merged into each other. The size was not uniform. Tiny crystals in the glass matrix.
24 hrs.	1 hr.	2 hrs.	Opal.	Lithium disilicate crystals merged together. High concentration of tiny crystals in the glass matrix.
24 hrs.	1 hr.	4 hrs.	Opal.	Lithium disilicate crystals merged together. High concentration of slightly bigger tiny crystals in the glass matrix.
24 hrs.	1 hr.	8 hrs.	Opal.	Lithium disilicate crystals merged together.

Table 15

Results of heat treatment of glass No.5

Heat treatment			Result	
550°C	550° - 750°C	750°C	Appearance	Crystals
24 hrs.	-	-	Light scattering.	None
24 hrs.	1 hr.	-	Light scattering.	High concentration of tiny crystals up to about 2 μ big.
24 hrs.	1 hr.	2 hrs.	Light scattering.	Similar to above.
24 hrs.	1 hr.	4 hrs.	Light opal.	High concentration of tiny crystals up to about 4 μ big.
24 hrs.	1 hr.	8 hrs.	Light opal.	High concentration of tiny crystals up to about 5 μ big.

III. STEADY STATE CRYSTAL GROWTH.

1. HOT STAGE MICROSCOPE.

(1) Design of various types of hot stage microscope.

Before deciding which form of hot stage microscope was going to be constructed, a survey of the design of hot stage microscope was made. Although numerous modifications had been used by different workers to suit their own purposes, all the designs could be allocated into one of the three groups described below.

a. Conventional furnace with an auxiliary lens system.

With this design, a conventional furnace is used. The real image of the specimen in the furnace is formed by the auxiliary lens system. The real image, which is outside the furnace, is then viewed by microscope. The general design of this type is shown diagrammatically in Fig. 13.

The temperature of the specimen can easily be measured and controlled to within close limits by conventional methods. The specimen can be quite big and the protection of the objective lens of the microscope is comparatively easy. The limitation of this design is the magnification that can be achieved. Owing to the auxiliary lens system, the resolving power is seriously diminished. Also it is difficult to use polarized light because normally reflected light is used in this design.

This type of hot stage microscope was tested at room temperature to investigate the characteristics of the optical system. A lens systems with 4.5 inches focal length and a 45° prism were used as the auxiliary lens system, to throw the image of the specimen outside the furnace. It was found that the distance of relay lens system from the specimen was long enough so that a water cooling system might not be necessary for

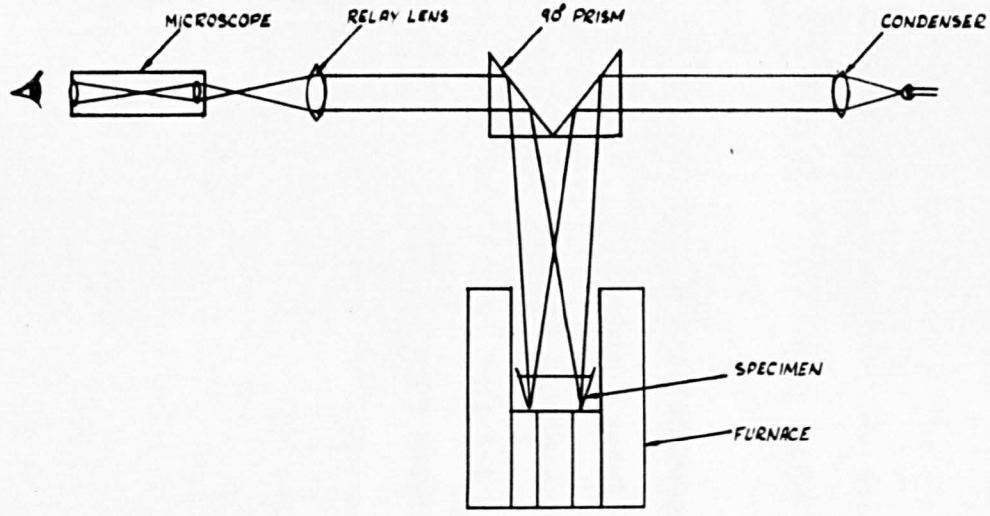

FIG 13 OPTICAL ARRANGEMENT OF HOT STAGE MICROSCOPE WITH RELAY LENS SYSTEM.

protection of the optical system. The magnification could also be varied within limits and it was possible to obtain a magnification of 50X without undue difficulties. However, the use of a relay lens system decreased the resolving power greatly. Different methods of illuminating the specimen were tried, but the resolution was still poor. It was felt that while this type of design could be improved by using a more suitable relay lens system, the improvement would not be likely to meet the present requirement. Also the thermal capacity of the conventional furnace would be too big and the change of the specimen temperature would not be quick enough. Therefore, this system was not investigated any further.

b. Hot wire furnace on the stage of microscope.

Several workers have used a noble metal wire or a thermocouple to form a loop to hold the specimen which is heated by a current flowing through the wire. This hot wire furnace is placed directly on the stage of the ordinary microscope. The temperature is measured by the emissivity of the metal wire or the e.m.f. of the thermocouple. With suitable design, the heating and the temperature measurements are essentially continuous.

The energy used in this type of the furnace is so small that the objective lens can be brought fairly close to the specimen without water cooling. Therefore, the resolution and magnification are higher than in any other design. The thermal capacity of the unit is small and the temperature can be changed very quickly. The incorporation of a controlled atmosphere chamber is relatively easy. By means of voltage stabilizer and closed specimen chamber, the temperature of the specimen can be controlled to close limits for reasonable periods. The chief limitation of this design is the small size of the specimen and the temperature gradient in the specimen.

A hot stage microscope of this design manufactured by Griffin and George Ltd. was tried. The hot wire furnace was a 5% Rh/Pt - 20% Rh/Pt thermocouple. Using a silican diode crystal in the circuit to separate the heating and thermo-electric currents, the thermocouple was heated at alternate half cycles of the supply voltage; in the intermediate half cycle when the heating current was cut off, a phased switching system was used to connect the thermocouple to the temperature measuring circuit. Therefore, the heating and the temperature measurements were practically continuous. The working temperature of this microscope was up to 1800°C in inert atmosphere. The temperature of the hot wire could be controlled to within 1°C for longer than six hours and could be changed very quickly. The specimen was held by surface tension at the junction of the thermocouple and its dimensions were about 0.15 mm. X 0.15 mm. X 0.7 mm.

Powdered specimen of composition 30 mol % Li_2O, 5 mol % ZnO, 65 mol % SiO_2 was used for the investigation. During the trial, it was found that the amount of specimen used, had a pronounced effect on the accuracy of the temperature measurement. When too big a specimen was used, the apparent liquidus temperature was up to 60°C higher than the actual liquidus temperature. When the right amount of specimen was used the liquidus temperature could be reproduced within 5°C easily. However the shape of the thermocouple junction was found to be very critical for correct temperature measurement. Magnification and resolution were good with this design. Therefore it would be very useful for liquidus temperature measurement, if equilibrium could be obtained in less than a few hours.

When this apparatus was tried for the study of crystal growth rate, difficulties were encountered. Owing to the small size of the specimen, the surface had an appreciable curvature. Therefore the specimen itself acted as a lens and accurate measurement of the dimensions of the crystal could not be obtained. The depth of the field of the long working distance objective was quite deep, so different dimensions could be assigned to the same crystal by adjusting the distance of the objective from the specimen, even though the crystal was still in focus all the time. Also crystals which grew from the thermocouple interfered with the observation of the crystal inside the melt and bubbles evolved continuously from the glass-thermocouple interface in a certain range of temperatures. The lithium silicate crystals grew very rapidly and it took less than 20 seconds for the crystal to grow from side to side even at comparatively moderate growing rates for the type of crystals. Owing to these difficulties, it was felt that this type of hot stage microscope would only be suitable for the determination of liquidus temperature but not for the study of crystal growth rate.

c. Unconventional furnace on the stage of microscope.

With this design, a micro-furnace is placed on the stage of the microscope. Transmitted light or reflected light can be used. To protect the objective lens, which is fairly close to the furnace top, an elaborate cooling system has to be incorporated into the design.

Magnification and resolution are between that of the conventional furnace design and that of the hot wire furnace design. The specimen cannot be very big, but up to 0.5 cm. is possible. The measurement of the specimen temperature is not easy owing to the thermal gradient in the furnace. It is not easy to incorporate

a micro-furnace with a controllable atmosphere. The temperature of the furnace is very sensitive to draughts because of its low thermal capacity. On the other hand, rapid temperature change is possible.

Although there are several disadvantages with this type of hot stage microscope, this design has been proved to be successful by J. G. Morley, studying the crystal growth rate of lithium silicate. The main disadvantage is that the construction is complicated, because of the provision of water cooling and the supply of very high a.c. current at low voltage. However, it was felt that this type of hot stage microscope would be most suitable for the study of the growth rate of crystal in glass. The detailed design of the instrument used in the present study is described in the next section.

(2) Design of the present hot stage microscope.

(a) Optical arrangement.

The design of the present hot stage microscope was based on that used by J. G. Morley, in investigating the crystal growth in binary lithium silicate glasses. Only slight modifications were made on the original design. The general arrangement was shown in Fig. 14a and 14b.

The design of the furnace depended mainly on the objective lens used in the microscope. To minimize the temperature gradient in that part of the furnace where the specimen would be, the furnace had to be very long compared with the size of the specimen. Therefore an objective lens with a long working distance and reasonable magnification and numerical aperture was necessary to obtain good magnification and resolution. During the design stage, the readily obtainable objective lens was that manufactured by Cook Troughton, and Simms, having an initial

Fig. 14a.

General arrangement of the hot stage microscope.

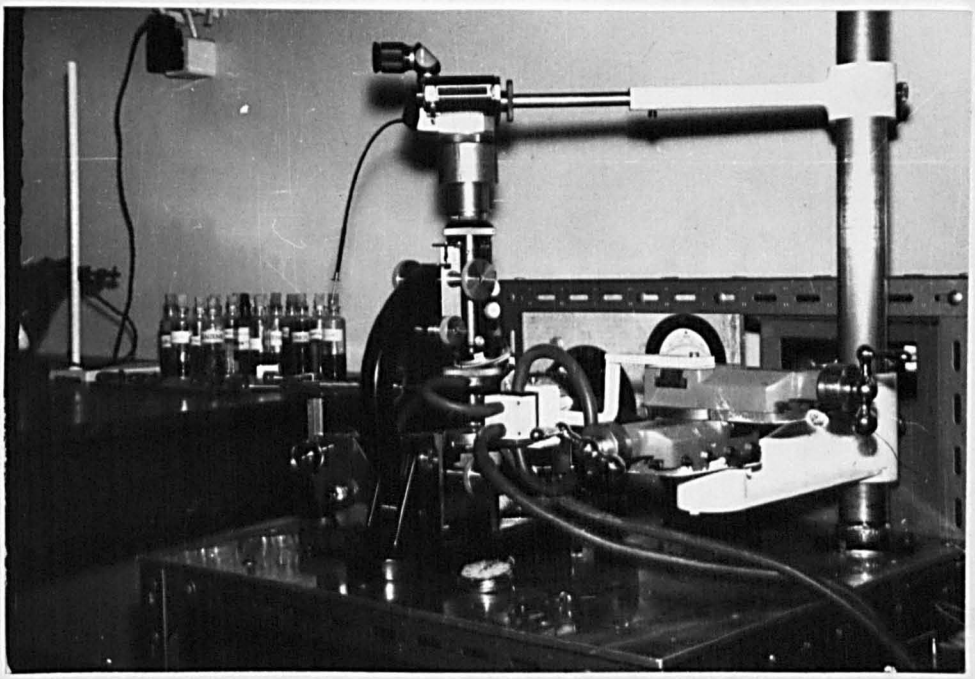

Fig. 14 b.

Showing microfurnace, thermocouple and water cooled objective and sub stage condenser.

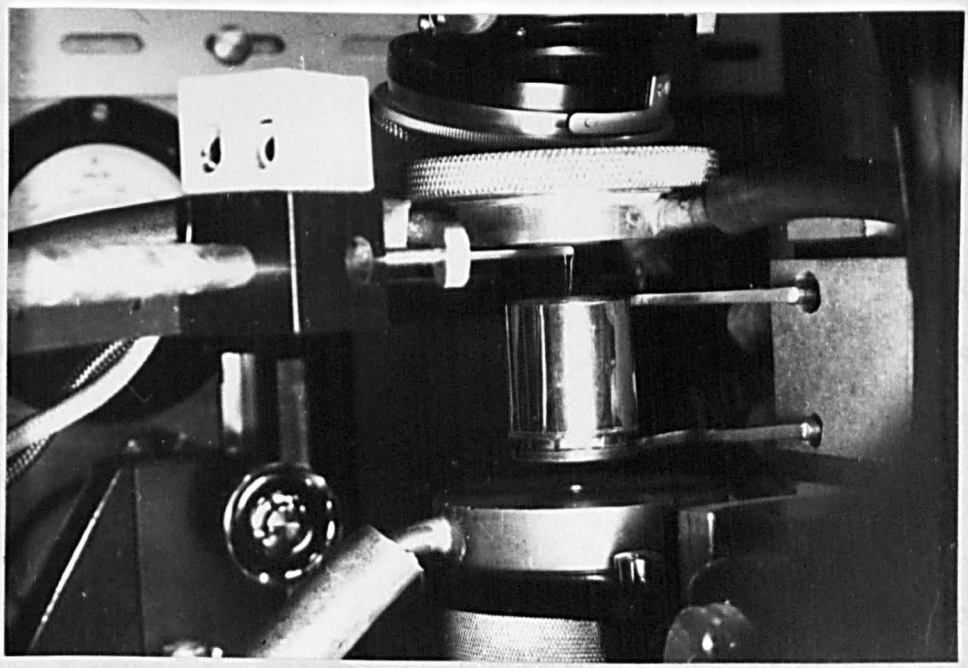

magnification of 5X, a numerical aperture of 0.15 and a working distance of 17 mm. The furnace was therefore designed according to this objective.

The microscope used was a polarizing microscope Model MP made by James Swift and Son Co. The body of the Pentax single lens reflex camera made by Asahi of Japan was used to photograph the specimen. The lens of the camera was taken off and a microscope adaptor was put into its place. Illumination was provided by transmitted light from a Swift ML microscope lamp.

The camera was first mounted on top of the microscope with a microscope adaptor which did not fit the eye piece of the microscope very well. A tube was then made to enable the adaptor to fit the microscope used. It was later found that the camera unit was so heavy that the microscope slipped slightly. Therefore the camera was finally mounted independently. A graticule with one hundredth of a centimeter scale was used in the eye piece. The adjustment of the top lens of the projecting eye piece was not enough, so a ring about one centimeter high was placed in between the graticule and the top lens of the eye piece to act as a spacer to project the eye piece scale onto the film.

The heat from the furnace was quite intense, so a water cooling jacket was used to protect the objective lens. The working distance of the original sub-stage condenser was not long enough, and an identical long working distance objective with a water cooling jacket was used in place of the substage condenser. The design of the water cooling jacket is shown in Fig. 15. A film of water about one millimeter thick was maintained in front of the lens by continuous pumping. The water was pumped through a close circuit from a tank to the water cooling jacket of the objective lens then the furnace terminal, the water cooling jacket of the sub-stage

FIG 15 DESIGN OF WATER COOLED OBJECTIVE AND CONDENSER.

(EXPLODED VIEW)

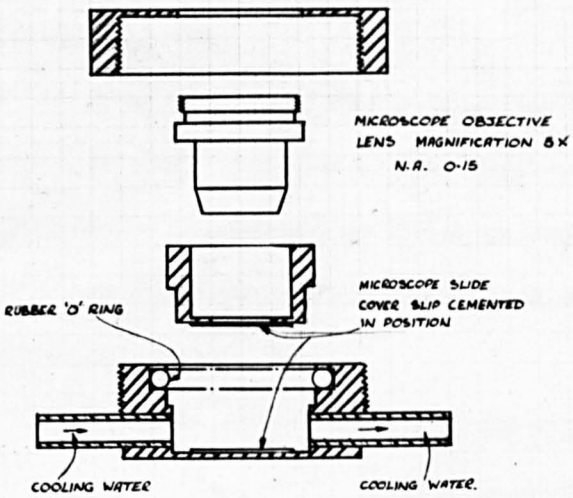

FIG 16

MICROFURNACE

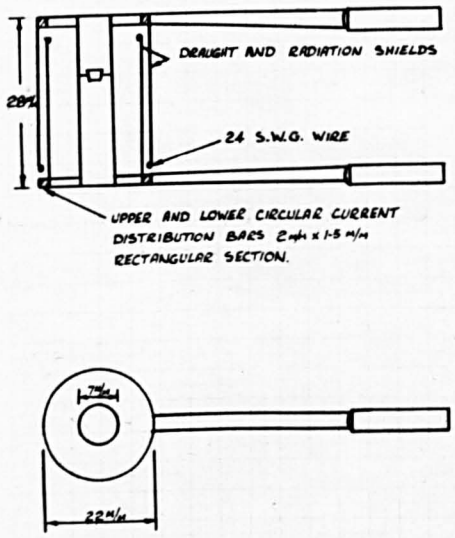

FIG 17

EFFECT OF THE NUMERICAL APERTURE
OF THE OBJECTIVE LENS ON THE FURNACE.

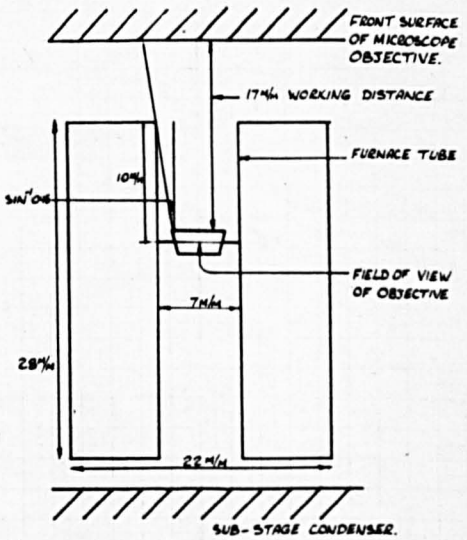

lens and finally back to the tank. This system did not seriously impair the optics of the system and protected the lens from overheating at furnace temperature up to 1400°C.

The polarizer of the microscope was in the optical system all the time, but the analyser could be put in and out of the optical system by operating a lever.

Throughout the present study, the microscope was screwed down onto the base plate of the unit; the camera support and the furnace terminal block support were secured at fixed points of the support column. Therefore the distance between the specimen and the camera body would be the same.

During the trial run of the instrument, it was found that the distance between the objective water cooling jacket and the top of the furnace was only three millimeters. Although the objective lens was not unduly heated, there was not enough room to operate the thermocouple. By this time, it had become known that James Swift and Son Ltd., produced an objective lens with working distance 26 mm, a numerical aperture of 0.16 and initial magnification of 5X. Since this objective was better in every respect for the present study, it was acquired and used throughout the study. The distance that the thermocouple could be moved vertically was now about one centimeter.

(b) Furnace Design.

The micro-furnace was constructed from thin 10% rhodium/platinum sheets according to the design shown in Fig.16. The heating element was a tube mounted vertically, having a circular diaphragm one centimeter from the top. This tube was welded onto the thin upper and lower circular plates which in turn were welded onto the circular current distribution bars.

This furnace was supported by two heavy current input leads terminated in the circular distribution bars. The outer radiation and draught shield was welded to the outside of the upper circular bar and the inner one was welded to the inside of the lower circular bar. The whole unit was made of the same material to minimize the unavoidable thermal stresses.

When the furnace was in operation, the furnace tube expanded. The thin upper and lower circular plates acted as buffers to minimize the thermal stress on the tube. The mechanical support was provided by the heavy current input bars and the circular distribution bars. The two radiation and draught shields were invaluable in improving the temperature distribution and decreasing fluctuation. The diaphragm was put at a point higher than the middle point of the furnace tube, because it had been found by previous worker that the highest temperature would be at this point. Also the temperature gradient in this region was expected to be very small. The specimen holder was actually a tapered ring which sat on the hole in the diaphragm. The melt was held in position by its own surface tension.

The dimensions of the present furnace were slightly modified. Since crystals growing from the side of the specimen holder interfered with observation of the crystal inside the melt, the specimen holder was enlarged from three to four millimeter. The geometry of the furnace was dictated by the size of the specimen holder and the numerical aperture of the objective lens. These effects were shown in Fig. 17. Therefore the diameter of the furnace tube was increased to seven millimeter to obtain the best result. Too wide a tube was avoided, because it was felt that this would increase the temperature gradient inside the furnace. The length of the tube was also increased from twenty to twenty seven millimeters to obtain better temperature distribution.

In order to carry the greater weight of the furnace and to withstand the mechanical resistance of the flexible heavy current leads connecting the furnace terminal block with the transformer, two "sliding heads" of small lathe mounted at right angles to each other, were used to construct the mechanical stage unit instead of using the ordinary mechanical stage. The two "sliding heads" provided means to adjust the horizontal position of the furnace so that the furnace tube would be in alignment with the microscope at all temperatures. The mechanical stage was mounted on a column which also provided the independent support for the camera.

(c) Power supply arrangement and temperature measurement.

Large low voltage current had to be used to provide the power. The circuit diagram was shown in Fig.18. A voltage stabilizer was used to steady the input voltage. A small Variac was placed between the stabilizer and the transformer to control the voltage input to the transformer. The reduction ratio of the transformer was one to eighty. The transformer was connected to the furnace terminals by seventy ordinary 5 ampere copper wires to provide flexibility. The copper furnace terminals were water cooled by close circuit water. The insulated furnace terminal block was fixed at the end of the mechanical stage unit. The two heavy current input leads of the furnace were secured onto the terminal block by screws.

During the experiment, 60 to 120 amperes at 0.8 to 2 volts was used. The relationship between the applied voltage on the primary phase of the transformer and the specimen temperature was shown at Fig. 19. The temperature achieved at the same applied voltage was not the same every time. The temperature seemed to be affected by the ambient temperature and the temperature of the cooling water.

FIG 18 CIRCUIT DIAGRAM OF MICROFURNACE.

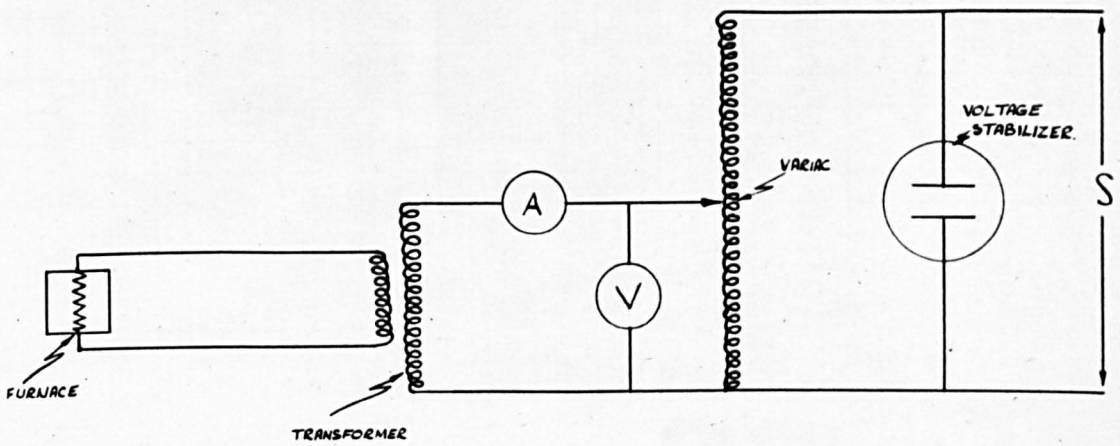

FIG. 19. PRIMARY PHASE VOLTAGE V SPECIMEN TEMPERATURE.

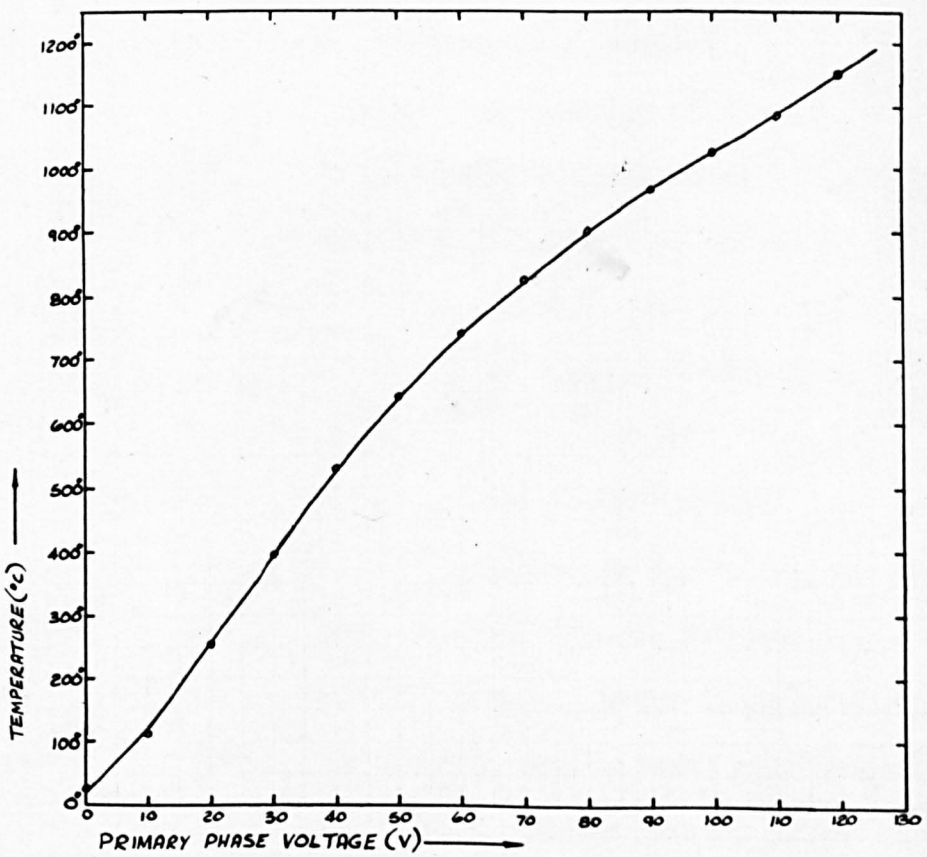

The thermocouples used were of 13% Rh/Pt - Pt. The wire diameter being only 0.004" in order to minimize errors due to thermal conduction up the thermocouple leads and to obtain a very small junction. These thermocouples were carried in twin bore fused silica sleeves. In the present study, one of the thermocouples was used to nucleate the crystals, and the other was used for periodical calibration purposes. Both of them had to be put into the confined space of the furnace tube. Therefore they were carried in two three-dimension micromanipulators to facilitate the accurate movement.

The thermocouple leads were connected to compensating leads in junction boxes situated at the micromanipulators. The compensating leads were connected at the ice junction to copper leads which terminated at the potentiometer. A two way switch was used to connect the unbalanced voltage from the potentiometer either to scale lamp galvanometer, or the Graphspot. The Graphspot is a spot follower device with a recorder, the speed of which can be varied widely by different combination of gears. The spot of light from the external light source is followed by a photocell, or an external electrical signal is converted into an internal light source by a built-in galvanometer. This instrument provides a convenient means of recording continuously an electrical signal or the movement of the spot of light from an external light source. The scale lamp galvanometer was used as the null-point instrument for standardizing the potentiometer or exact temperature measurement. The graphspot was used to provide a continuous record of the specimen temperature. When the graphspot was used, the potentiometer was set at six millivolt and the excess e.m.f. was fed into the Graphspot, so that a more sensitive scale could be used. Under these conditions, the scale on the chart was about three degree centigrade to one millimeter. This was accurate enough for the crystal growth study.

During the periodic calibration of the thermocouples, the scale lamp was used and an accuracy of 0.1°C could be achieved.

2. EXPERIMENTAL WORK.

(1) Calibration of the graticule, the Graphspot and the thermocouples.

A graticule graduated in tenth of a millimeter was fitted into the microscope eye piece, and it appeared superimposed upon the photographs. It was necessary to calibrate the scale on the graticule so that the actual length of the crystals could be deduced. The camera and the microscope were independently supported so that the microscope could be focused onto various depths of the specimen which was about two millimeter thick. Therefore it was also necessary to investigate whether the vertical position of the crystals in the specimen could affect the magnification.

During the calibration, the microscope and the camera were fixed at the same position as in the experiment with the cooling water system operating. The furnace was first fixed at the usual position and the microscope was focused on top of the specimen. The furnace was then taken off. A stage micrometer calibrated in $\frac{1}{50}$th of a millimeter was carried by a three dimension micro-manipulator. Its position was adjusted to bring the stage micrometer into sharp focus. The scale of the stage microscope was at the same position as that of the top of the specimen. A photograph was taken. The stage micrometer was then lowered one millimeter and was at the same position as that of the middle of the specimen. The microscope was then readjusted to focus the stage microscope. Another photograph was taken. The same procedure was repeated with the stage micrometer at the same position as that of the bottom of the specimen. From this series of photographs, it was found that there was no detectable change of magnification due to variation of the positions of the stage micrometer. Under this

condition, the ratio between the two scales was found to be about two to three, and one small scale division on the graticule was about thirty-three microns. These photographs are reproduced as Fig.20.

The range used in the Graphspot was 0-10 MV. However it was found that the calibration was not exactly linear as stated in the operation manual of the instrument. Therefore calibration curves were obtained so that the temperature could be read off from the scale reading on the 250 millimeter wide chart in the Graphspot.

During the calibration, the output of a thermocouple in a furnace at constant temperature was used as the source of e.m.f. This was first balanced exactly by the potentiometer using the scale lamp galvanometer as null-point instrument. The potentiometer was then turned down at steps of one millivolt, and the unbalanced voltage was fed to the Graphspot. Four curves, two of which were with increasing voltage and the other with decreasing voltage were obtained. This chart was reproduced as Fig. 21. A calibration curve of scale reading - voltage applied was constructed from the data obtained from the chart. 6 MV was added to the data and the resultant millivolt was converted to temperature by appropriate conversion table. The calibration curve of scale reading-temperature was then plotted from these results, and was used in the experiment, during which the potentiometer was set at six millivolts. These calibration curves were shown in Fig.22.

In the present study, two thermocouples were used. Both of them were calibrated by specimen of known liquidus temperature, and the measured liquidus temperature was found to be within $\pm$ 2°C. In the determination of liquidus temperature or crystal growth rate, one of these thermocouples was immersed in the melt to measure the temperature and to nucleate the melt. This thermocouple was cleaned in hydrofluoric acid after an experiment on one specimen and was then calibrated by the other thermocouple. During the calibration, both thermocouples were put into the furnace and

Fig. 20.

Micrograph for the Calibration of Graticule.

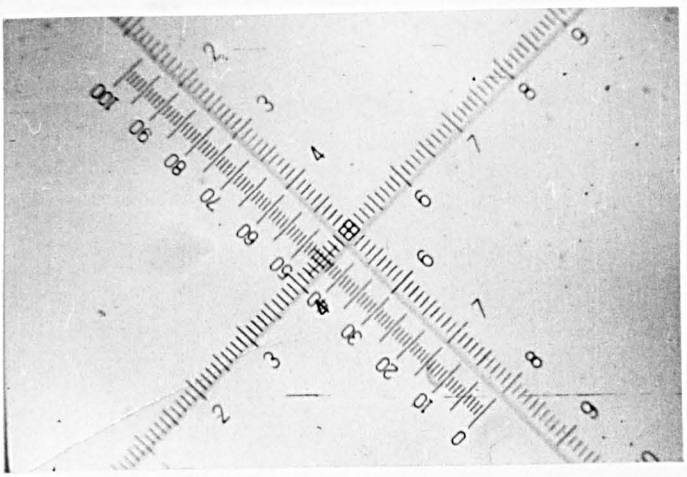

(a)

Stage micrometer at the top position.

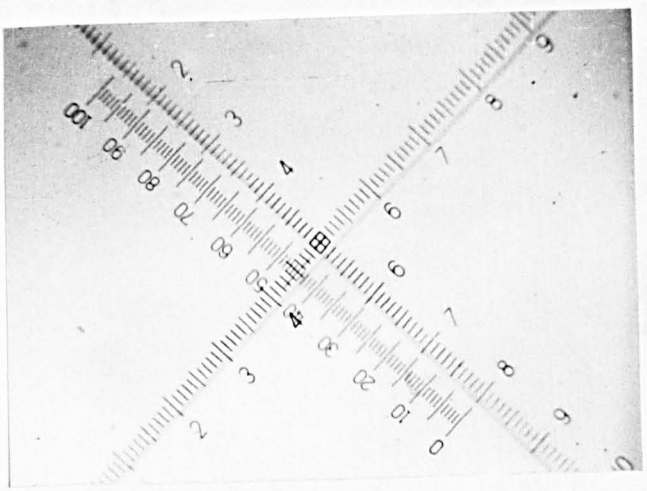

(b)

Stage micrometer at the middle position.

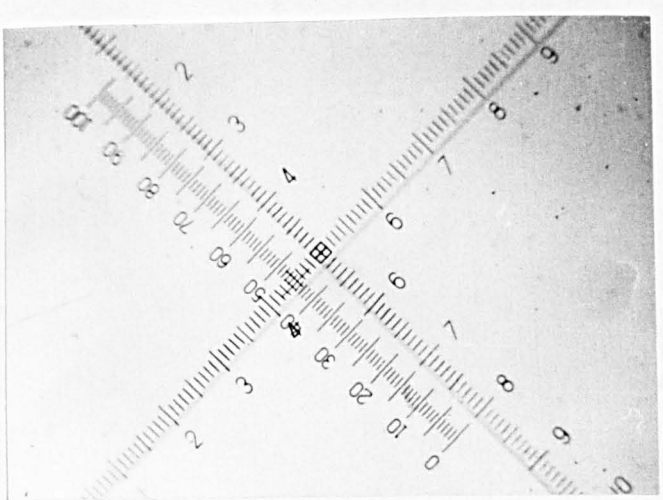

(c)

Stage micrometer at the bottom position.

FIG 21 GRAPHSPOT CHART FOR CALIBRATION OF SCALE READING.

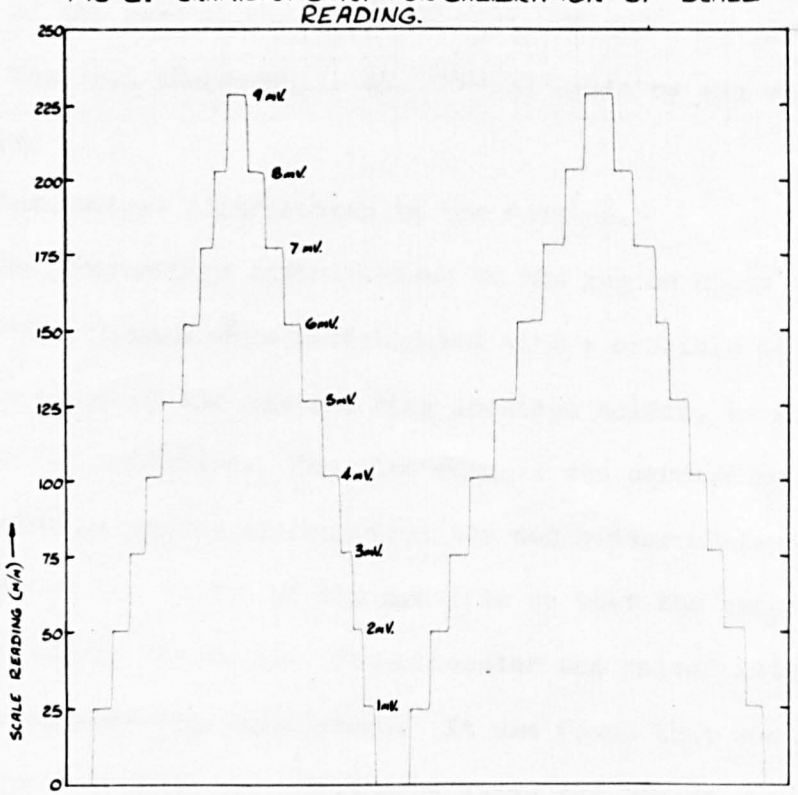

FIG 22 CALIBRATION CURVES OF SCALE READINGS.

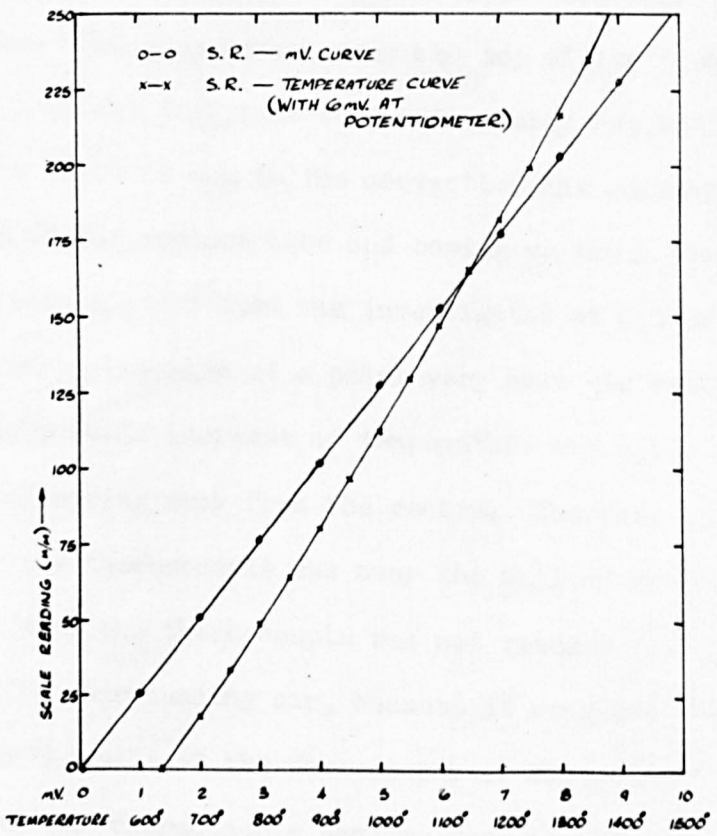

were placed very close together above the surface of a specimen. When the indicated temperatures differed more than 5°C, about one centimeter of the used thermocouple was cut off and a new junction was made. The used thermocouple was checked again by the standard thermocouple.

(2) Temperature distribution in the furnace.

The temperature distributions in the region above the specimen of the furnace were investigated with a crucible of the same size in place of the tapered ring specimen holder, to similate the experimental condition. The thermocouple was carried in the graduated three dimension micromanipulator and measurements started at the centre of the bottom of the crucible so that the exact position of the thermocouple was known. Potentiometer and galvanometer unit were used to measure the temperature. It was found that the maximum temperature was at about one millimeter above the rim of the crucible. The axial temperature variation, up to three millimeter above the crucible, was slight. The maximum variation in the crucible was about seven degrees. The temperature near the top of the furnace dropped rapidly and it was difficult to obtain steady reading at these points. This might be due to the convection air current going down at the centre of the furnace tube and coming up along the wall. The radial temperature distribution was investigated at 0.5 mm above the rim of the crucible and also at a point very near the bottom of the crucible. A very rapid increase of temperature was noted when the thermocouple was moving away from the centre. Increase of 26°C/mm. was noted when the thermocouple was near the wall of the furnace tube. It was felt that the thermocouple was not reading correctly the temperature of the surrounding air, because it received fairly high radiation from the wall of the furnace tube. Since this survey was done with the thermocouple hanging free in the air, the apparent temperature variation would be higher than the actual temperature variation of the air due to error introduced by the

radiation from the wall. Owing to this interference, the radial temperature distribution in the specimen was investigated. The thermocouple was immersed in the melt about one millimeter below the top surface. The maximum temperature variation was found to be only six degrees compared with about twenty degrees in the previous investigation. The axial temperature distribution was not investigated because it was found impractical to push the thermocouple into the bottom of the melt. However it would be safe to conclude that the maximum temperature variation at different points of the specimen was less than ten degrees centigrade. The temperature distribution curves were shown in Figure 23 and 24.

Earlier, it had been stated that this type of furnace was sensitive to draught and it was difficult to hold the temperature for a long period. It was found during this survey that, when the thermocouple was hanging free above the specimen, the temperature of the thermocouple junction dropped, up to 50°C, by just blowing into the furnace tube. However, if precautions were taken to avoid creating a disturbance in the room and the thermocouple was immersed in the melt, the recorded temperature was found to be within $\pm$ 2°C. for at least half of an hour. Since the time needed to study the growth rate at each temperature was ranging from thirty seconds to fifteen minutes in the present study, it was felt that the temperature of the specimen was steady enough for its present purpose.

(3) Determination of liquidus temperature.

A small piece of specimen of the composition under investigation was put in the specimen holder which was placed in a rider in a platinum crucible. The whole unit was then put into an ordinary electric furnace holding at temperature near the liquidus temperature of the specimen. After the specimen had melted and adhered to the specimen holder, the platinum crucible was taken out of the furnace. Some more specimen was filled into the specimen holder which was then returned to the furnace. This procedure was

FIG. 23. AXIAL TEMPERATURE DISTRIBUTION OF MICROFURNACE.

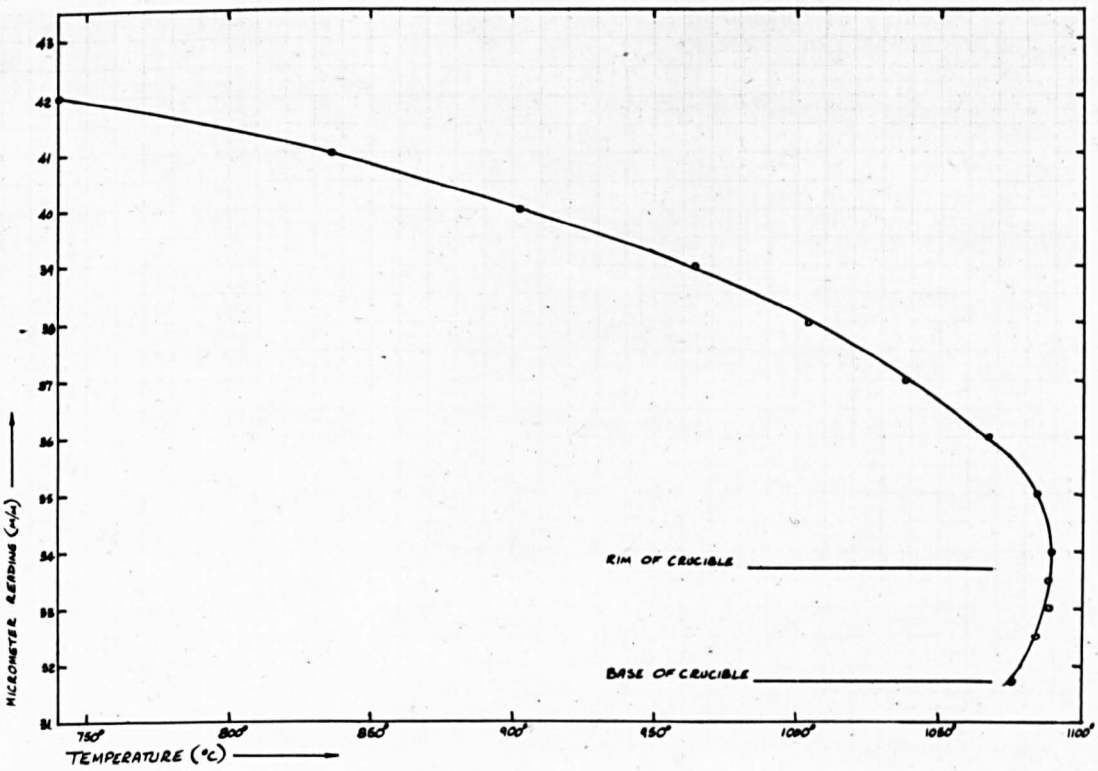

FIG. 24. RADIAL TEMPERATURE DISTRIBUTION OF MICROFURNACE

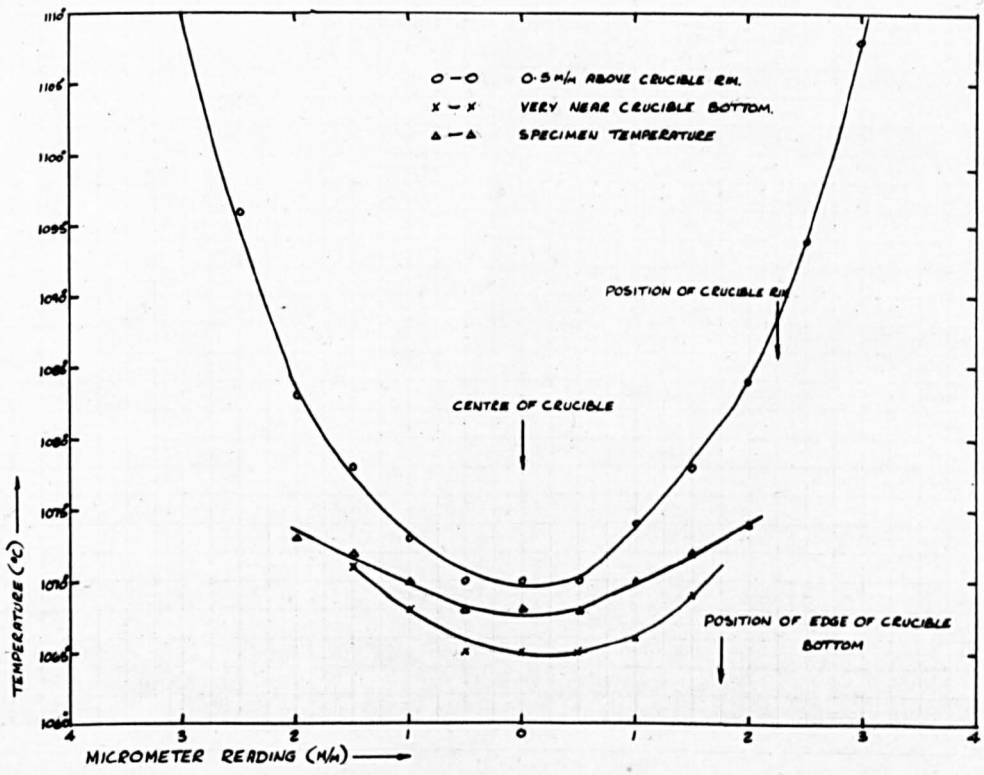

repeated until enough specimen had been filled in the holder. With this method, a specimen with a reasonable flat upper and lower surface could be obtained. Also it avoided the difficulty of filling the specimen holder without spilling while it was in the micro-furnace of the hot stage microscope.

The specimen was carefully placed in the diaphragm of the furnace, so that its surfaces would be as horizontal as possible, and the furnace was secured in its terminal block. The camera unit was taken off, so that the specimen could be observed visually more easily. The furnace was heated up slowly to just above the liquidus temperature of the specimen to melt all the crystals that might be present. With the aid of the microscope, the thermocouple was lowered into the melt until its junction was just immersed. The thermocouple was then raised to a position at temperature about 50°C. below the melt. The temperature of the melt was then lowered to about 50°C. below the liquidus. The glass coating on the junction of the thermocouple would then devitrify fairly quickly. Then the thermocouple was again lowered into the melt and crystal growth would start from the junction. The temperature of the furnace was raised to about 15°C below the liquidus temperature. The temperature was measured accurately with the potentiometer and galvanometer unit. Normally a small ball of crystals would form at the junction surrounded by the melt. This crystalline mass was observed until it reached its equilibrium size, usually taking about only one minute. The temperature of the furnace was raised in about 5°C. steps, and the furnace was held at each temperature for about five minutes and the crystals were observed. During that time, the temperature was measured. This procedure was repeated until all the crystals were dissolved. The liquidus temperature was taken as the middle temperature between that when the last trace of crystals had persisted and that when all the crystals had dissolved. The determination of the liquidus temperature was repeated three times and the results were within 5°C.

(4) Determination of the rate of crystal growth.

After the determination of liquidus temperature, crystal growth characteristics at three or four different temperatures were observed visually. The camera unit was then put back into position and illumination was adjusted. The potentiometer was set at six millivolt and the unbalanced voltage was fed into the Graphspot. After all the adjustmen had been made, the measurement of crystal growth rate could then begin.

In the determination of the rate of crystal growth, the position of the crystals was controlled by nucleating the melt with the thermocouple. The temperature of the melt was raised well above the liquidus temperature and held there for a while to dissolve any crystal that might be present and also to destroy the "memory" of the crystals in the melt. At this moment, the thermocouple was above the melt. The temperature of the furnace was then lowered by decreasing the applied voltage to a pre-selected level. The thermocouple junction was lowered into the melt. The amount of immersion was so chosen that the interference of the meniscus of the melt upon observation was at a minimum. The microscope was readjusted if necessary to focus the thermocouple junction inside the melt. By virtue of its low thermal capacity, the temperature of the melt would approach the steady temperature in a few seconds. After the crystals had grown to an observable size, photographs were taken at regular time intervals ranging from five seconds to two minutes, depending upon the prevailing growth rate, until the crystals grew to outside the field of the camera, or the observation was interfered with by other crystals. The temperature of the furnace was again raised above the liquidus temperature to dissolve all the crystals, and the thermocouple was then raised above the melt. The same procedure was then repeated for another temperature at about 10°C interval. The rate of the crystal growth was studied from just

below the liquidus temperature down to the lowest temperature, at which the observation was practical with the present apparatus.

While the thermocouple was above the melt, there was a coating of the melt at the junction. Due to the much smaller heat capacity of the thermocouple junction than that of the melt, its temperature dropped much faster, when the applied voltage was turned down. As soon as the junction was lowered down into the melt again, its temperature would rise because the melt was at a higher temperature. The indicated temperature then dropped again and approached a steady level in a very short time, showing that the melt was then at a steady temperature. These were recorded on the chart in the Graphspot, and the record for the experiments at several temperatures was reproduced as Fig. 25. Since the thermocouple junction was at a lower temperature for a longer time and reheated on entering the melt, usually the coating of the melt at the junction surface would crystallize. Shortly after the junction was in the melt, these crystals would start to grow into the melt. Therefore the crystals were normally around the junction and at the centre of the photographs.

Depending upon the temperature and composition, crystals sometimes started to grow from the side wall of the specimen holder, but the central mass around the thermocouple always grew to an appreciable size before this occurred. Therefore enough photographs could normally be taken to determine the growth rate. At lower temperature, difficulties were encountered. While the crystalline mass around the thermocouple was growing steadily, crystals started to grow on the surface of the melt, and this interfered with the observation of the crystals at the middle. Therefore the thermocouple was left in the melt when the temperature of the furnace was dropped. Crystallization would normally start at the thermocouple junction immediately and this would give

FIG. 25

GRAPHSPOT CHART DURING OBSERVATION OF CRYSTAL GROWTH.

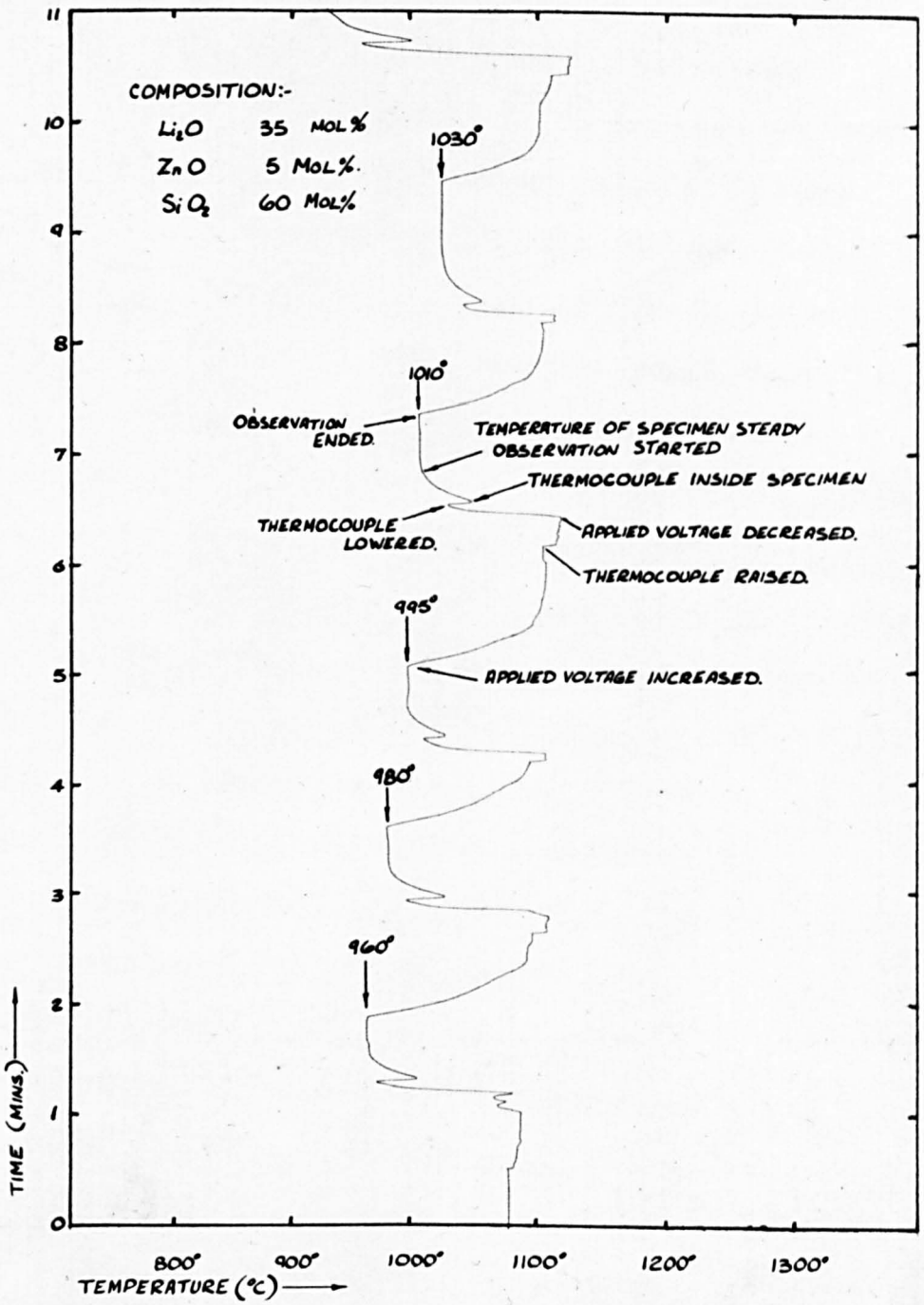

a longer time to observe the growth of the crystals at the middle. At still lower temperatures, even this method did not help very much, because the crystals started to grow at the surface very quickly and the number of crystals on the surface was quite large. In a very short time, the whole surface was occupied by a lot of tiny crystals. This was found to be the limiting factor at the lowest temperature that observation could be carried out.

At the lower temperature range, the thermocouple was lowered immediately after the applied voltage was lowered. At higher temperature, it was found necessary to wait for a while before the junction was lowered into melt to give some time for the melt on the junction to crystallize. This time interval ranging from a few seconds to about two minutes increased with the temperature.

At temperatures just below the liquidus temperature, crystals did not start to grow immediately after the junction was lowered into the melt. A few minutes might be taken before the crystals appeared at the junction, even in composition having a very high crystal growth rate at this temperature range. In this temperature range, the thermocouple junction was normally raised to a position, the temperature at which was much lower than that of the melt. When the temperature of the furnace was lowered, the junction would be at a temperature range at which crystals would grow immediately. Therefore, before the junction was lowered, the coating of the melt on the junction would have crystallized already. Under this condition, crystals would start to grow in the melt shortly after the junction was in the melt.

An attempt was made to grow the same crystalline mass at different temperatures. In this attempt, the thermocouple junction was left in the melt all the time and the temperature of the furnace was increased to about 5°C. higher than the liquidus

temperature, after the observation at one temperature was completed. In the low temperature range, the time necessary to heat the specimen to above the liquidus temperature was quite long, and the whole mass was completely crystallized during the heating up period. Under this condition, the last trace of crystals was normally on the surface of the melt and also away from the thermocouple junction. When the temperature was lowered again, these crystals started to grow before that at the thermocouple junction. Therefore the observed crystalline mass was not the same for successive experiments at different temperature. At higher temperature range, the specimen did not crystallize completely during the heating up period. However, the crystalline mass normally started to dissolve from the bottom. The crystalline mass became thinner and thinner, and at the later stage only a few long crystals were left radiating out from the junction. When the temperature of the furnace was lowered again, the crystals normally grew downward instead of at horizontal direction. This made the observation very difficult. Also the time for the last trace of crystals to dissolve was only about a second. This made it very difficult to control the size of the last trace of crystals. Due to the above practical difficulties, this technique was not used in the present study, instead a new crystalline mass was nucleated for the experiment at each temperature.

In one specimen with composition of lithium oxide 25 Mol % zinc oxide 15 Mol % and silica 60 Mol %, some special difficulty was encountered. When the thermocouple junction was lowered into the melt with the furnace temperature below the liquidus temperature, the crystals originally in the coating of the melt on the junction detached from the junction and flew to the surface quickly. These crystals were very close to each other, and grew into each other at a very short time. This made the observation very difficult. Therefore this composition was not studied.

After the study of crystal growth rate at various temperatures was finished, the liquidus temperature of the specimen was redetermined twice with the same experimental procedure already described. The liquidus temperature of the specimen was always found to be within 5°C to that determined before the study of the rate of crystal growth. Normally a liquidus temperature of 3°C higher was obtained after the study of the growth rate. Therefore the change of the composition due to selective volatilization was very slight and this did not significantly affect the results obtained.

In the temperature range with a very high crystal growth rate, the indicated temperature rose up to twenty degrees Centigrade during the crystallization. This was mainly due to the release of latent heat of crystallization. Under this condition, the average temperature was taken to be the temperature of the experiment. The indicated temperature was the temperature of the thermocouple at the centre of the crystalline mass, and the increase of temperature at the crystals and melt interface would have to be higher. There was no way to measure the temperature precisely. Therefore the actual temperature of the experiment was in doubt. However, this was met at only two or three temperatures at each specimen. For the experiment at all other temperatures, there was no observable change of temperature during the experiment.

(5) Identification and measurement of the crystalline phase.

After the study of liquidus temperature and crystal growth rate, the crystalline phase at different temperatures was identified. A small crystalline mass was allowed to grow as in the study of crystal growth rate. The thermocouple was raised out from the melt bringing with it the crystalline mass, at the same time the applied voltage to the furnace was cut off to freeze the crystals at the thermocouple junction. This crystalline mass was then immersed in liquids of different refractive

indices. The Becke line technique was used to identify the crystalline phase at the edge of the crystalline mass.

The rate of the crystal growth was deduced from the photographs taken. Films of different speed were tried. Since there was fairly low contrast between the crystalline mass and the melt in the negatives, it was necessary to increase the contrast. This was done by slightly under-exposing and over-developing a slow film. The best result was obtained with Ilford FP3. The intensity of the transmitted light was so adjusted that an exposure of one thirtieth of a second would give a negative slightly under exposed. The developer used was Ilford Microphen Fine Grain Developer, and the developing time was increased from the normal seven and a half minutes to eleven minutes.

It was quite easy to deduce the length of the crystals from an image projected from a negative by a photographic enlarger. The negatives taken in the calibration of the graticules were used for standardization. It was found that when the image of the two millimeter stage micrometer was ten inches long, the image of the sixty division of the graticule was 9.1 inches long. When the length of the crystal was measured, the photographic enlarger was so adjusted that the superimposed image of sixty division of the graticule would be 9.1 ins. long. Under this condition, 0.1 in. on the base plate of the enlarger was equivalent to twenty microns. A graph paper with 0.1 in. graduation was placed on the base plate of the enlarger and the distance between a reference point and the edge of the crystalline mass was read off from the graph paper. The edge with the fastest growth rate was measured; the edge with a slower growth rate was neglected, because at this point, the crystal was not growing in the plan of observation, or this line was not parallel to the direction of the growth.

3. Results.

These glasses were investigated. Their compositions, liquidus temperatures and primary phase crystals were listed in Table 16.

Table 16

Glasses used in the crystal growth experiment.

Glass No.	Composition			Liquidus Temperature	Primary Phase Crystal
	Li_2O	ZnO	SiO_2		
4	20	15	65	$1120^\circ \pm 5^\circ C.$	Tridymite.
6	30	5	65	$1010^\circ \pm 5^\circ C.$	Lithium disilicate.
7	35	5	60	$1188^\circ \pm 5^\circ C.$	Lithium metasilicate.

The length of crystal versus time curve and the growth rate versus temperature curves are shown in Fig. 26-32. A series of micrographs showing the growth of $Li_2O \cdot ZnO \cdot SiO_2$ were reproduced as Fig. 33. All the length of crystal versus time curves are straight lines indicating linear growth rate. The growth rates at various temperatures were obtained from the slopes of the length of crystals versus time curves. The usual hump shaped growth rate versus temperature curves were obtained.

A high scattering of results were obtained with glass No. 7. The main cause of the scattering was the measurement of temperature. A very high growth rate of over three thousand microns per minute were obtained with this glass. During the growth of the crystals, the temperature of the specimen increased up to $30^\circ C.$ The temperature was measured at the centre of the crystalline mass, so the increase of

FIG. 26. GROWTH OF LITHIUM DISILICATE AT DIFFERENT TEMPERATURES.

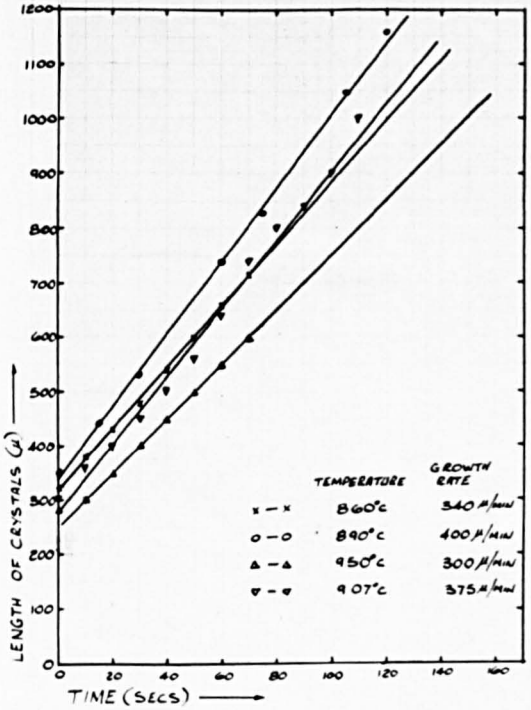

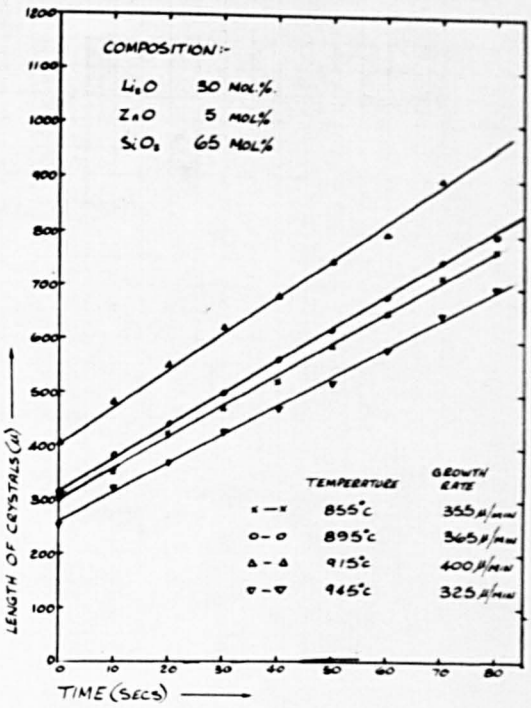

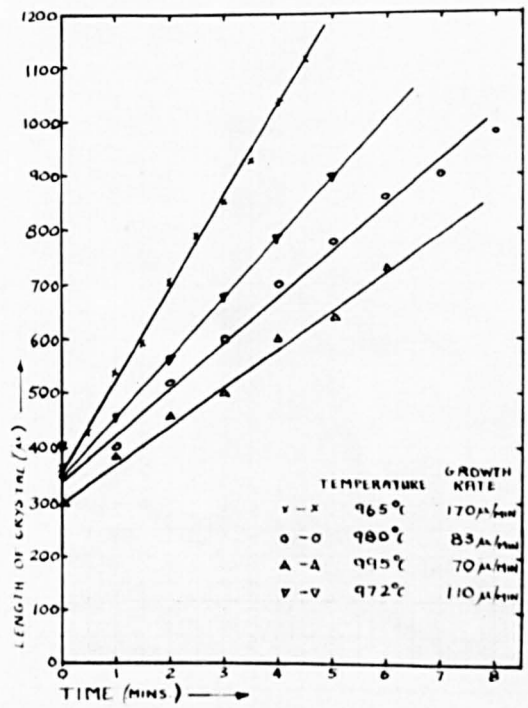

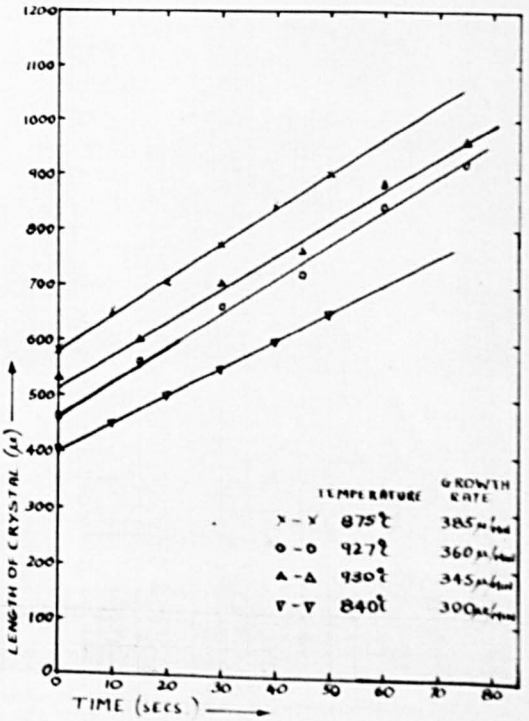

FIG. 27

RATE OF GROWTH OF LITHIUM DISILICATE

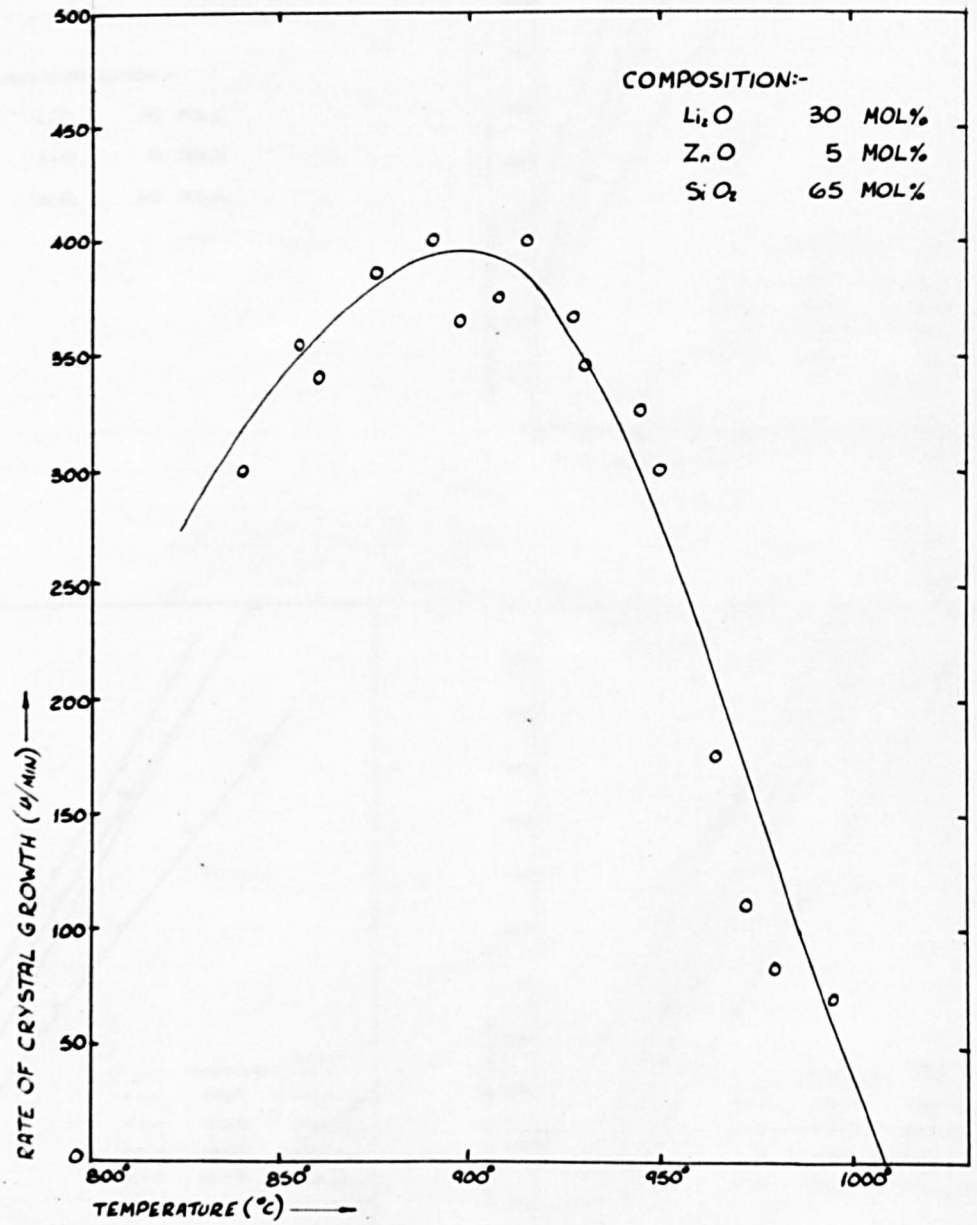

FIG. 28.

GROWTH OF LITHIUM META SILICATE CRYSTALS AT DIFFERENT TEMPERATURES.

GLASS COMPOSITION :—

Li_2O	35 MOL%
$Zn O$	5 MOL%
$Si O_2$	60 MOL%

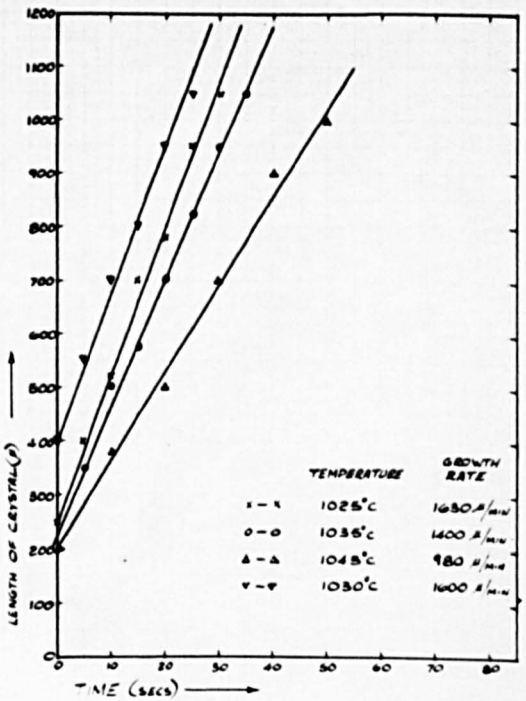

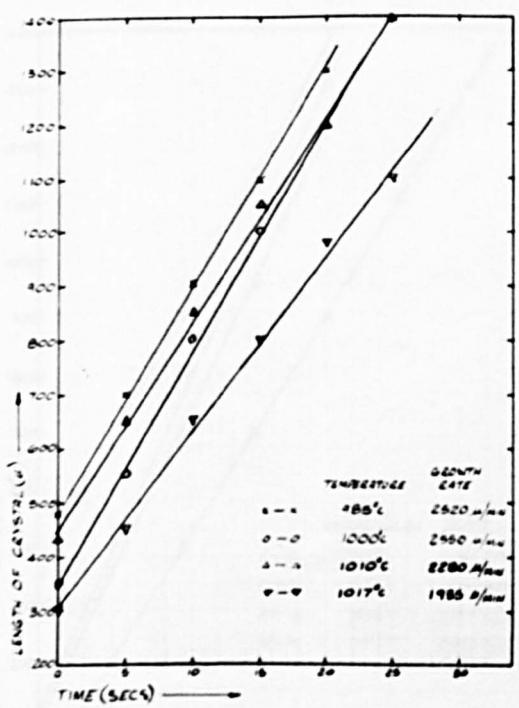

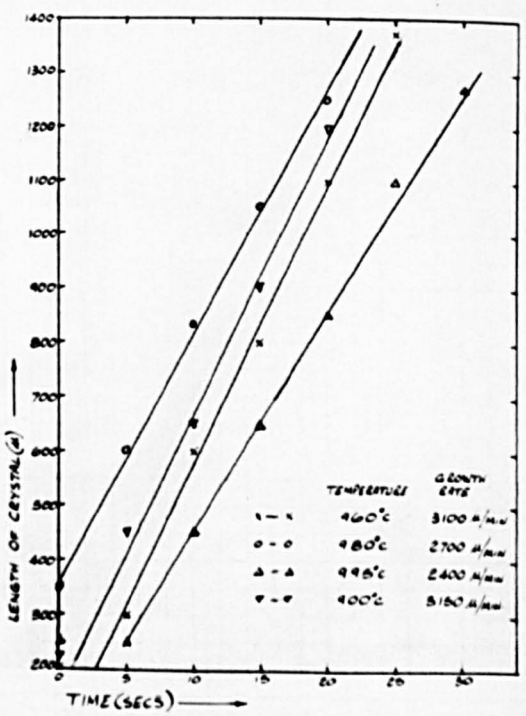

FIG. 29. GROWTH OF LITHIUM META SILICATE CRYSTAL AT DIFFERENT TEMPERATURES.

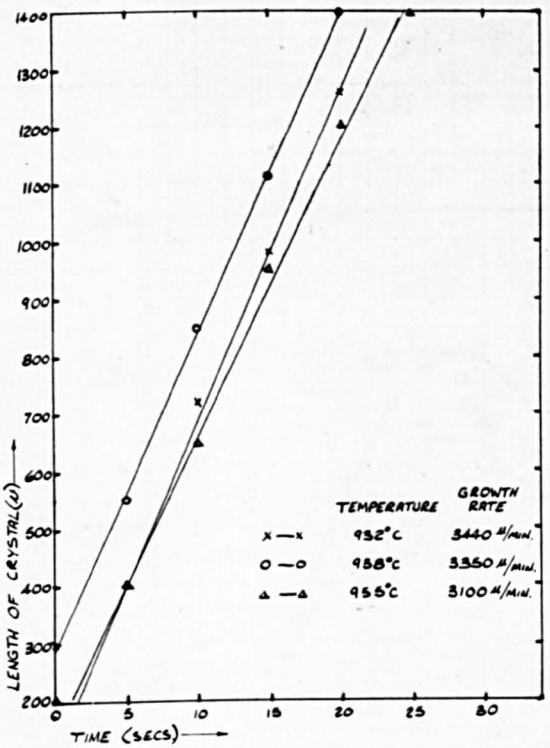

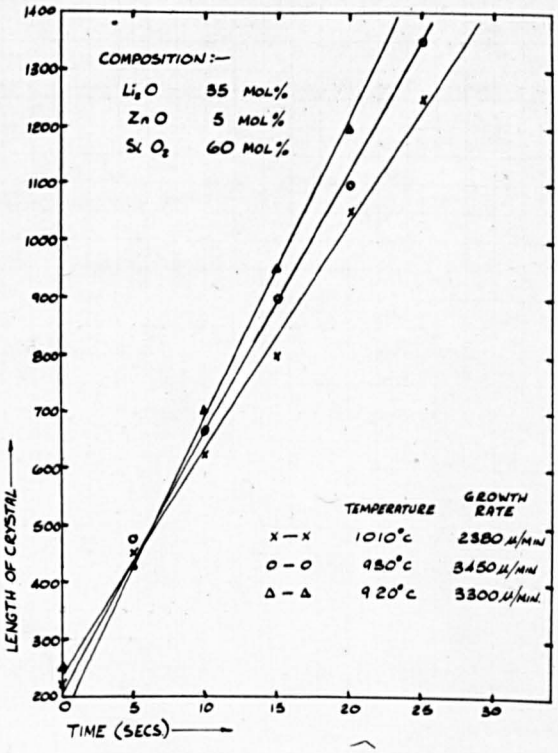

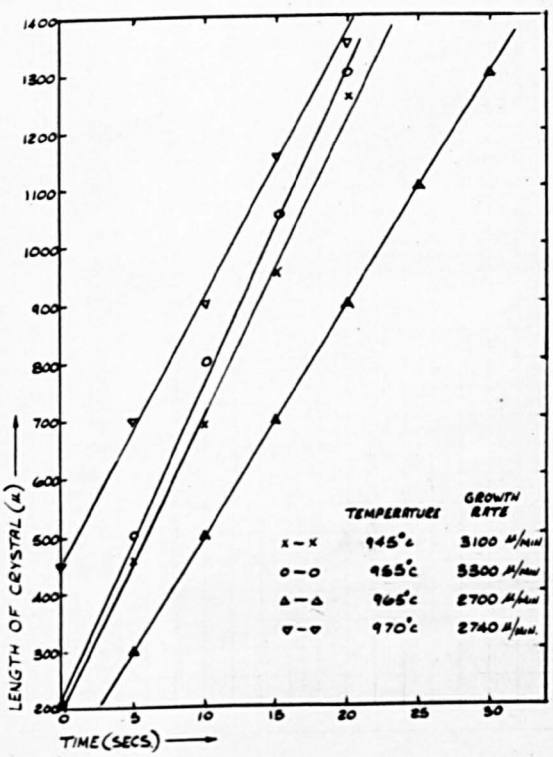

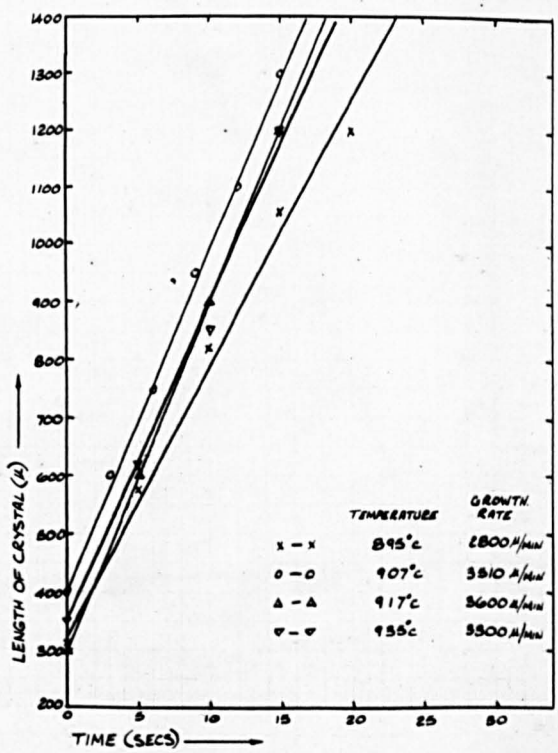

FIG. 30

RATE OF GROWTH OF LITHIUM META SILICATE

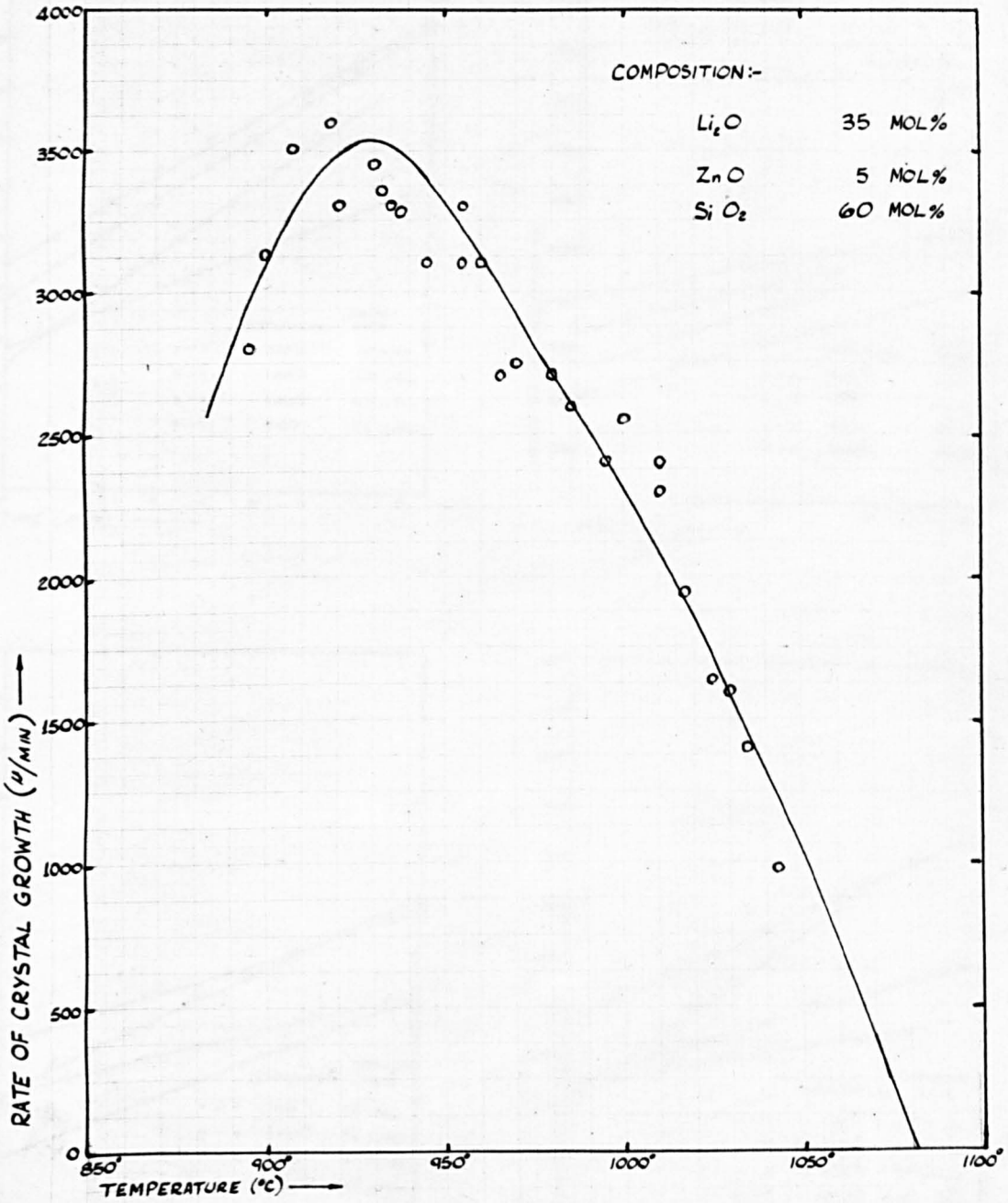

Tridymite And $Li_2O \cdot 2nO \cdot SiO_2$

FIG. 31. GROWTH OF ~~LITHIUM META SILICATE~~ AT DIFFERENT TEMPERATURES.

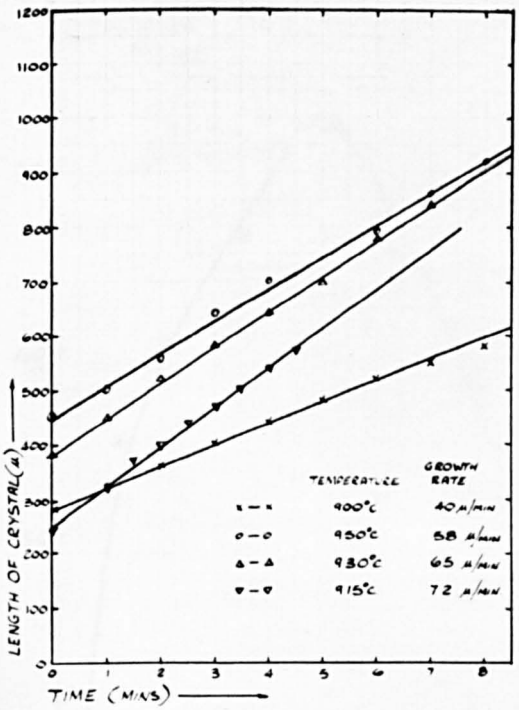

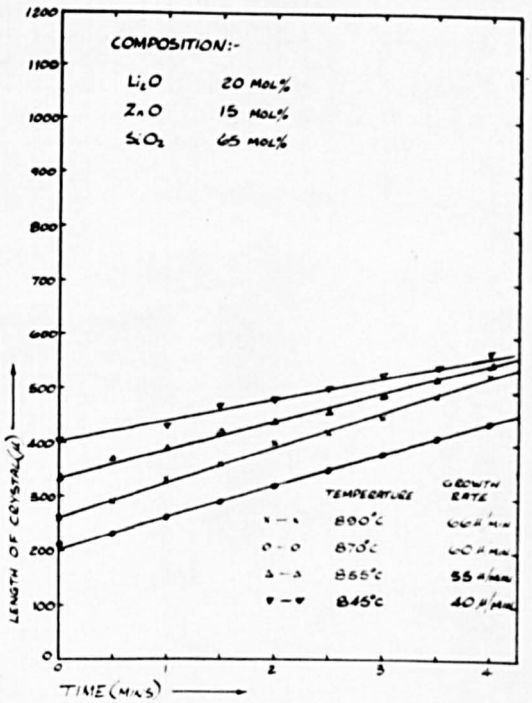

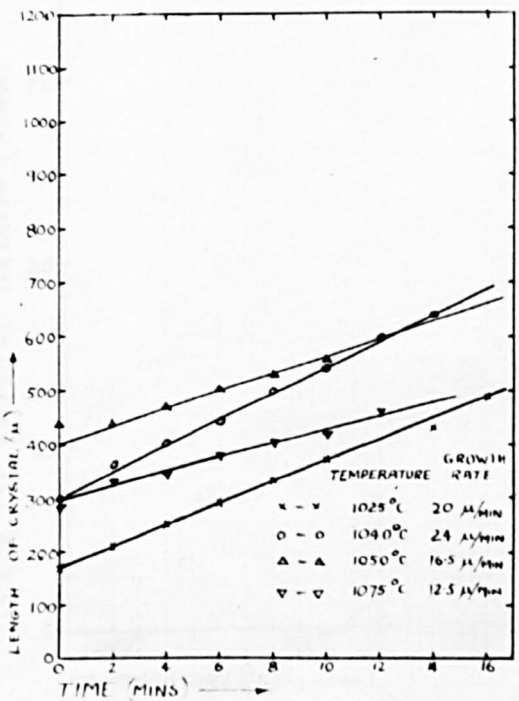

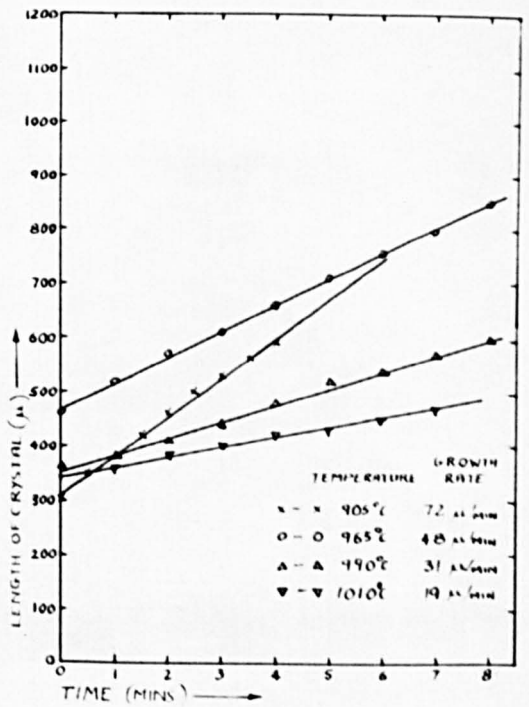

FIG 32

RATE OF GROWTH OF TRIDYMITE AND $Li_2O \cdot ZnO \cdot SiO_2$

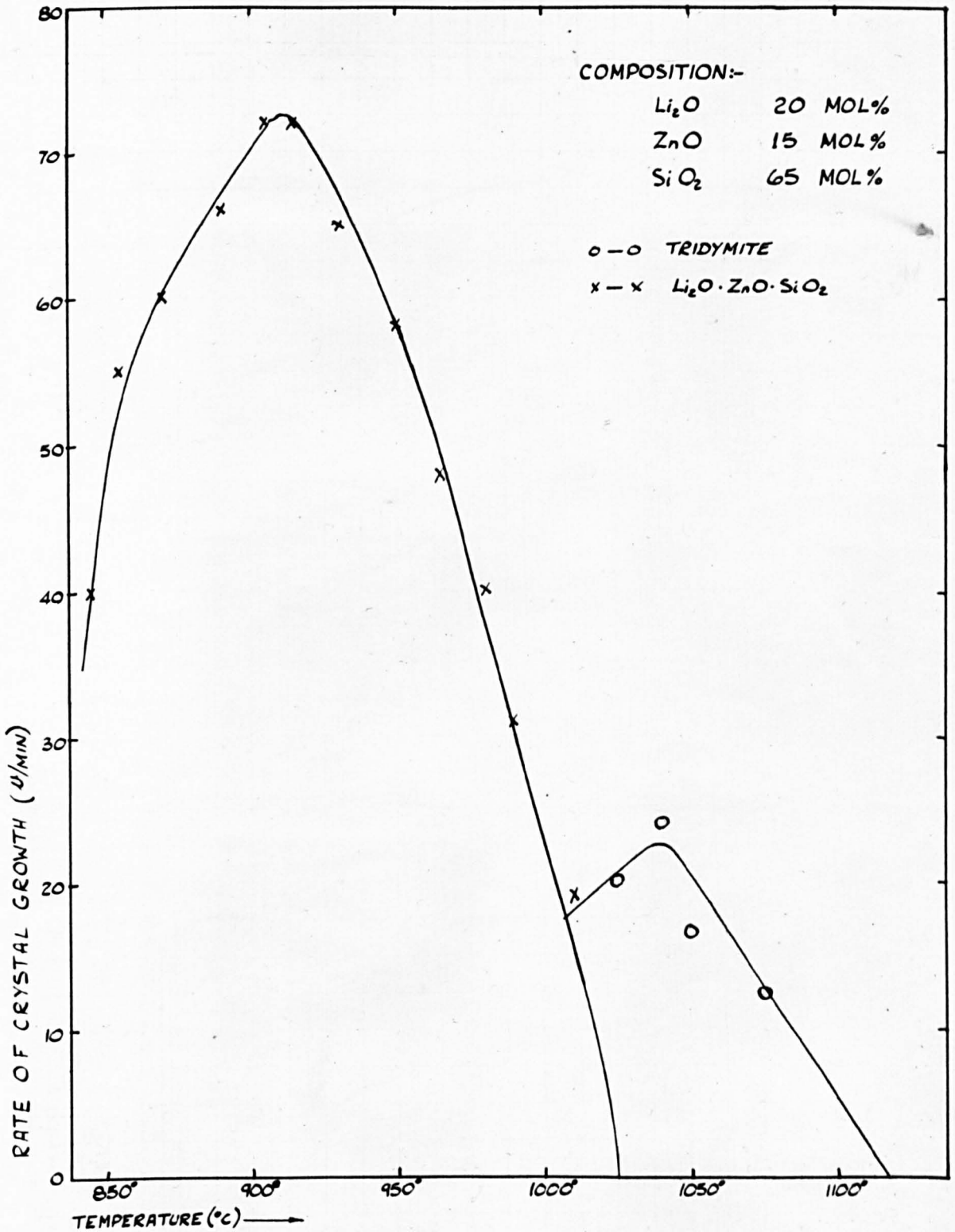

Fig. 33.

Growth of $Li_2O \cdot ZnO \cdot SiO_2$ crystals in glass No. 4 at 915°C.

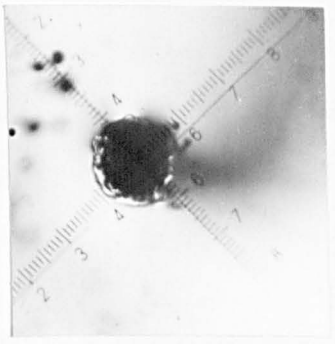

0 minute

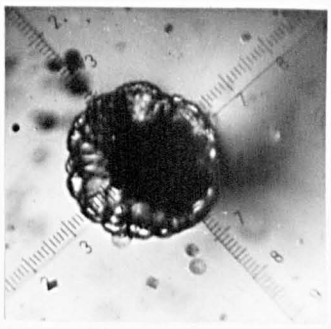

2½ minutes

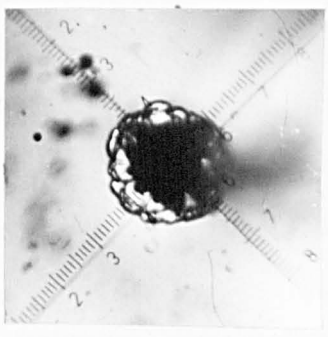

1 minute

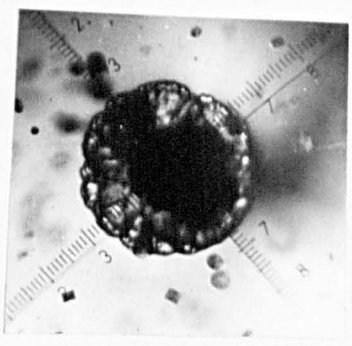

3 minutes

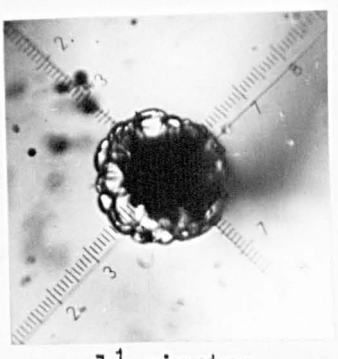

1½ minutes

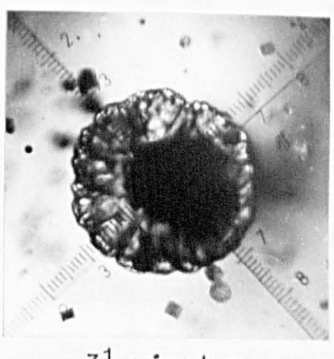

3½ minutes

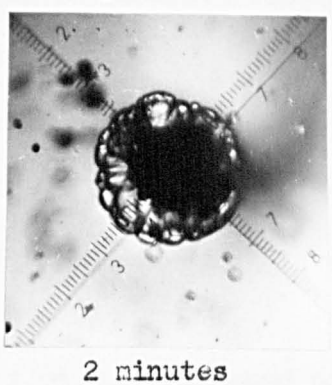

2 minutes

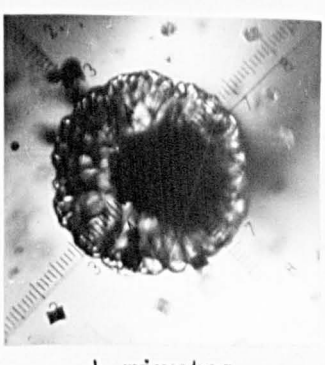

4 minutes

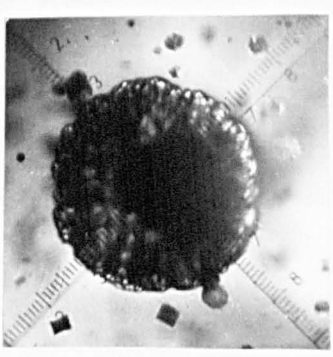

4½ minutes

temperature at the crystal and melt interface was much higher. There was no way to measure the temperature of the interface very accurately. At present, the average temperature during growth was used to plot the curves. This uncertainty of temperature measurement caused the wide scattering.

Owing to the high rates of growth, the time to observe the crystal was limited to about half a minute. Five second intervals were found to be the shortest time for operating the camera accurately. If three second intervals were used, it was difficult to take the photographs at the right moment. Therefore, only five photographs were taken to obtain the growth rate. Owing to the rapid change of temperature, the growth rate changed as well. This made the points on the length of crystal versus time curves scatter. The best straight lines were drawn through the points to obtain the growth rate. This would also introduce some error.

At the lower rate of growth, the data obtained was more accurate. In glass No. 4, the growth rates of which were below seventy five microns per minute, the points were all falling on the growth rate versus temperature curves. Except for very high growth rate curves, the points of the length of crystals versus times all fall on the straight line fairly accurately.

The linear growth rates obtained ranged from about ten microns per minute to over three thousand microns per minute. The maximum growth rates of different crystals ranged from about twenty microns per minute in tridymite to over three thousand microns per minute in lithium metasilicate. J. G. Morley found that the maximum growth rates in the lithium silicates were about eight hundred microns per minute in the glasses he investigated. He suggested that the rate at which the latent heat of crystallization could be conducted away might be the limiting factor of the growth rate. From the much higher growth rate obtained in the present study, it could be concluded that his suggestion was not correct.

With the present experimental procedure, only the higher rate of growth could be obtained, when different types of crystals were growing simultaneously, because the crystal and melt interface was that of the crystal which had a higher rate of growth. In glasses No. 6 and 7, the growth rates of the primary phases were higher than that of the secondary phases, therefore only the growth rates of the primary phases could be obtained. In glass No. 4, the growth rate of the secondary phase crystal was obtained below about 1000°C, because its growth rate was higher than that of the primary phase.

The present hot stage microscope proved to be very useful to study the growth rate of the crystal at high temperature. A wide range of growth rates could be studied with the present apparatus. The error in the observation of high growth rate is an inherent difficulty of the study and cannot be eliminated by using other apparatus, because it is impossible to measure the temperature of the moving interface between the crystal and melt continuously. However this apparatus is limited at low temperature ranges by the high tendency of the surface of the melt to devitrify, so that the position of the growing crystal could not be controlled by the measuring thermocouple and the tiny crystals on the surface interfered with observation. In the present study, the temperature range studied extended from just below the liquidus temperature to about 850°C.

IV. DISCUSSION OF RESULTS.

G. Tammann's concept of the mechanism of crystallization has been accepted as the classical theory of nucleation. By consideration of the total free energy change during the initial stage of the phase transformation from an unstable phase to a stable phase, he concluded that there is an energy barrier in the formation of the new phase. In this theory, only the direct transformation of the unstable phase to the stable phase is considered, the other paths with intermediate steps are not considered. In the transformation of a pure material, the direct transformation of the unstable phase into the stable phase is the only path. However in the precipitation of a stable phase from a complex solution, different paths with various intermediate steps are conceivable. If the energy barrier of each intermediate step is lower than that of the direct formation of the stable phase, it is more likely that the path of the direct formation will not be followed. The separation of a second liquid phase seems to be an easier step, because the surface tensions of the liquids are similar.

In the classical theory, the concept of the interface between the stable phase and the unstable phase is of a macroscopic scale. In the absence of precise knowledge of the properties of the interface of the small nuclei, the concept of the interface of macroscopic scale, is a reasonable assumption. However, S. D. Stookey[29] has pointed out in his discussion of the crystallization of the photosensitive glass that the minimum size of the stable gold nuclei in the homogeneous nucleation was found to be one to three gold atoms. These results were obtained independently from light scattering experiments and from the latent image stabilization experiment. If the minimum size of a stable nucleus is in the order of one to three atoms, it is difficult to conceive the concept

of interface surrounding this group of atoms. Even the concept of an interface in the macroscopic scale is accepted, the properties of this interface may be completely different from that of a particle in the macroscopic scale. With a particle consisting of only one to three atoms, some other factors (e.g. the relative geometrical position between them) may be more important than the surface energy term in the consideration of the classical theory. Owing to the foregoing reasons, the classical nucleation theory can only serve as the background knowledge of the processes of crystallization of complex systems and it cannot be applied directly in most cases.

It has been reported by other workers and observed in the present study of the growth rate of crystal that over a range of temperature just below the liquidus temperature, the crystals do not grow immediately after the specimen is below the liquidus temperature, even the growth rates of the crystals are very high in this temperature range. This indicates the very high energy barrier of the formation of the new phase in this temperature range. If the various processes of conditioning the specimen, before the crystals are able to begin the steady state crystal growth, are regarded as the "nucleation process", instead of limiting the term nucleation to the formation of stable nuclei, the classical theory can be extended considerably to include more phenomena. In other words, the processes of overcoming the energy barrier of the steady state crystal growth can be considered as the "nucleation" stage.

During the present study of nucleation, only surface crystallization was observed in the commercial soda lime silica glass. Also in the crystal growth study, surface crystallization was the limiting factor of the low temperature limit for the observation of the crystal growth. Actually in the present technique, to study the crystal growth rate, the coating of glass on the thermocouple junction was placed in favourable

conditions for heterogeneous nucleation by providing a large platinum and melt interface, air and melt interface and the suitable temperature. The crystals formed in the coating on the thermocouple were used as "nuclei" for the crystallization of the specimen. Therefore the crystals were actually nucleated heterogenously. The easiness of the heterogeneous nucleation may be due to the differences between the structure of the specimen and that of the interior, or due to the lower energy barrier in the nucleation processes, or due to impurities. In the acid etching experiment on the heat treated specimen, it was found that the properties of the surface were different from those of the interior. A higher differential acid resistance was found on the surface than in the interior of the glass. This indicates a higher inhomogenity on the surface than in the interior. On the surface, the condition is different, and the energy barrier should be different. Turnbull(33) had shown in the study of crystal growth in fused silica that impurities have a pronounced effect on the easiness of the "nucleation" stage.

In the glass ceramic process, phase separation was found to be the initial essential step for the formation of the high concentration of the tiny crystals at the later stage. Therefore the uniform crystallization of the glass ceramic materials is actually a heterogeneous nucleation process, instead of a homogeneous nucleation process. The success of the glass ceramic process is actually the introduction of an evenly distributed liquid and liquid interface into the interior of the material and hence the energy barrier of crystallization in the interior is lowered to the same, or even lower, level of that on the surface. Therefore a lot of crystallization centres are introduced in the interior of the material and a lot of crystal will form simultaneously to convert the material to an essentially polycrystalline material.

In the present study of the nucleation of the glasses in the lithium oxide - zinc oxide - silica ternary system, uniform crystallization was found in every specimen. Therefore the tendency to crystallization of the interior of the glass will be comparable to that of the surface. However the results of the acid etching experiment indicate that higher segregation occurred on the surface of the specimen. This may mean a slightly higher tendency to crystallization of the surface than that of the interior. In the present study, the effects of different heat treatment were not studied. Possibly, a more suitable heat treatment schedule may eliminate this slightly higher tendency to crystallization of the surface.

The primary phase crystals of the two of the three glasses studied are tridymite and that of the third is $Li_2O \cdot ZnO \cdot SiO_2$. The compositions of these three glasses are very similar and close to the eutectic point E of the composition triangle of SiO_2 - $Li_2O \cdot SiO_2$ - $Li_2O \cdot ZnO \cdot SiO_2$. Big lithium disilicate crystals as well as a lot of tiny crystals were found in these three specimens, although the primary phase of these glasses are not lithium disilicate. From the effect of time in nucleation experiments, the growth rate of the lithium disilicate was found to be much higher than that of the tiny crystals in the temperature range of the experiment. Since these crystals were found to grow simultaneously, the different sizes of these two types of crystals would be mainly due to the different growth rate instead of the difference between the easiness of their "nucleation". Therefore in the sub-solidus temperature, the growth rate of the different crystals have a higher effect on the size of the crystal, and hence the crystalline content of the final product, than whether a particular crystal is the primary phase of this specimen or not, if the heat treatment is not continued to the equilibrium condition.

The formation of the spherical crystals and their outward growth of them should not be taken as the proof that these crystals grow from the stable nuclei as described in the classical nucleation theory, because Oldberg, Golob and Strickler[23] had shown that crystals originated from the interface of a spherical droplets also form spherical crystals.

It was observed that the heat treated specimen broke along the cleavage plane of the crystals. Therefore these crystals seem to weaken the materials. In any case, uniform size of crystals is advantageous in the glass ceramic process. In the effect of time in nucleation experiment, the compositions of the glasses No. 4 and 5 are further away from the composition of lithium disilicate. Much less and smaller lithium disilicate crystals were found in the specimen of glass No. 4 than in glass No. 1 to 3, after heat treatment at the lower temperature. After heat treatment at 550° - 750°C for one hour, the lithium disilicate in glass No. 4 seemed to be bigger than that in glass No. 1 to 3, possibly due to the higher growth rate of lithium disilicate in glass No. 4 than in glass No. 1 to 3, in this temperature range.

In glass No. 5, which is outside the silica - lithium disilicate - $Li_2O \cdot ZnO \cdot SiO_2$ composition triangle, no lithium disilicate was identified, and only a very high concentration of tiny crystals were found in the heat treated specimens. Therefore the compositions on the right of the SiO_2 - $Li_2O \cdot ZnO \cdot SiO_2$ join seem to be more suitable for the production of glass ceramics.

In the crystal growth experiment, the growth of the crystal was found to be linear with time. In the literature, only Turnbull[31] and his Associates had reported root time relationship in the crystal growth in glasses. They found in their study of the crystal growth of cristobalite in fused silica that the atmosphere has a pronounced effect and they suggested that the diffusion of catalytic oxygen, water vapour or impurity in the crystalline layer was the controlling factor of the growth

rate. If the oxides other than silica in the glass are regarded as "impurities", then in a complex system, the diffusion of "impurities" will not be the controlling factor of the growth rate because the concentration of "impurities" is so high in every part of the glass already.

The temperature ranges of the crystal growth investigation in the present study are quite narrow, and it was found difficult to deduce any information of the mechanism of the growth rate from them. Several workers had suggested that viscosity is the dominant factor of the growth rate below the maximum growth temperature. By plotting the product of the growth rate and viscosity versus temperature, Littleton[37] had demonstrated that the straight line from high temperature extended to far below the maximum growth temperature, suggesting that viscosity is the dominant factor over this temperature range.

In their investigation of growth rate of cristobalite in fused silica containing small amounts of alumina, Kistle and Brown[32] had found that the growth rates at the same temperature increased with the amount of alumina, but the viscosities at the same temperature also increased with the amount of alumina. They had suggested that this was a contradictory case to the generally observed effect of viscosity. In the temperature range they studied, the growth rate of the same glass increased with temperature, indicating that the temperature range was below the maximum growth rate temperature. Turnbull[31] showed that the growth rate of cristobalite increased with temperature up to about fifty degrees below the liquidus temperature. By comparing the temperature range, it was found that the temperature range in which Brown and Kistle[32] studied was below the maximum growth rate temperature. From the phase diagram of the binary alumina - silica system, it is noted that the liquidus temperature of silica is lowered greatly by small addition of alumina. Since the growth rate versus temperature curve are normally of

the same hump shape. The lowering of the liquidus temperature by addition of alumina will move the growth rate versus temperature curves to a lower temperature. When the growth rates of different glasses at the same temperature were compared, the different part of the growth rate versus temperature curves were used. This does not present the true picture of the crystal growth process, because the effect of viscosity is masked by the effect of liquidus temperature. The comparison of the maximum growth rate may have more meaning.

In the present study of the growth of crystal, a very wide range of maximum growth rate from about twenty micron per minute to over three thousand micron per minute was obtained. The ratio between them is over a hundred. This phenomena is very striking, because the compositions of the glasses are not widely different. In the absence of reliable viscosity data of these glasses, it is difficult to assess the effect of viscosity. Since the maximum growth rates were found in approximately the same temperature range, the difference of viscosity of these glasses at the maximum growth rate temperature will not be large. Therefore some other factors may be important. These maximum growth rates are not obtained from the same kind of crystal. Therefore the difference between the structure of the melt and the crystals may be important.

The crystallization characteristics of glasses in this ternary system were only studied slightly. With the results obtained so far, it is noted that the glasses crystallized uniformly. This may make these glasses suitable for the glass ceramic process. The compositions on the right of the SiO_2 - $Li_2O \cdot ZnO \cdot SiO_2$ join will be more suitable, because the high growth rate crystals of lithium metasilicate and lithium disilicate are elminated. The $Li_2O \cdot ZnO \cdot SiO_2$ solid solution and

$2\ Li_2O \cdot 4\ ZnO \cdot 3\ SiO_2$ solid solution fields seem to be more suitable owing to the existence of solid solutions, which will assist the precipitation of crystals.

The physical properties of the partially crystallized material have not been studied. Since the physical properties of glass ceramic materials depend on the properties of the constituent crystalline phases and the glass matrix, desirable properties may be obtained by choosing suitable compositions and heat treatments to give the desired crystals. The effect of heat treatment on the microstructure of the final product and their physical properties of compositions in the $Li_2O \cdot ZnO \cdot SiO_2$ solid solution and $2\ Li_2O \cdot 4\ ZnO \cdot 3\ SiO_2$ should be investigated further.

References.

1. S. D. Stookey, Corning, U.S.A. Patent 2,920,971 (1960).

2. Corning. B.P. 869, 328 (1961).

3 Corning. B.P. 863, 569 (1961).

4. Corning. B.P. 863, 570 (1961).

5. Corning. B.P. 863, 776 (1961).

6. Corning. B.P. 869, 315 (1961).

7.(a) R. Ricke and H. Endell, Sprechsaal (43) 683 (1910).
(44) 97 (1911)

(b) Ballo and Dittler, 2. Anorg. Chem. (76) 42 (1912).

(c) Schwarz and Sturm, Berichte (47) 1737 (1914)

(d) R. Wallace, Z.Anorg.Chem. (63) 15 (1909).

(e) H. S. Van Klooster, Z.Anorg.Chem. (69) 136 (1911)

(f) F. M. Jaeger and H. S. Van Klooster, Proc.Amst.Acad.Sci. (16) 857 (1914).

8. F. C. Kracek, J.Phy.Chem. (34II) 2645 (1930).
J.Amer.Chem.Soc. (61) 2870 (1939).

9. (a) Stein, Z.Anorg.Chem. (55) 159 (1907).

(b) H. S. Van Klooster, Z.Anorg.Chem (69) 142 (1910).

(c) F. M. Jaeger and H. S. Van Klooster, Proc.Amst.Acad.Sci. (18) 896 (1916).

(d) Ebelmen, Ann.de Chim.Phy. (33) 34 (1851).

(e) Schulge and Stelgner, Neues Tahrb.Min. (1) 150 (1881).

(f) Traube, Berichte (26) 2735 (1893).

(g) Mulert, Z.Anorg.Chem. (75) 220 (1912).

(h) Gorgen, Comp.rend. (104) 120 (1887).
J.Amer.Ceram.Soc. (13) 8 (1930).

10. E. N. Bunting, Bur.Standards J.Research (4) 134 (1930).

11. H. S. Van Klooster, Z.Anorg.Chem. (69) 135 (1910).

12. I. M. Stewart and G. J. P. Buchi, Tran.Brit.Ceram.Soc. (61) 615 (1962).

13. A. W. Bastress, Glass Science Bull. (4) 135 (1946).

14. A. E. Austin, J.Amer.Ceram.Soc. (30) 218 (1947).

15. G. Donnay and J. D. H. Connay, J.Amer.Mineral. (38) 163 (1953).

16. R. Roy and E. F. Osborn, J.Amer.Chem.Soc. (71) 2085 (1949).

17. G. Rindone, J.Amer.Ceram.Soc. (45) 7 (1962).

18. G. Tammann, J.Soc.Glass Tech. (9) 166 (1925).

19. R. J. Jacodine, J.Amer.Ceram.Soc. (44) 472 (1961).

20. O. Knapp, Glass Ind. (36) 262 (1955).

21. T. B. Yee and A. I. Andrews, J.Amer.Ceram.Soc. (39) 188 (1956).

22. R. D. Maurer, J.Appl.Phys. (29) 1 (1958).

23. S. M. Ohlberg, H. R. Golob, and D. W. Strickler, Nucleation and Crystallization Symposium, p.55. ¥
W. Vogel and K. Gerth, Nucleation and Crystallization Symposium, p.11. ¥

24. R. D. Maurer, Nucleation and Crystallization Symposium, p.5. ¥

25. J. P. Williams and G.B. Carrier, Glass Tech. (4) 183 (1963).

26. R. Roy, Nucleation and Crystallization Symposium, p.39. ¥

27. W. B. Hillig, Nucleation and Crystallization Symposium. ¥

28. F. P. H. Chen, J.Amer.Ceram.Soc. (46) 476 (1963).

29. S. D. Stookey, Progress in Ceramic Science, Vol.II, Pergaman Pres, London (1962).

30. W. D. Scott and J. A. Park, J.Amer.Ceram.Soc. (44) 181 (1961).

31. N. G. Hinslie, C. R. Morelock and D. Turnbull, Nucleation and Crystallization Symposium, p.97. ¥

32. S. D. Brown and S. S. Kistle, J.Amer.Ceram.Soc. (42) 263 (1959).

33. E. Preston, J.Soc. Glass Tech. (24) 139 (1940).
J. O. Jones, Glass, Methuen and Co. Ltd., London (1956).

34. A. J. Milne J.Soc.Glass Tech. (36) 275 (1952).

35. H. R. Swift, J.Soc.Glass Tech. (30) 170 (1947).

36. O. H. Grabier and E. H. Hamilton, J.Res.Nat.Bur.Stad. (44) 495 (1950).

37. J. T. Littleton, J.Soc.Glass Tech. (15) 263 (1931).

38. J. G. Morley, Ph.D. Thesis, Nottingham University (1962).

39. G. Rindone, J.Amer.Ceram.Soc. (41) 41 (1958).

¥ Symposium on Nucleation and Crystallization in Glasses and Melts. The American Ceramic Society (1962).